IMPACT OF CARBON NANOTUBES ON BACTERIAL VIABILITY: INDICATORS, MITIGATION, AND ROLE OF PHAGE SHOCK PROTEINS

A Dissertation
Submitted to the Graduate Faculty
of the
North Dakota State University
of Agriculture and Applied Science

By

Tu Thi Anh Le

In Partial Fulfillment of the Requirements
for the Degree of
DOCTOR OF PHILOSOPHY

Major Program:
Environmental and Conservation Sciences

March 2014

Fargo, North Dakota

North Dakota State University
Graduate School

Title

IMPACT OF CARBON NANOTUBES ON BACTERIAL VIABILITY: INDICATORS, MITIGATION, AND ROLE OF PHAGE SHOCK PROTEINS

By

Tu Thi Anh Le

The Supervisory Committee certifies that this ***disquisition*** complies with North Dakota State University's regulations and meets the accepted standards for the degree of

DOCTOR OF PHILOSOPHY

SUPERVISORY COMMITTEE:

Dr. Eakalak Khan

Chair

Dr. John McEvoy

Dr. Kalpana Kati

Dr. Achintya Bezbaruah

Approved:

7/10/2014	Dr. Eakalak Khan
Date	Department Chair

ABSTRACT

The toxicity of single walled carbon nanotubes (SWCNTs) to a model bacterium, *Escherichia coli* ATCC 8739 was investigated. Estimates of *E. coli* viability following treatment with SWCNTs were similar using four viability methods: plate count, galactosidase enzyme assay, LIVE/DEAD® Baclight™ assay, and RNA quantificatio. Pristine SWCNTs, carboxylic functionalized SWCNTs (SWCNT-COOHs) and hydroxyl functionalized SWCNTs (SWCNT-OHs) were used to assess toxicity. Regardless of the length of SWCNTs, the toxicity was in the following order: SWCNT-OHs < SWCNTs < SWCNT-COOHs. While there was no difference in the impact of short and long SWCNT-OHs, the long pristine SWCNTs and SWCNT-COOHs were more toxic than the corresponding short SWCNTs. The viability of cells exposed to all three types of SWCNTs was greater with increasing cell density. Alterations of cell morphology ware observed after the cells were exposed to SWCNTs.

Entrapment of cells in alginate and polyvinyl alcohol (PVA) as a means to limit the antibacterial effect of SWCNTs was examined. The results showed that cell entrapment could reduce the bactericidal effects of SWCNTs. Calcium alginate and PVA provided equivalent cell protection against SWCNTs. The toxicity of SWCNTs for entrapped cells depended on the length and concentrations of SWCNTs, the presence of functional groups, and the initial cell density.

Transcriptomic and proteomic analyses were used to study the molecular mechanisms by which SWCNTs induce bactericidal activity. Expression levels of genes and proteins, particularly phage shock proteins (Psp) that are known to react under membrane stress such as

pspA, pspB, and *pspC*, changed following cell exposure to SWCNTs. Expression of the Psp operon was affected by the length, concentration, and functionalization of SWCNTs.

Overall, this study provided multiple methods that can be used to quantify the toxicity of SWCNTs for bacterial cells. A way to mitigate the bactericidal effects of SWCNTs was identified and verified. Gene and protein expression, particularly expression of the Psp operon, were reported in cells stressed by exposure to SWCNTs.

ACKNOWLEGEMENTS

My deepest gratitude goes first and foremost to my advisers, Dr. Eakalak Khan and Dr. John McEvoy, for providing me the opportunity to work under their supervision. My sincere thanks go to them for their constant encouragement and guidance during all phases of my graduate research and education. Throughout the years, I have learned so much from them about science and life, which will be greatly cherished, in my future life.

I would like to thank my committee members Dr. Kalpana Katti and Dr. Achintya Bezbaruah. Without their advice and help, this dissertation would not have been possible. I acknowledge Vietnam International Education Development (VIED), National Science Foundation, USA, and Environmental and Conservation Sciences Program and Graduate School of North Dakota State University for financial support.

I gratefully thank Cathy Giddings and Scott Hoselton for their guidance and friendly cooperation during my research. I would like to thank Dr. Birgit Pruess, Dr. Jane Schuh, Dr. Eugene Berry, and Dr. Glenn Dorsam for providing me valuable suggestions and laboratory facilities.

I could not have done this work without Sita Krajangpan, Yaping Chi, Jun Yang, and Pumis Thuptimdang, my comrades for life, who shared their time, love, and lives. I would like to thank all former and current members of Dr. McEvoy's and Dr. Khan's research groups that have made the labs a great and fun work environment.

Last but not least, I am forever indebted to my parents, my dearest husband – Nam Nguyen, and my lovely son - Manh Nguyen. Without their continuous support and encouragement, I would have a much more difficult time. Knowing they were always behind me helped push me to complete this journey.

TABLE OF CONTENTS

LIST OF TABLES

LIST OF FIGURES

LIST OF ABBREVIATIONS

ANOVA……..Analysis of variance

cDNA …….Complementary deoxyribonucleic acid

CFU…….Colony forming unit

COOH…….Carboxylic

CNTs…….. Carbon nanotubes

DNA …….. Deoxyribonucleic acid

DI…….Deionized

FITC……Fluorescein isothiocyanate

IPTG……Isopropyl-beta-D-thiogalactopyranoside

MWCNTs ……...Multiple walled carbon nanotubes

MUF ……Methylumbelliferone

MUGAL……..4-methylumbelliferyl-β-D-galactoside

NA …….. Nutrient agar

NB ……..Nutrient broth

OH……Hydroxyl

PBS……..Phosphate buffer saline

Psp……Phage shock protein

RT-PCR……Quantitative reserve transcriptase polymerase reaction

RNA…….Ribonucleic acid

SDS-PAGE……. Sodium dodecyl sulfate polyacrylamide gel electrophoresis

SEM…… Scanning electron microscopy

SWCNTs ……. Single walled carbon nanotubes

LIST OF APPENDIX FIGURES

LIST OF APPENDIX SCHEMES

CHAPTER 1: INTRODUCTION

1.1. Background

Over the past decade, the development in nanotechonology and nanosciences has led to the expansion of nanoparticle and nanomaterial uses in various industries. Among nanomaterials, interests in carbon nanotubes (CNTs) have dramatically grown. CNTs are cylindrical structures of graphene sheets. They come in different lengths, shapes, surface modifications, and graphene sheet numbers. Their unique physical and chemical properties, such as electrical, optical, mechanical, and diffusion, have made them a potential material for several applications, such as conductive and high-strength composites, energy storage and energy conversion devices, sensors, field emission display, and semiconductor devices.

The increasing uses and mass production of CNTs have raised concerns about their safety and environmental impact. CNTs have three properties that are toxicity related: (1) They are a few nanometers in diameter making them more toxic than larger size particles; (2) They have a fiber morphology which is similar to asbestos and other pathogenic needle-shaped fibers; and (3) the essential graphite may make them biologically persistent (Donaldson et al., 2006). Many investigations on CNT toxicity have been reported but the results remain controversial (Francis et al., 2012). Discrepancies among studies may be due to differences in size and functionality of CNTs, experimented organisms, and the approaches used.

Studies have reported potential CNT toxicity for humans (Akasaka and Watari, 2009; Monteiro-Riviere et al., 2005; Tabet et al., 2011). The high aspect ratio of CNTs makes them airborne and easy to inhale. Acute pulmonary toxicity, subpleural fibrosis, and immune suppression have been observed when sensitive organs are exposed to CNTs. The potential toxic effects of CNTs on plants and plant cells have been investigated (Lin and Xing, 2007; Parvin

et al., 2012; Stampoulis et al., 2009). While some studies reported that CNTs enhanced rape, radish, lettuce, corn, and cucumber growth without damaging the plants or inhibiting seed germination (Lin and Xing, 2007), CNTs severely inhibited root elongation in tomatoes (Canas et al., 2008). Several studies have addressed the toxicity of CNTs in aquatic and terrestrial invertebrates and vertebrates (Blaise et al., 2008; Handy et al., 2011; Handy et al., 2008; Philbrook et al., 2011; Scott-Fordsmand et al., 2008). Mortality induction, fertilization reduction, inflammation, and alterations in behavior were observed (Cheng et al., 2007; Leeuw et al., 2007; Liu et al., 2009a; Philbrook et al., 2011; Scott-Fordsmand et al., 2008; Smith et al., 2007).

CNTs also have an antimicrobial effect. Membrane integrity disruption (from direct contact between CNTs and bacteria), DNA damage, protein inactivation by reactive oxygen species, and impurity toxicity (mainly from heavy metals) are the proposed mechanisms of toxicity of CNTs (Arias and Yang, 2009; Kang et al., 2007a; Liu et al., 2009a; Luongo and Zhang, 2010; Vecitis et al., 2010; Young et al., 2012). Generally, CNTs reduced bacterial viability or retarded growth rate. CNTs exhibited antimicrobial activity on suspended, deposited bacteria and prevented formation of bacterial films. Kang et al. (2007a, 2008a) reported the reduction in viability of bacteria after exposure to CNTs. The purity of CNTs influences the bactericidal activity. The metal residue of CNTs induced bacterial toxicity in addition to the CNTs themselves (Vecitis et al., 2010). CNTs reduced enzyme activity of soil microorganisms (Jin et al., 2013). CNTs also reduce the formation of biofilm both in natural and industrial environments (Rodrigues and Elimelech, 2010).

1.2. Research Problems and Justifications

CNTs possess unique properties making them a leading material for many desirable applications. CNTs are currently being reviewed by the U.S. Environmental Protection Agency (EPA) for possible regulation (EPA, 2010). Until the EPA decides on the final ruling, there are few restrictions on CNT usage and disposal. The increasing production of CNTs increases the potential for their release into the environment. Studies have primarily focused on the effects of CNTs on humans and plants; however, bacteria in the environment are also vulnerable. Any effects on these microorganisms could alter the ecological balance. Therefore, before CNTs become more widespread in the environment, it is important that their toxicity for bacteria is studied and known.

The effects of CNTs on bacteria have attracted more interest and many studies have investigated the toxicity of CNTs on bacteria (Arias and Yang, 2009; Kang et al., 2007a; Yang et al., 2010; Young et al., 2012). However, these previous studies have primarily aimed to evaluate the toxicity of CNTs without investigating potential mitigation strategies. Several studies proposed that direct physical contact leading to physical membrane perturbation and oxidative stress are the most likely toxicity mechanisms for single wall CNTs (SWCNT) (Arias and Yang, 2009; Kang et al., 2008a; Kang et al., 2009; Kang et al., 2008b; Kang et al., 2007a; Liu et al., 2010a; Liu et al., 2010b; Vecitis et al., 2010; Yang et al., 2010; Young et al., 2012).

Several studies used cell viability as a key indicator of CNT toxicity for bacteria (Arias and Yang, 2009; Kang et al., 2007a; Olivi et al., 2013). Cell viability can be detected by culture based and non-culture based methods. Culture based methods have limitations, including the time required, an inability to detect viable but non culturable bacteria, and their application is

limited to suspended cells. It is necessary to find alternative methods, particularly non-culture based methods that can be applied under a variety of conditions.

The small sizes, large surface areas, and needle shape of CNTs are the main factors contributing to their toxicity (Buzea et al., 2007). The toxicity mechanisms include physical contact and oxidative stress (Alazzam et al., 2010; Rajavel et al., 2014; Yang et al., 2010; Young et al., 2012). However, the reaction of cells exposed to CNTs at a molecular level is not clear. To further understand the biological mechanisms by which bacteria respond to CNT insults, the interaction between cells and CNTs needs to be investigated at the cell, transcriptome, and proteome levels.

1.3. Research Goals and Approaches

The goals of this study were to identify alternative methods for examining the effects of CNTs on bacterial cell viability, to offer a method to mitigate the effects of CNTs on cell viability, and to understand molecular mechanisms of CNT-induced stress. To achieve these goals, *Escherichia coli* was used as a model organism for experiments since it has been widely used in studies related to the effects of CNTs on bacteria (Kang et al., 2007a, 2008a; Al-Hakami et al., 2013; Arias and Yang, 2009). In addition, the abundant genome and protein database of *E. coli* will benefit this research. Four different cell viability indicators were examined: plate count, galactosidase enzyme assay, LIVE/DEAD® Baclight™ assay, and RNA quantification. Cell entrapment was considered as a method to mitigate the effects of CNTs on cells. Phage shock proteins and genes responding cell membrane perturbations were the focus of studies on molecular mechanisms.

1.4. Objectives and Hypotheses

The objectives of this dissertation research are:

1. To evaluate the plate count, galactosidase enzyme assay, LIVE/DEAD® Baclight™ assay, and RNA quantification as indicators of bacterial viability in studies of SWCNT toxicity

   Hypothesis: The plate count, galactosidase enzyme assay, LIVE/DEAD® Baclight™ assay, and RNA quantification provide similar results when assessing the viability of *E. coli* exposed to SWCNTs.

2. To investigate the influence of SWCNT length on the antimicrobial activity of SWCNTs on free and entrapped cells.

   Hypothesis: The reduction in viability of free and entrapped cells exposed to long SWCNTs is greater than shorter ones

3. To examine the influence of SWCNT functional groups on the antimicrobial activity of SWCNTs on free and entrapped cells.

   Hypothesis: The reduction in viability of free and entrapped cells exposed to functionalized SWCNTs is greater than the pristine ones

4. To investigate the effect of initial bacterial cell density on the antimicrobial activity of SWCNTs on free and entrapped cells.

   Hypothesis: A high-density bacterial population resists SWCNTs better than the lower density for both free and entrapped cells.

5. To investigate antibacterial effects of CNTs on entrapped cells.

   Hypothesis: Entrapment can reduce toxicity effect of SWCNTs on *E. coli* cells.

6. To analyze the impact of CNTs on gene and protein expressions, particularly on genes of Psp operon including *pspA, pspB,* and *pspC* of *E. coli* cells after exposure to CNTs.

   Hypothesis: CNTs alter the expressions of *pspA, pspB,* and *pspC*.

1.5. Dissertation Organization

This dissertation is divided into 6 chapters. Chapter 1 (this chapter) includes background, research problems and justifications, research goals and approaches, objectives and hypotheses, and dissertation organization. Chapter 2 is a literature review that provides information about carbon nanotubes such as synthesis, properties, applications, fate and transport, and toxicity. Cell entrapment is also reviewed in this chapter. Chapter 3 is derived from a manuscript entitled "The effect of single walled carbon nanotubes on Escherichia coli: multiple indicators of viability". This manuscript is under revision for possible publication in *Journal of Nanoparticle Research*. The materials in Chapters 4, 5 and 6 are based on manuscripts that will be submitted for publication in peer reviewed journals. Chapters 4 and 5 describe the work titled "Mitigation of bactericidal effect of carbon nanotubes by cell entrapment" and "Bactericidal effect of single wall carbon nanotubes on entrapped cells is functionality dependent", respectively. The title of Chapter 6 is "Effects of carbon nanotubes on the protein and gene expression of *Escherichia coli*." Lastly, conclusions and recommendations for future work are presented in Chapter 7.

CHAPTER 2: LITERATURE REVIEW

2.1. Nanomaterials

A nanomaterial (NM) is commonly described as a material that has at least one dimension under 100 nm (Klaine, 2009). Nanomaterials have different physical and chemical properties to macroscale materials. Nanomaterials in the environment are from natural sources (e.g., clay, organic matter and iron oxides) (Klaine et al., 2008) and anthropogenic sources (Sadik, 2013). Nanomaterials from the anthropogenic sources are manufactured nanomaterials (MNM) and include: (1) carbon nanomaterials, (2) metals, (3) metal oxides, (4) quantum dots and semi-conductors, (5) nanoclays, (6) dendrimers which are multi-functional polymers, and (7) emulsions (Batley and McLaughlin, 2010).

"Nanotechnology is the understanding and control of matter at dimensions between approximately 1 and 100 nanometres, where unique phenomena enable novel applications." (NNI, 2008). Nanotechnology consists of designing, synthesizing, modifying, and manipulating nanoscale functional structures for specific applications (NNI, 2008). Nanotechnologies are booming and becoming a part of society with an estimated global economic impact in industrial, consumer and medical products of $292 billion dollars in 2010 (Tinkle, 2008). The market for nanotechnology-based products is projected to reach $3 trillion dollars globally and employ 2 million workers in the U.S. by 2020 (NSF, 2011). Many nano-based products are available commercially, such as electronics components, cosmetics, cigarette filters, antimicrobial and stain-resistant fabrics and sprays, sunscreens, and cleaning products (Invernizi et al., 2011). The widespread use of MNMs will increase the likelihood of their release into environment. Carbon nanomaterials, including carbon nanotubes, fullerenes, and amorphous carbon nanoparticles, are widely used and therefore have gained great attention related to their toxicity.

2.2. Carbon Nanotubes

CNTs are allotropes of carbon. Since their discovery in 1991 by Iijama (Iijima et al., 1991), CNTs are among the best-known and most promising nanotechonology products because of their unique physical, chemical, electrical, and mechanical properties (Smart et al., 2006). CNTs are carbon (grapheme) sheets rolled in to a cylinder with sp^2-hybridized bonds between carbon atoms (Hirlekar et al., 2009).

The first generation of CNTs was built from two to fifty graphene sheets (multiple walled carbon nanotubes; MWCNTs) (Iijima et al., 1991) (Fig. 2-1). Single walled carbon nanotubes (SWCNTs) that have walls built from one graphene sheet were discovered later (Iijama et al., 1993) (Fig. 2-1). There are three types of CNT chiralities (structures): zigzag, armchair, and chiral, depending on the direction that the graphene sheet is rolled (Fig. 2-2).

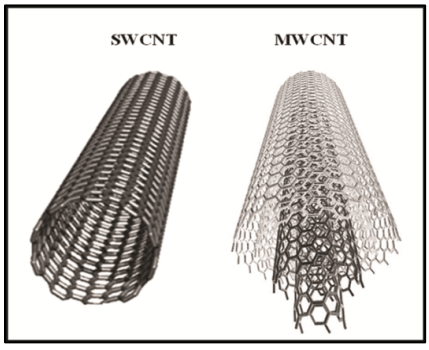

Figure 2-1: Schematic diagrams of SWCNT and MWCNT (Choudhary and Gupta, 2011).

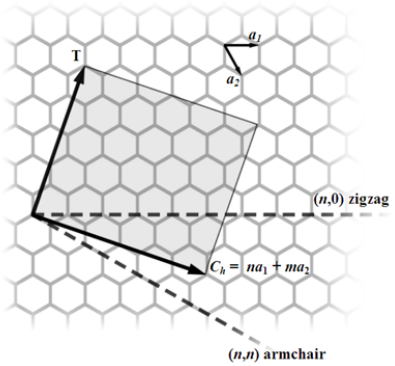

Figure 2-2: Structure of 2d grapheme sheet is shown along with the vector, which specifies the chiral nanotube (Dresselhaus et al., 2002).

2.2.1. Synthesis Methods

2.2.1.1. Arc discharge synthesis

Iijima first observed CNTs during an arc discharge in 1991. The arc discharge method is used to produce both SWCNTs and MWCNTs. A low voltage (~12 to 25V) and high current power supply (50 to 120 amps) are used in this method (O'Connell, 2006). A direct current arc voltage is applied across two graphite electrodes immersed in an inert gas of 100 to 1000 Torr of He or Ar. A metal catalyst is added to the anode for SWCNTs synthesis. The commonly used catalysts are Fe, Co, Ni, Y or Mo (Iijima, 1991; O'Connell, 2006). CNTs produced from the arc discharge method are inexpensive but need extensive purification.

2.2.1.2. Laser ablation synthesis

In 1995, Guo and co-workers first produced CNTs on a large scale using a laser ablation technique (Guo et al., 1995). CNTs are manufactured by using a high power laser to vaporize carbon from a graphite composite target (1.2% cobalt/nickel and 98.8% carbon) at a high temperature. An inert gas such as Ar or He, at a pressure of 500 Torr, in a 1200^{o}C quartz furnace is used as the atmosphere for the reaction (Thess et al., 1996). Both SWCNTs and MWCNTs can

be produced by this method. Similar to the arc discharge method, a metal catalyst must be added to the graphite target to produce SWCNTs. This method achieves a high yield of CNTs that are purer than those produced by the arc discharge method.

2.2.1.3. Thermal synthesis

2.2.1.3.1. Chemical vapor deposition

In 1993, Endo first reported the production of MWCNTs by using a chemical vapor deposition technique (CVD) (Endo et al., 1993). Three years later, SWCNTs were produced successfully by using an adapted carbon monoxide-based CVD (Dai et al., 1996). Gaseous carbon feedstock is fed through quartz tubes at medium to high temperature (550-1200°C). The hydrocarbons are broken to produce the pure carbon molecules that will diffuse toward the heated substrate that is coated with a catalyst such as Ni, Fe, or Co. The carbon molecules will bind and form CNTs. Either SWCNTs or MWCNTs will be formed depending on the generated temperature. A large-scale high purity production can be achieved by using this technique.

2.2.1.3.2. High-pressure carbon monoxide synthesis

High-pressure carbon monoxide synthesis is a technique related to CVD that provides high-quality, high-quantity, and narrow-diameter distribution SWCNTs. This technique was first developed at Rice University in 1999 (Nikolaev et al., 1999). Catalyst reaction is in a gas phase after a catalyst and a hydrocarbon gas are fed in a furnace. Carbon monoxide gas is used as a hydrocarbon gas and at 900 to 1100°C, at a pressure of 30 to 50 atm, reacts with $Fe(CO)_5$ or $Ni(CO)_4$ to form SWCNTs. SWCNTs can be generated continuously; therefore, SWCNTs can be produced on a large scale by this technique.

2.2.1.3.3. Flame synthesis

CNTs are generated in a flame environment that is fed with inexpensive hydrocarbon fuels and a metal catalyst (Vander-Wal et al., 2001, 2002). Common used hydrocarbon fuels are methane (CH_4), ethylene (C_2H_4), and acetylene (C_2H_2). The metal catalyst (Co, Fe, or Ni) inserted in the flame forms small aerosol metal catalyst islands that provide the sites for deposition of solid carbon. The catalyst particle size and carbon deposition rate control the formation of carbon nanotubes (MWCNTs and/or SWCNT) downstream.

2.2.1.3.4. Plasma enhanced chemical vapor deposition

Plasma enhanced chemical vapor deposition (PECVD) is considered to be the most promising way to produce uniform, vertically aligned CNTs (Mauger et al., 2006; Meyyappan et al., 2003). PECVD is a general term encompassing several different synthesis methods such as hot filament PECVD (Ren et al., 1998), microwave PECVD (Bower et al., 2000), glow discharge PECVD (Chhowala et al., 2001; Merculov et al., 2000), and inductively coupled plasma PECVD (Delzeit et al., 2002). In the PECVD, nanotubes are only generated where the catalyst is located on the substrate. Therefore, CNTs can be specifically positioned on the substrate. This has been enabled the use of CNTs in microelectronic field applications such as emission devices.

2.2.2. Properties and characteristics

2.2.2.1. Electronic property

The electrical properties of CNTs depend on four parameters: chirality, curvature, diameter, and applied magnetic field along the cylinder axis (Su et al., 2011). Therefore, how the graphite sheets roll up and tube size will affect the electronic properties. The structure of CNTs can be defined by two indices, labelled n and m. Based on the value of (n-m), either semiconducting or metallic tubes can be determined. Tubes that have (n-m) of zero or

multiple of 3, are called metallic nanotubes. Metallic nanotubes have electrons in their conductive bands at room temperature, and conduct electricity well. The remaining nanotubes, which are semiconducting, have band gaps between 0.5 and 3.5 electron Volts.

Electrons easily flow through CNTs. The electrical resistance of individual CNTs is similar to copper wires of the same size. In bundles, electrons move in the tubes and sometimes jump to other tubes. Carbon nanotube ropes have a resistivity of 10^{-4} ohm-cm at room temperature (Thess et al., 1996). Therefore, they are considered as the most electrically conductive fibers known.

2.2.2.2. Thermal property

Prior to CNTs, pure diamond was known for having the highest thermal conductivity. The thermal conductivity of pure diamond is 2000-2500 $Wm^{-1}K^{-1}$, while for copper it is 400 $Wm^{-1}K^{-1}$. For an individual carbon nanotube, the thermal conductivity is about 3000 $Wm^{-1}K^{-1}$ (Dresselhaus et al., 2002). The thermal transport also depends on the temperature, and the tube diameter (Dresselhaus et al., 2002).

2.2.2.3. Mechanical property

CNTs have unique mechanical properties. Their stiffness is larger than that of any other known materials. The Young's modulus is up to 1.4 TP (Yu et al., 2000). The tensile strength is up to about 50 GPa (Walters et al., 1999), while the Young's modulus and tensile strength of high-strength steel are around 200 GP and 1-2 GPa, respectively. Therefore, CNTs are considered as the stiffest fibers.

2.2.3. Functionalization of carbon nanotubes

Pristine CNTs are chemically inert and incompatible with most of organic and inorganic solvents (Zhang et al., 2010). This has limited CNTs in the desirable applications.

Functionalization of CNTs is a promising way to overcome this drawback (Chen et al., 2012). Carbon nanotubes can be derived both covalently and non-covalently. Covalent functionalization is a procedure to generate carboxylic groups or carboxylated fractions on the tube by highly oxidized carbon atoms on the sidewalls or at the end of CNTs. The derived groups then can be modified by amidation or esterification (Sun et al., 2011). Many polymers (Sun et al., 2011), metals (Lordi et al., 2001), and biological molecules (Huang et al., 2002) can be anchored on the surface of CNTs through these bridges. The advantage of covalent functionalization is that it is robust and controlled, and can therefore be used in multiple functionalization (Zhang et al., 2010).

For non-covalent functionalization, molecules adhere to the CNT sidewall, such as wrapping of polymers around CNTs (Star et al., 2001), or the loading material is grafted to the surface of CNTs by the interaction between π aromatic rings of functional groups and π of electrons associated with the graphite sheets (Chen et al., 2002; Petrov et al., 2003). Functionalized CNTs show increased solubility and improved biocompatibility (Chen et al., 1998a; Zhang et al., 2010). Therefore, applications of functionalized CNTs attract more interest.

2.2.4. Applications

2.2.4.1. Electronics

2.2.4.1.1. Field emissions

Due to the high electrical conductivity, the sharpness of the tubes, and the high ratio of height to diameter, CNTs are the best field emitter of any known sources (Eletski et al., 2010). Electric fields of millions of Volts cm^{-1} can be generated near the tip when a few volts are applied to an electrode (that is a few microns from the nanotube tip). Over 4 amp/cm^2 could be produced from CNTs based cathode electron emitters, and the current is stable (Wei et al.,

2001). The CNT based electron field emitters can be exploited to develop new types of vacuum electronic devices such as the flat panel displays (Mauger et al., 2006; Sohn et al., 2001; Wang et al., 2001), cathode ray tubes (Saito et al., 2000), X-ray sources (Yue et al., 2002) and microwave radiation sources and amplifiers (Kawakita et al., 2006; Teo et al., 2005).

2.2.4.1.2. Transparent conductive CNT films

CNTs can form thin films that are highly conductive and almost transparent. The thickness of these films is about 50 nm. The transparent conductive CNT films are considered as a promising candidate that could replace the indium tin oxide (ITO) films that have been used widely. The CNT films are more flexible, durable, stretchable, and easy to manufacture than the ITO films (Hecht et al., 2011). Therefore, films have desirable applications for multiple types of touch screens in games, portable computers, cell phones, personal digital assistant, and many others. They are also ideal for large area transparent conductors such as liquid crystal displays (LCDs), plastic solar cells, and the organic lighting.

2.2.4.1.3. Printable transistors

The mass production of large area flexible electronic circuits with low cost has been achieved by using a novel technology named printable flexible electronics. The unique properties of CNTs such as semiconducting, high mobility, high on/off ratio, and small operation voltage (Javey et al., 2003; Kang et al., 2007b) make them ideal materials for creating printable transistors (Artukovic et al., 2005; Bradley et al., 2003; Snow et al., 2003). Schindler et al. (2007) reported that the mobilities of CNT-based transistors employing a sparse nanotube network reached 1 cm^2/V-s, while CNT-based transistors using an aligned array of single-walled nanotubes achieved the mobilities as high as 480 cm^2/V-s (Kang et al., 2007b). Due to the unique current carrying capacity of CNTs, the organic light emitting diode (OLED) displays

manufactured from CNT thin film transistors (TFTs) have a higher resolution than that of organic TFTs.

2.2.4.2. CNT composites

Due to their exceptional mechanical properties, CNTs, considered as the stiffness fibers, are excellent load-bearing reinforcements in composites (Zu et al., 2013). The applications of carbon nanotubes of superior mechanical properties as toughening agents in polymer, ceramic, or metal matrix composites have been getting attention. By using CNTs to reinforce polymer films, the polymer's mechanical properties, thermal stability, and gas barrier properties were improved compared to pure polymer films (Njuguna and Pielichowski, 2003). CNTs play the role of a nucleating agent that provides a template to improve the polymer orientation. Chae et al. (2007) reported that the composite of 1 wt % of CNTs and polyacrylonitrile (PAN) increased the tensile strength and modulus of the resulting carbon fiber by 64% and 49%, respectively. Silicon glass rods, synthesized from surfactant-CNT co-micelles as templates, were added to inorganic ceramics. About 100% enhancement on hardness in the presence of 6 wt% of CNTs was observed (Hwang et al., 2001).

Hyperion, an auto body and paint company, has used the composites of MWCNTs in epoxy resin for electrostatically applying paint onto car components (Baughman et al., 2002). The composites achieve percolation at loadings of 0.01%. Another use of nanotubes composites is as antistatic shielding on airplane wings and fuselages, tennis rackets, aircraft body parts, and bicycle rims.

2.2.4.3. Energy

Large surface area, good electrical conductivity, chemical stability in acidic environment, and low resistivity make CNTs suitable for applications in electrochemistry. CNTs are effective materials for electrodes in batteries, capacitors, and fuel cells. Gao et al. (2000) reported that CNTs have the highest reversible capacity of any carbon material for use in lithium-ion batteries (Gao et al., 2000; Frackowiak et al., 2002). CNTs improve the conductivity of the electrode and the electrolyte penetration into the electrodes, and enable the electrodes to maintain their mechanical integrity during the charge-discharge cycles as they absorb and desorb lithium ions (Endo et al., 2004).

2.2.4.4. Life sciences

Functionalized CNTs have several potential applications such as biosensors, drug and vaccine delivery devices, medical treatment, and tissue engineering. Cancer treatment is the prominent potential clinical application of CNTs including antitumor chemotherapy, antitumor immunotherapy, and antitumor hyperthermia therapy. The high surface area of CNTs results in effective loading of chemotherapy drugs (Liu et al., 2007). The permeability and retention effect of CNTs with drugs are enhanced (Cho et al., 2008); therefore CNT loading drugs can get in to the tumor tissues over time and keep the drug concentrations in tumor higher than plasma (Liu et al., 2007). CNTs have the ability to translocate across the cell membranes and enhance the immune response when attached to an antigen. Therefore, CNTs are a good candidate for vaccine delivery tools that may be applied in antitumor immunotherapy (Salvador-Morales et al., 2006).

The efficacy of antitumor immunotherapy in mouse liver tumor was enhanced by conjugate of MWCNTs and tumor cell vaccine (Meng et al., 2008). Due to the ability of strong absorbance in the near-infrared region (NIR; 700-1000) (O'Connell et al., 2002), CNTs can

be applied for optical imaging inside living cells (Welsher et al., 2008). Another application of the NIR absorbance is a local thermal ablation of tumor cells by excessive heating of SWCNTs (in tumor cells) (Kam and Dai, 2005). High sensitive detecting devices are another potential application of CNTs in viral disease therapy. A biosensor made of Au nanoparticles and SWCNTs has been studied for detecting HIV-1PR (Mahmoud and Luong, 2008). CNTs also can be used to reinforce the mechanical strength of tissue scaffolding that is applied in tissue engineering (Bhattacharyya et al., 2008).

2.3. Fate and Transport of CNTs in Environment

Increasing the commercial products related CNTs might lead to the negative consequences after their release to the natural environment. Many studies reported the potential pathways of CNTs in various matrices such as air, soil, water, and sediment (Gottschalk et al., 2009; Gottschalk et al., 2010; Mueller and Nowack, 2008).

2.3.1. Release pathway of CNTs to environment

2.3.1.1. Polymer CNT composites

One of the main sources of CNT release into environment is CNT composite based products. Most of the commercial products related to CNTs are made in polymer/CNTs based composites while CNT-containing products that are expected in biomedical applications are not commercially available yet (Petersen et al., 2011). CNTs may be released during manufacturing as an air-borne contaminant during handling of CNT dry powder (Nowack et al., 2013) and blending with polymer to prepare CNT composites (Han et al., 2008). CNTs from these products are also released to the environment during their life cycles (Petersen et al., 2011). CNTs in CNT based products are likely released during use and discharge through mechanical pathways (abrasion, scratching, sanding, washing, and diffusion), degradation, and incineration.

Harsh conditions such as ultraviolet (UV) radiation, moisture, high temperature, or ozone also speed up the CNT emission.

2.3.1.2. Wastewater treatment plants

CNTs may end up in wastewater treatment plants (Gottschalk et al., 2010; Mueller and Nowack, 2008; Nowack et al., 2013). CNTs get in to the sewer system mainly from manufacturing use, degradation of CNT-based textiles (Kohler et al., 2008), and research and development sources (Gottschalk et al., 2010). However, new applications of CNTs may reveal more sources that release CNTs to wastewater (Petersen et al., 2011). CNTs in wastewater treatment facilities may have effects on the activity of microbial/sludge communities and in turn the treatment efficiency.

2.3.2. Environmental transport

The mobility and colloidal stability of CNTs influence their impact on ecosystems as CNTs are released to environment (Petersen et al., 2010). It is important to understand potential CNT migration through different matrices in the environment.

2.3.2.1. Mobility in the subsurface environment

CNT mobility depends on the physicochemical properties of CNTs and environment chemistry (Zhang et al., 2011). The interaction among the CNTs (sorbate), the porous media (sorbent) and the solution determined the CNT behavior in the environment. Therefore, the shape of CNTs (Jaisi and Elimelech, 2009; Jaisi et al., 2008), presence of organic matter, surfactants, and bio-macromolecules (Bouchard et al., 2012; Jaisi and Elimelech, 2009; Jaisi et al., 2008; Saleh et al., 2010; Wang et al., 2008), surface oxidation (Yi and Chen, 2011), pore water velocity (Liu et al., 2009b) and porous media grain size (Mattison et al., 2011) play an important role in the fate and transport of CNTs.

Jaisi et al. (2008) reported that the shape of SWCNTs limited their flow through porous media. Organic matter containing both negative and positive charge and the charges of the functional groups of CNTs affected the electrostatic interaction that mainly determined the transport of CNTs in soil (Zhang et al., 2011). Wang et al. (2008) reported that the increase of stability and mobility of SWCNTs in the porous media were observed with the presence of humic acid. A similar trend was observed with MWCNTs when dissolved organic matter (DOM) was present (Petersen et al., 2011; Zhang et al., 2010). CNT stability and mobility through the porous media (Bouchard et al., 2012) and water (Han et al., 2008) are enhanced in the presence of sodium dodecylsulfate. Due to the steric repulsion, biomacromolecules and humic acids are effective in stabilizing and mobilizing of CNTs (Saleh et al., 2008; 2010). Liu et al. (2009) reported that the mobility of CNTs increased with increasing pore water velocity.

2.3.2.2. Aggregation and colloidal stability

Aggregation and colloidal stability play an important role in the fate and transportation of CNTs in the aquatic systems (Holbrook et al., 2010; Lin et al., 2010; Schwyzer et al., 2011). The aggregation of CNTs controls their mobility, biocompatibility and sedimentation rate in natural aquatic systems (Chen et al., 2010; Pertersen et al., 2011). Functional groups influence their aggregation behavior. Pristine CNTs that are highly hydrophilic tend to aggregate and accumulate in the environment. Functionalization or employing surfactants are routes to enhance the CNT dispersibility in the aqueous solutions. The aggregation kinetics of CNTs is also determined by the solution chemistry and the presence of natural organic matter in the aquatic systems. Saleh et al. (2008) reported that dispersibility of CNTs increased with increasing pH of the solution from acidic (3) to basic (11). The authors also found that humic acid and polysaccharides enhanced the CNT stability in the solution.

2.3.3. Transformation in environment

Most of the studies on CNT transformations in the environment are in vitro studies that investigated chemical reactions. However, the information provided potential routes that CNTs may transform in the natural environment. There are two ways for transformation to take place, covalent reactions and biodegradation.

2.3.3.1. Covalent reactions

The CNT surface structure is inert in general. However, the sidewalls contain defect sites such as pentagon-heptagon pairs called Stone-Wales defects, sp3 – hybridized defects, and vacancies in the nanotube lattice (Hirsch et al., 2002). The end caps and the defects on the sidewalls are expected to be sites susceptive to oxidation (Niyogi et al., 2002).

Chemical oxidation of CNTs needs strong oxidative forces such as concentrated HNO_3 (Hu et al., 2005) mixtures of concentrated HNO_3/H_2SO_4 (Schierz et al. 2009), $KMnO_4/H_2SO_4$, $K_2Cr_2O_7/H_2SO_4$ (Zhang et al. 2003), OsO_4 (Niyogi et al., 2002), and H_2O_2/H_2SO_4 (Kuznetsova et al., 2001) and strong energy inputs but these conditions do not often occur naturally in the environment. However, oxidants used in wastewater treatment are effective in oxidizing CNTs, such as ozone (Banerjee et al., 2004; Hemraj-Benny et al., 2008), Fenton's reagent (Li et al., 2005; Wang et al., 2007; Ying et al., 2003), and photo-Fenton's reagent (Fan et al., 2007). Reactive oxidants species (ROS) such as O_2, O_2^-, and $^{\bullet}OH$ can modify the CNT surface under the sunlight or lamps (Chen et al., 2010). After being oxidized, the end caps are opened and oxygen-containing surface functional groups such as carboxyl, hydroxyl, carbonyl, and ester attach on either the ends or the sidewalls of the tubes (Escobar et al., 2009; Fan et al., 2007; Kuznetsova et al., 2001; Li et al., 2005; Wang et al., 2009). The aromatic ring system of CNTs

was also disrupted in strong oxidation processes (Kuznetsova et al., 2001). The common results of these processes are increasing surface charge and stability in water.

2.3.3.2. Biodegradation

Soil enzymes such as horseradish peroxidase can transform carboxylated SWCNTs via mediation. The results of this transformation are the SWCNT length reduction, more carboxyl groups on the sidewalls, and release of CO_2 (Allen et al., 2008). SWCNTs were degraded by the neutrophil myeloperoxidase, a peroxidase of human cells. After the degradation, no inflammatory response into the lung of mice was observed (Kagan et al., 2010). A phagolysosomal stimulant, a membrane-enclosed organelle forming when a phagosome fuses with lysosome, also degraded carboxylated SWCNTs in 90 days. After the degradation, the SWCNT length shortened and ultrafine solid carbonaceous debris were found (Liu et al., 2010b). Therefore, the potential degradation pathways of CNTs in the natural environment may diminish their environmental risks.

2.4. CNTs Toxicity

With the increase of CNT applications, the potential hazard of CNTs to the human health and environment has been getting more attention.

2.4.1. Factors contributing to toxicity of CNTs

2.4.1.1. CNT size

Physicochemical properties such as the size and surface area are the factors determined the toxicity of CNTs (Podila and Brown, 2013). The smaller-sized and functionalized CNTs could facilitate particles translocating through the cellular barriers and entered easily into a wide range of cells (Lacerda et al., 2007) or the biological systems (Panyam et al., 2003). The large aggregates of MWCNTs were formed in the living tissue without any transport, while the

smaller SWCNTs were phagocytosed by macrophages and translocate to the local lymph node (Fraczek et al., 2008). Oberdorster et al. (1994) reported that the smaller-sized CNTs exhibited more pulmonary toxicity. CNTs with an average size of 80 nm exhibited less translocation and accumulation than that of 20 nm CNTs in mouse (Kreuter, 2007).

2.4.1.2. CNT shape

The tubular structure of CNTs could facilitate CNTs transport through capillaries and adhesion on blood vessel of rat. The results were stimulation platelet aggregation and acceleration of the rate of vascular thrombosis (Radomski et al., 2005). The length of CNTs also influences the toxicity.

2.4.1.3. CNT surface area

The surface charge of CNTs can affect their agglomeration and translocation (Vaisman et al., 2006). The surface charge also plays a role in cellular uptake and cytotoxicity. Acid-functionalized SWCNTs exhibited more embryo toxicity than pristine SWCNTs (Saxena et al., 2007). SWCNTs have a tendency to aggregate into bundles due to van der Waals forces. This might impact their toxicity; for example, aggregates with a much larger diameter than a SWCNT could deposit in an organ with a different anatomic pattern when compared to a SWCNT. Wick et al. (2007) reported that larger aggregates had an increased toxicity compared to the smaller bundles of SWCNT when testing with a lung cell model (Mesothelioma cell line MSTO-211H).

2.4.2. CNT toxicity on human and mammals

The CNT nano scale size leads to larger area per mass unit compared with the larger particles; therefore, they are easy to enter human body and more biologically active (Oberdorster et al., 2005). Large surfaces also enhance their ability to adhere to other molecules, including pollutants, facilitating their transport in the environment (Kleiner and Hogan, 2003).

Additionally, CNTs have potential to become airborne. A variety of aerosol types was produced by different SWCNT synthesis methods (Maynard et al., 2004). Therefore, the toxicity potential of each type of CNTs has to be researched individually.

Huczko et al. (2001) found that CNTs had no effect on the pulmonary function of guinea pigs. Subsequent studies showed that CNTs could induce pulmonary pathology in guinea pigs, or induce inflammation of the lung tissue of mice (Warheit et al., 2004). Warheit et al. (2004) showed that 15% of rats died within 24 h of exposure to SWCNTs. A study published by the U.S. National Institute for Occupational Safety and Health found that human keratinocyte cells were damaged after exposure to CNTs (Shvedova et al., 2003). SWCNTs were taken up by macrophage cells (Cherukuri et al., 2006) and evoked an oxidative stress within hours (Kagan et al., 2006). However, other studies showed that SWCNTs had very low toxicity to human lung cells (Davoren et al., 2007). Human epidermal keratinocytes took up MWCNTs in vacuoles and reduced 20% of the cell viability after 24-hour exposure to 400 μg/ml MWCNTs. Interleukin (IL)-8 also was detected up to 6 times compared with control cell cultures (Monteiro Riviere et al., 2005). MWCNTs induced the cell cycle arrest and increased apoptosis and necrosis of human skin fibroblast cells (Ding et al., 2005).

2.4.3. CNT toxicity on plants, invertebrates, and vertebrates

There are number of studies reported that CNTs also affect the plants and plant cells. Pristine CNTs enhanced the root elongation of onion but inhibited that of tomato (Canas et al. 2008). Khodakovskaya et al. (2009) observed the increase of germination and growth of seedling in tomato with the presence of CNTs. MWCNTs reduced the cultured rice cell density. MWCNTs caused apoptosis and necrosis at low and high concentrations, respectively

(Tan et al.,2007, 2009). The endonucleolytic cleavage of DNA from Arabidopsis protoplast cells exposed to SWCNTs was observed (Shen et al., 2010).

CNTs have potential for transport in the natural environment; therefore impact of CNTs on ecosystems is possible. CNTs are expected to enter the aquatic environment. Due to the hydrophobic and non-biodegradable properties (Donaldson et al., 2006), CNTs can accumulate in aquatic biota and may affect the aquatic organism health. The hatching of zebrafish (*Danio rerio*) embryos was induced in the presence of pristine CNTs (Cheng et al., 2007). The larvae of the second generation had a lower survival rate (Cheng et al., 2009). *Daphnia magna* could ingest the lysophophatidylcholine coated CNTs (Roberts et al., 2007). CNTs were also found on the external surface of *D. magna* (Roberts et al., 2007), or on the gill of fish (Mouchet et al., 2008).

2.4.4. CNT toxicity on bacteria

CNTs exhibited bactericidal activity. Chung et al. (2011) reported that high concentrations of MWCNTs reduced the microbial activity and biomass (C and N) in soils by inhibiting enzyme activities such as 1,4-β-glucosidase, cellobiohydrolase, xylosidase, 1,4-β-N-acetylglucosaminidase, and phosphatase. The change in activity of soil microorganisms may have an effect on ecosystem functions. Goyal et al. (2010) carried out a study on the effect of SWCNTs on activated sludge. Members of three families, *Sphingomonadaceae, Cytophagaceae,* and *Zoogloea*, that are important in activated sludge communities were studied. SWCNTs had more negative impact on the spingomonad in term of the phylogenic intensity than the other two groups. SWCNTs adversely affected the soil microbial communities that involved in the carbon and phosphorous biogeochemical cycles (Rodrigues et al., 2013).

CNTs inhibited the survival rates of the human bacteria. The effects are influenced by the length and surface functional groups of CNTs and the shape of bacteria (Chen et al., 2013). In addition, CNTs antimicrobial activity was enhanced by combining with other factors such as microwave radiation or near-infrared radiation (NIR). Ninety eight percent of *E. coli* K12 cells were inactivated after exposure to CNTs combined with microwave radiation (Al-Hakami et al., 2013). The reduction in viability of *Bacillus anthracia* spores and *Samonella* cells were observed after exposure to CNT-NIR (Dong et al., 2013; Mamouni et al., 2011).

Functionalized CNTs exhibited the antibacterial ability. Arias and Yang (2009) reported that CNTs with different surface groups (-OH and -COOH) inactivated bacterial pathogens. Incubation of *Salmonella* cells with 200-250 μg/ml SWCNTs (-OH and -COOH) for 15 min completely inactivated 10^7 cfu/ml. However, MWCNTs (-OH and -COOH) did not show any significant toxicity to bacterial cells at concentrations up to 875 μg/ml. The surface functionalization has an indirect effect on the CNT toxicity through the impacts of the CNT aggregation (Pasquini et al., 2012).

Akasaka and Watari (2009) reported that CNTs (SWCNTs and MWCNTs) could capture bacteria. CNTs exhibit strong adhesion to bacterial cells and may be used to eliminate oral pathogens. Kang et al. (2007a, 2008b) investigated the effects of SWCNTs and MWCNTs on *E. coli* K12 cells. Direct contact between both types of CNTs and the cells caused cell lysis leading to alterations of cell morphology and mortality. MWCNTs have more effect when they were short, uncapped and functionalized. The mechanical disruption of the cell membrane and biochemical changes may account for the antimicrobial activity of CNTs (Zarubina et al., 2009). It was observed that after 4 days of incubation of *E. coli* K12 with SWCNTs, the cell surface changed and cytoplasm was lost partially. The intensity of oxygen consumption and bacterial

luminescence intensity decreased substantially. Enzyme leaking was an evidence of the cell membrane damage after exposure to CNTs (Amarnath et al., 2012).

2.5. Entrapped Cells

Immobilized cells are cells that are attached to or entrapped in an inert support (Wijffels et al., 2000). Methods used to immobilize the cells include adsorption, covalent bonding, crosslinking and entrapment. One of the frequently used methods for microbial cell immobilization is cell entrapment in matrices. In the entrapment, the microbial cells are enclosed in a rigid network to prevent the cells from releasing into the surrounding media. The network is porous to allow the diffusion of substrates and products (Park and Chang, 2000). The entrapment process starts with the suspended microbial cells in a solution of the matrix. Based on the type of reactors, the entrapment may be formed to different shapes such as the spheres, film fibers, or cylinders.

Common matrices used for cell entrapment include hydrogels (alginate, k-carrageenan, and chitosan), thermogels (agar, agarose, and cellulose), and synthetic polymers (polyvinyl alcohol, polyurethane, and polyacrylamide) (Hung et al., 2008; van der Sluis et al., 2000). The ideal characteristics of the entrapment matrix are insoluble, biocompatible, high mechanical and chemical stability, and non-biodegradable (Leenen et al., 1996; Smidsrød and Skjåk-Braek, 1990; Van Veen et al., 1997).

Sodium alginate, a natural hydrogel, is one of the most common cell entrapment matrices. Sodium alginate is extracted from the cell walls of brown algae (*Laminaria*). Sodium alginate comes in white powder and is soluble in water. The structural unit of sodium alginate is a flexible chain formed by the coordination between alginate and sodium. The molecular formula and weight of sodium alginate are $(C_6H_7O_6Na)n$ and 198.11, respectively (Fig. 2-

3). The melting, boiling and flash points of sodium alginate are >300°C, 495.2°C (at 760 mm Hg) and 211.1°C, respectively. The whole microbial cells are mixed with the water-soluble alginate. The mixture then is dropped into a calcium chloride solution in which alginate beads are formed. During the bead formation, sodium is replaced by calcium, and each calcium ion coordinates with two alginate chains and forms an egg box structure (Fig. 2-4) (Smidsrød and Skjåk-Braek, 1990).

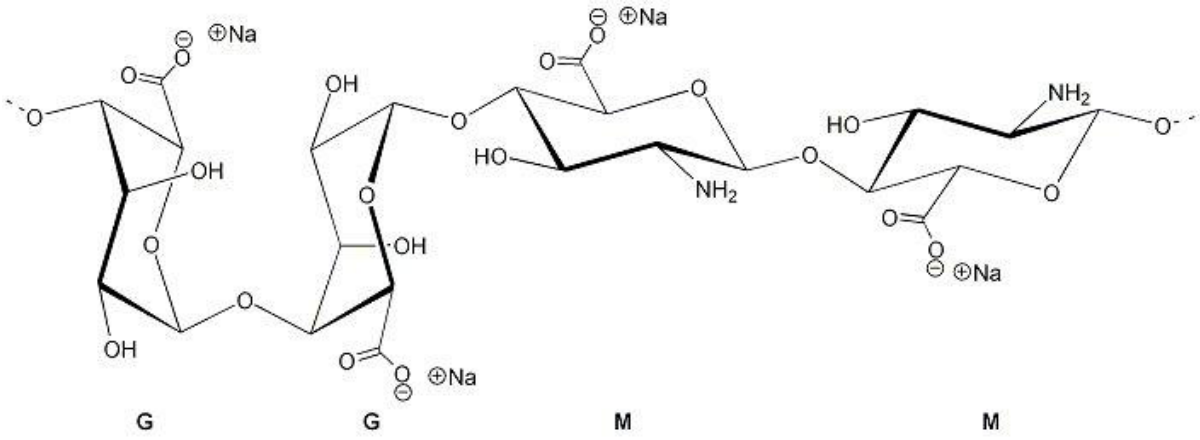

Figure 2-3: Structure of sodium alginate (Smidsrød and Skjåk-Braek 1990).

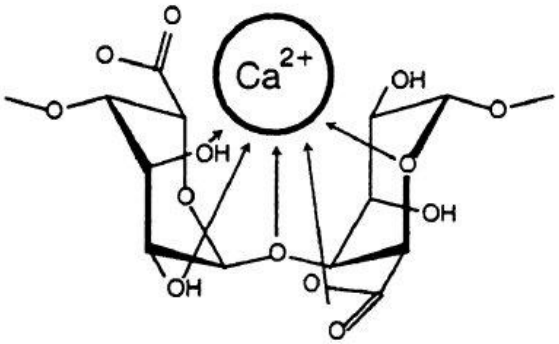

Figure 2-4: Structure of calcium alginate (Smidsrød and Skjåk-Braek 1990).

Another commonly used entrapment material is polyvinyl alcohol (PVA) because of its low cost and strong gel strength (Hashimoto et al., 1987). Raw PVA is a white, free-flowing granule and moderately soluble in water. The properties of PVA are based on the polymer chain

length (molecular weight) and degree of hydrolysis. PVA is a polymer of about 2,000-vinyl alcohol units when dissolved in water (Fig. 2-5). The cell entrapment process begins with the mixture of the solution of water-soluble PVA and suspended microorganisms. The mixture is dropped in to a boric acid solution resulting in formation of a viscoelastic gel that creates by PVA-boron cross-linkage (Fig. 2-6). In a phosphorylated PVA entrapment method, the gels are then placed in an orthophosphate solution. Phosphate groups are incorporated in to PVA resulting in enhanced surface gel strength without affecting other PVA gel properties. The structure of phosphate bonded PVA is presented in Figure 2-7 (Sreenivasan et al., 2004; Wu and Wisecarver, 1992).

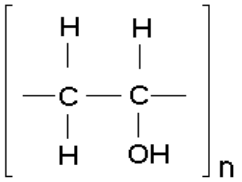

Figure 2-5: Structure of PVA.

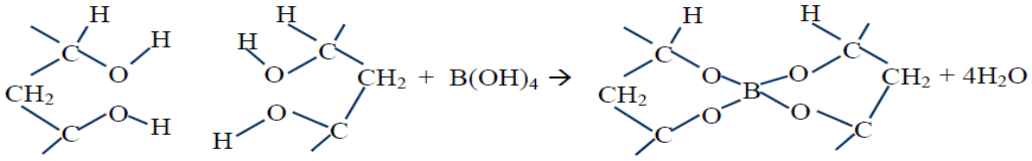

Figure 2-6: Structure of PVA-boric acid gel.

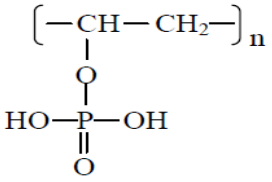

Figure 2-7: Structure of phosphate bonded PVA (Sreenivasan, 2004).

Entrapped cell systems have technical and economical advantages over free cell systems such as an ability to separate cell mass from the liquid for possible reuse, reactor productivity enhancement, lower cost of downstream processing, and protection of cells from shear damages (Galazzo et al., 1990; Groboillot et al., 1994 Kierstan et al., 1977; Zang et al., 1989). Therefore, the microbial cell entrapment is one of the most widely used biotechnologies in food and pharmaceutical fields.

The uses of the entrapped cells in environmental fields have been mainly for remediation and treatment of contaminated soil and water (Hu et al., 1994; Zhon et al., 1993). Entrapped *Rhodococcus chlorophenolicus* cells in alginate biodegraded pentachlophenol more effectively than the free cell inoculation (Salkinoja-Salonen et al., 1989). Entrapped cell systems have been used to treat specific pollutants such as phenol, sulfate, dye, and toxic heavy metals (Chen et al., 1998; Kuo and Shu, 2004; Leung et al., 2000) in wastewater. Cells entrapped in polyurethane have been used in the groundwater remediation (Hu et al., 1993; Tampion et al., 2001). Activated sludge cell entrapment has been studied and applied in sewage treatment plants to remove nitrogen (Chen et al., 1998b).

The prominent applications of cell entrapment are in pharmaceutical industry for production of steroids and antibiotics. A variety of antibiotics including penicillin G, bacitracin, actinomycin D, candicidin, patulin, neomycin and cyclosporin A have been produced by using entrapped cells (Chun and Agathos, 1993; Constantinides and Mehta, 1991; Dalili and Chau, 1988; Deo and Gaucher, 1984; Deo and Gaucher, 1985; Morikawa et al., 1980; Park et al., 1994).

In food industry, cell entrapment is commonly used for fermentation and enzyme production. It has been used for ethanol production in order to decrease the inhibition of the high product concentrations resulting in yield increases and cost reduction (Julianna et al.,

2013; Najafpour et al., 2004). Entrapped cells have been successfully used to produce enzymes such as α-amylase, glucoamylase, chloroperoxidase, lipase, xylanase, invertases and proteases (Ariga et al., 1991; Carmichael et al., 1986; Federici et al., 1990; Ghosh and Nanda, 1991; Hasal et al., 1992; Grozeva et al., 1993; Johri et al., 1990). Entrapment cells have been also used to produce amino acids and organic acids (Brodelius et al., 2001).

CHAPTER 3: THE EFFECT OF SINGLE-WALLED CARBON NANOTUBES ON *ESCHERICHIA COLI*: MULTIPLE INDICATORS OF VIABILITY

3.1. Background

CNTs are extensively commercialized and widely used nanomaterials because of their outstanding physical, chemical, and mechanical properties, including high tensile strengths, ultra-light weight, thermal and chemical stability, and metallic and semi-conductive electronic properties (Ajayan and Ebbesen, 1997; Dresselhaus et al., 2002; Gwon et al., 2012; Smart et al., 2006; Yu et al., 2000). Increasing commercial demand for CNTs will inevitably lead to their increased presence in the environment because of point- and non point-source pollution. After entering the environment, CNTs may agglomerate and persist in solutions (Saxena et al., 2007). Research on the environmental impacts and fate of CNTs has not kept pace with the rapid development of the technology.

Most research to date has focused on the impact of CNTs on human health (Arias and Yang, 2009; Cavallo et al., 2012; Delogu et al., 2012; Patlolla et al., 2010a; Patlolla et al., 2010b; Simate et al., 2012; Ursini et al., 2012), and less is known about their environmental impact. Many bacterial species are critical to element cycling and remediation of environmental pollutants, and damage to these beneficial bacteria by CNTs could negatively impact the environment and ecosystems. High concentrations of CNTs reduce microbial activity and biomass (C and N) in soils by inhibiting the activity of enzymes including 1,4-β-glucosidase, cellobiohydrolase, xylosidase, 1,4-β-N-acetylglucosaminidase, and phosphatase (Chung et al., 2011). It has been shown that such affects by CNTs also can negatively impact microbial communities in activated sludge used in wastewater treatment (Goyal et al., 2010).

Physicochemical properties of CNTs can affect their toxicity for bacterial species. Functional groups have varying effects on toxicity; for example, –OH and –COOH are more toxic than $–NH_2$ (Arias and Yang, 2009). Other toxic functional groups include n-propylamine, phenylhydrazine, hydroxyl, phenydicarboxy, phenyl, sulfonic acid, and 1-octadenol (Al-Hakami et al., 2013; Pasquini et al., 2012). Toxicity is also affected by the size of CNTs (Simon-Deckers et al., 2009; Yang et al., 2010), with SWCNTs reported to be more toxic than larger-diameter MWCNTs (Kang et al., 2008a). SWCNTs were also shown to be more toxic when long than short (Yang et al., 2010), which appears to be due to greater aggregation with bacterial cells. Aggregation may be the result of long CNTs wrapping around the bacterial cell, as shown by Chen et al. (2013); in contrast, it appears that short CNTs exhibit their toxicity by piercing the cell membrane (Chen et al., 2013).

CNTs can trigger an oxidative stress response in bacterial cells, as evidenced by an increased expression of oxidative stress-related genes (Kang et al., 2008a; Kang et al., 2007a; Vecitis et al., 2010). Vecitis et al. (2010) showed that metallic CNTs caused greater oxidative stress than semi-conducting CNTs, and they proposed a three-stage mechanism of CNT-induced toxicity involving CNT contact with bacteria, membrane damage, and electronic structure-dependent oxidation.

Many bacterial populations affected by CNTs in the environment are entrapped in biofilm communities. Culture based methods are limited by the need to physically disrupt the biofilm structure in order to create a suspension of bacteria for analysis. Non-culture based methods can be used to quantify bacteria *in situ*, and have the added advantage of detecting sub-populations of viable but non-culturable bacteria. Despite this, culture based methods remain the gold standard for bacterial viability assessment. Although a number of studies have compared culture and

non-culture based methods, few comparisons have been made using CNT-treated bacteria. A goal of this study was to compare non-culture based methods to the gold-standard plate count, with a view to adopting them in future studies of CNT toxicity for entrapped bacteria. Three different measures of viability – beta galactosidase enzyme activity, membrane integrity, and total RNA were focused. Beta galactosidase enzyme activity was previously used to rapidly quantify *E. coli* and other coliforms in water (George et al., 2000; George et al., 2001; Ozkanca, 2002; Rompre et al., 2002; Tryland and Fiksdal, 1998). A limitation of this approach is that beta galactosidase activity is generally only found in *E. coli* and other coliforms. In contrast, the membrane integrity-based LIVE/DEAD® BacLight™ assay and total RNA can be more broadly used for bacterial viability assessment.

In this study, the toxicity of short and long SWCNTs for *E. coli* ATCC 8739 was compared. *E. coli* was selected because it is a model Gram negative that has been extensively characterized at the molecular and cellular level, and it has been widely used in previous studies of CNT toxicity (Arias and Yang, 2009; Chen et al., 2013; Kang et al., 2008a; Kang et al., 2009). The issue of the metal impurities by examining the toxicity of a leachate of SWCNTs was also addressed. In addition to proposing tools to study the interactions between CNTs and bacteria, the comprehensive efforts reported in this study are expected to provide a more thorough understanding of the impact of SWCNTs on bacterial cells.

3.2. Materials and Methods

3.2.1. Chemicals and cell culture

4-methylumbelliferyl-β-D-galactoside (Mugal), isopropyl-beta-D-thiogalactopyranoside (IPTG), and Xgal were purchased from Sigma Chemical Company (MO, USA). *E. coli* ATCC 8739 strain was obtained from the Global Bioresource Center (American Type culture

collection, VA, USA). The strain was plated onto nutrient agar (NA) and incubated overnight at 37°C. A single colony from the overnight incubation was used to prepare a liquid culture in the tryptic soy broth for experiments. This liquid culture was incubated overnight at 37°C with continuous orbital shaking at 150 rpm (Lab-line® orbit shaker 3590, IL, USA) and was harvested during stationary growth phase. The timing of stationary growth was determined during preliminary growth curve experiments. Cells were pelleted at 4500× *g* for 15 min and washed twice in phosphate buffered saline (PBS) before use in experiments.

3.2.2. Single-walled carbon nanotubes

Short and long SWCNTs, 0.5-2 μm and 5-30 μm in length, were obtained from Cheap Tube Inc. (Brattleboro, VT, US.). Both types of SWCNTs have a diameter of 1-2 nm. They were purified to remove silica, cobalt, and amorphous carbon before being used in experiments. The purification procedure was modified from the method of Kang et al. (2007b). Briefly, silica was removed by refluxing SWCNTs two times in 1 M NaOH for one hour. Following treatment, SWCNTs were collected by filtration through a 5 μm pore-size membrane (Omnipore, Fisher Scientific, PA, USA) and washed three times with deionized water. Cobalt was removed by refluxing twice in 37% HCl for 7 hours. SWCNTs were collected by filtration and heated for 30 min at 400°C between acid refluxes. After the second reflux, SWCNTs were collected by filtration and washed in deionized water before drying at 100°C for 24 hours.

3.2.3. Treatment of *Escherichia coli* 8739 with SWCNTs

All treatments were carried out in 50 ml flat-bottomed glass bottles. Washed *E. coli* 8739 cells were suspended in PBS to achieve a density of 6.5 $\log_{10}$ CFU (Low density inoculum) and 9 $\log_{10}$ CFU (High density inoculum) per treatment. SWCNTs were added from a purified 10 mg/ml stock to achieve final treatment concentrations of 5, 10, 20, 50, 100, 200, 500,

and 1000 μg/ml. Duplicate controls containing *E. coli* 8739 without SWCNTs were included with each experiment. Treatments and controls were stirred using a magnetic stirrer at approximately 75× *g* for 90 min at room temperature. Immediately following, an aliquot was removed and used to determine viability by one of four methods: plate count, beta galactosidase assay, a LIVE/DEAD® BacLight™ assay, or total RNA quantification. All experiments were carried out in triplicate.

As a control, *E. coli* 8739 cells were treated with SWCNT washing solution. To determine the extent to which SWCNT toxicity is caused by chemical leaching from the SWCNT surface, *E. coli* 8739 cells were treated with a SWCNT wash solution. Wash solutions were prepared from different concentrations of SWCNTs (5, 10, 20, 50, 100, 200, 500, and 1000 μg/ml), which were incubated with stirring at 800 rpm for 90 min at room temperature. Following incubation, SWCNTs were removed by filtering three times through 0.2 μm pore-size membrane (Omnipore, Fisher Scientific, PA, USA) with 2 ml of Celite 545 filter aid (Fisher Scientific, PA, USA) deposited on the membrane surface. Low and high densities of *E. coli* 8739 (6.5 $\log_{10}$ CFU and 9 $\log_{10}$ CFU, respectively) were exposed to the filtrate (washing solution) from different SWCNT concentrations and stirred using a magnetic stirrer at approximately 75× *g* for 90 min at room temperature. Immediately following, an aliquot was removed and used to determine viability by plate count on NA, a beta galactosidase assay, a LIVE/DEAD® BacLight™ assay, and RNA quantification.

3.2.4. Viability assays

Beta galactosidase assay. The beta galactosidase enzymatic assay of whole cells was modified from a protocol by Fiksdal et al. (1994). A 20 ml aliquot from the treatment was filtered through a 0.2 μm pore-size, 47 mm diameter polycarbonate filter (Millipore

Isopore Polycarbonate membrane filters, Fisher scientific, PA, USA). The filter with retentate was placed in a 250 ml flask containing 20 ml of a PBS solution supplemented with 500 g/l 4-methylumbelliferyl-β-D-galactoside (Mugal), 0.2 g/l sodium dodecyl sulfate, and 0.1% nutrient broth. The flask was incubated in a reciprocal shaking bath (Thermo electron corporation 2879, OH, USA) at 44.5°C. One milliliter aliquots were collected at 5, 10, 15, 20 and 25 min intervals and placed in Costar clear Polystyrene 96 well plates with 40 µl of 10 M NaOH. Fluorescence intensity was measured using a spectrophotometer (Synergy HT, Biotek, VT, USA) at an excitation wavelength of 360±20 nm (10 nm slit width) and an emission wavelength of 440±20 nm (20 nm slit width). The fluorometer was calibrated by using 100% of fluorescence intensity of methylumbelliferone (MUF) at concentrations ranging from 50 to 30000 nmol/l. The measured fluorescence intensity was converted to MUF concentration. The enzyme activity was determined based on the slope of a least-square linear regression of MUF versus time (MUF released per minute).

Plate count. Serial decimal dilutions of the sample were prepared in PBS and 100 µl of diluted samples were spread on NA plates. Plates were incubated overnight at 37°C before enumeration.

LIVE/DEAD® BacLight™ assay. The L7012 LIVE/DEAD® BacLight™ Bacterial Viability Kit (Molecular Probe, Invitrogen, OR, USA) was used to assess the viability of *E. coli* 8739. The method was carried out as described by the manufacturer. Fluorescence was quantified using a microplate reader (Synergy HT, Biotek, VT, USA) at an excitation wavelength at 485 nm and emission wavelengths at 530 nm (emission green F_G) and 630 nm (emission red F_R) for SYTO 9 and propidium iodine (PI), respectively. The ratio of F_G/F_R was plotted to calculate the percentage of live cells.

RNA quantification. Due to its rapid degradation in non-viable cells, RNA can be a useful surrogate for bacterial cell viability. Total RNA was extracted and purified using the GenElute™ Bacterial Total RNA Miniprep Kit in accordance with the manufacturer's instructions (Qiagen, MD, USA). The total RNA concentration and purity was determined from 260 nm to 280 nm (*A*260/*A*280) absorbance values, which were obtained using a Nanodrop 1000UV/VIS spectrophotometer.

*Scanning electron microscopy (SEM)***.** Three milliliters of sample, including visible sediment, was aspirated into a syringe equipped with a 0.2 μm sterile filter. The filter was then flushed with 2.5% glutaraldehyde in sodium phosphate buffer to fix the sample, rinsed with distilled water, and dehydrated with absolute ethanol. After air-drying, the filter housing was cracked open to allow removal of the filter material and sample. The filter was mounted sample side up on an aluminum stub using carbon tape and coated with carbon using a Cressington 208C carbon coater. Images were acquired using a JSM-7600F Field Emission Scanning Electron Microscope.

*Raman spectroscopy***.** Raman spectra were recorded on an Aramis Confocal Raman Imaging System. The instrument is equipped with an Olympus confocal microscope. Excitation wavelengths of 532 and 784.42 nm (spectro of 1399.88) were used.

Energy dispersive spectroscopy. Energy dispersive spectra were detected by using energy dispersive spectroscopy, JEOL JSM-6300 to characterize the elemental composition of SWCNTs before and after purification. The voltage of 15.00 kV was used.

3.2.5. Statistical analysis

Analysis of variance (ANOVA) and Bonferroni's t-test at 5% significance level were performed for data analysis. ANOVA F test and Bonferroni's t-test were used together to

analyze the difference in the cell viability provided by different experimental conditions (SWCNT concentrations, type of SWCNTs, cell viability indicator, and bacterial density). The Minitab Program was used for statistical analysis.

3.3. Results and Discussion

3.3.1. Results

3.3.1.1. Plate count

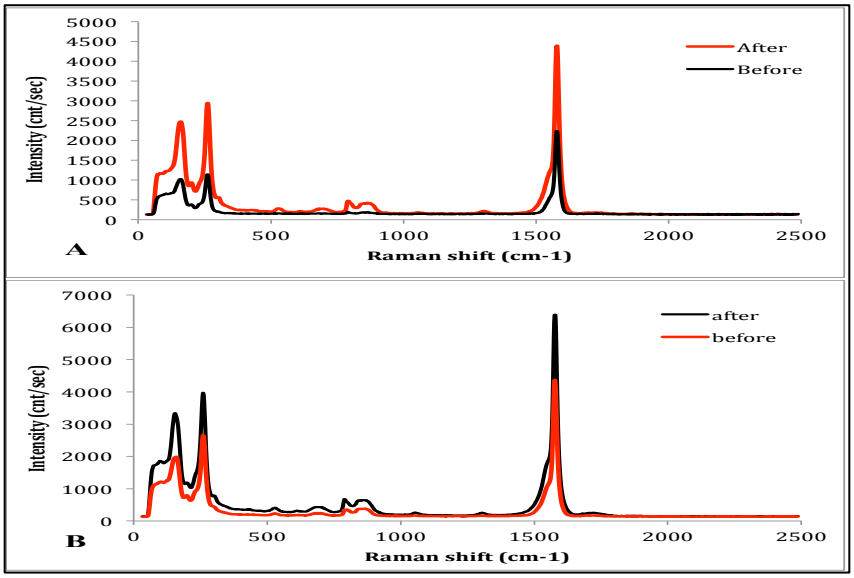

Figure 3-1: Raman spectroscopy (785nm) of (A) Short and (B) Long SWCNTs before and after purification.

A mild acid cleaning procedure reduced cobalt levels to less than 0.6 wt% and did not affect SWCNTs structures (Table 3-1, Fig. 3-1). Fig. 3-2 shows the effect of short and long SWCNTs on 6.5 $\log_{10}$ CFU of *E. coli*. Viability was assessed using the plate count assay and expressed as a percentage of the control. The reduction in viability of *E. coli* cells increased with increasing concentrations of both short and long SWCNTs (Fig. 3-2A). However, the differences were less pronounced at lower concentrations of long SWCNTs. At 500 and 1000 μg/ml, similar reductions of 93-95% were observed for both short and long SWCNT treatments ($p = 0.137$).

Table 3-1: Composition of elements of short and long SWCNTs before and after purification based on energy dispersive spectra.

Chemical formula	Mass (%)			
	Short SWCNTs		Long SWCNTs	
	Before purification	After purification	Before purification	After purification
C	91.76	94.8	93.66	94.59
O	5.75	4.46	4.67	4.06
Mg	0.1	0	0.08	0
Al	0.08	0	0.06	0
Si	0.33	0	0.01	0.01
Ca	0.22	0	0.13	0
S	0.12	0.07	0.11	0.09
Cl	0.1	0.18	0.05	0.05
Cr	0.1	0	0.38	0.37
Fe	0.71	0	0.26	0.18
Co	0.73	0.49	0.60	0.5

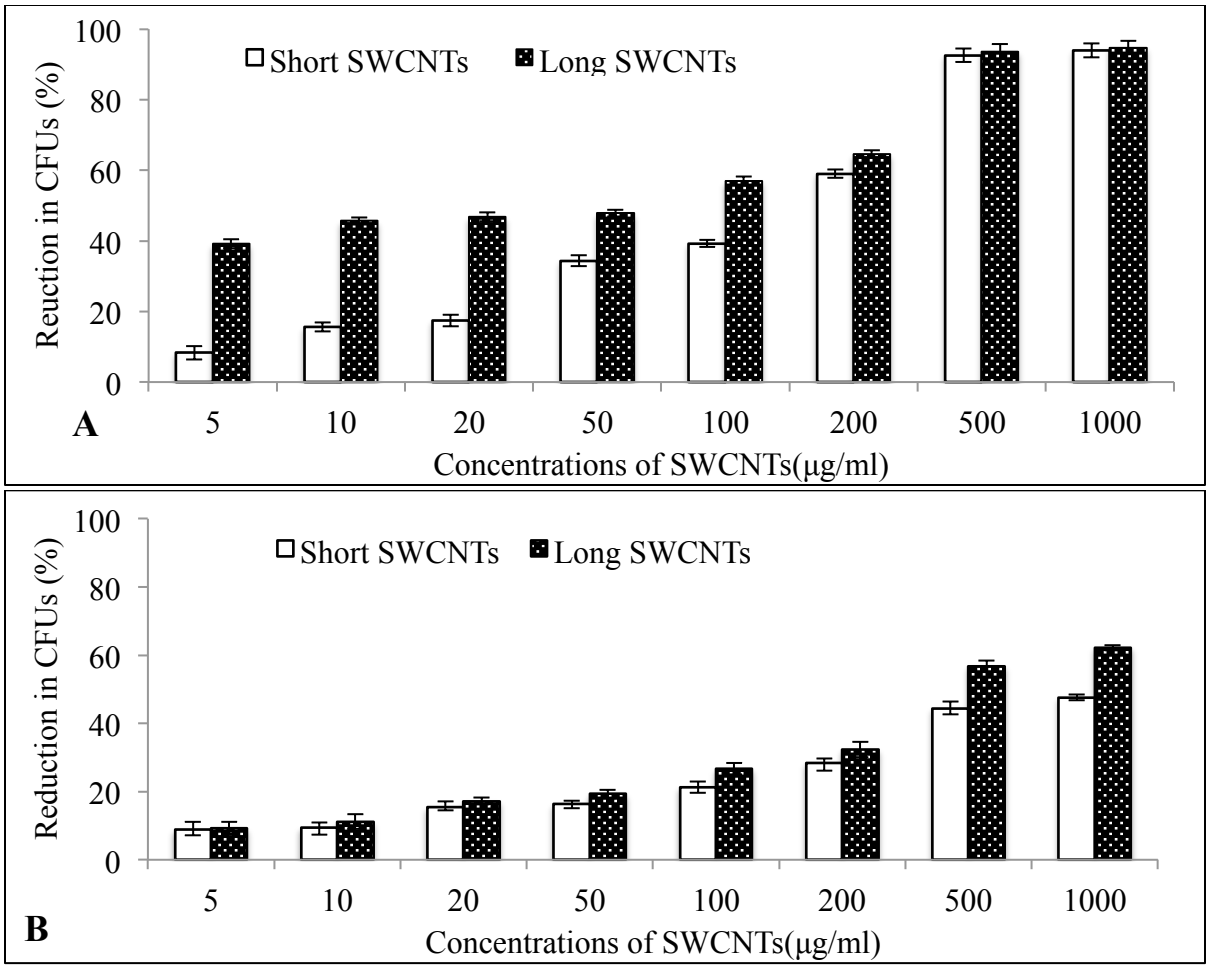

Figure 3-2: Effect of SWCNTs on viability of *Escherichia coli* detected by plate count method. (A) Starting *E. coli* cell density 6.5 $\log_{10}$ CFU $Test^{-1}$, (B) Starting *E. coli* cell density 9.0 $\log_{10}$ CFU $Test^{-1}$.

Less dramatic reductions in viability were observed when treatments were carried out using 9 $\log_{10}$ CFU *E. coli* (Fig. 3-2B). Treatments with short or long SWCNTs at concentrations of 500 and 1000 μg/ml resulted in only a 50% reduction in viability. The long SWCNTs resulted in a greater reduction in viability than short SWCNTs ($p < 0.05$) with the exception of the 5 μg/ml treatment.

3.3.1.2. Beta galactosidase activity

Experiments were carried out using beta galactosidase activity as an indicator of *E. coli* viability (Fig. 3-3A and B). Experimental conditions, including the *E. coli* density (6.5 $\log_{10}$ CFU and 9 $\log_{10}$ CFU per test) and concentration of short and long SWCNTs were as described for the plate count assay. Viability generally decreased with the increasing SWCNT concentration. This trend was observed for both short and long SWCNTs.

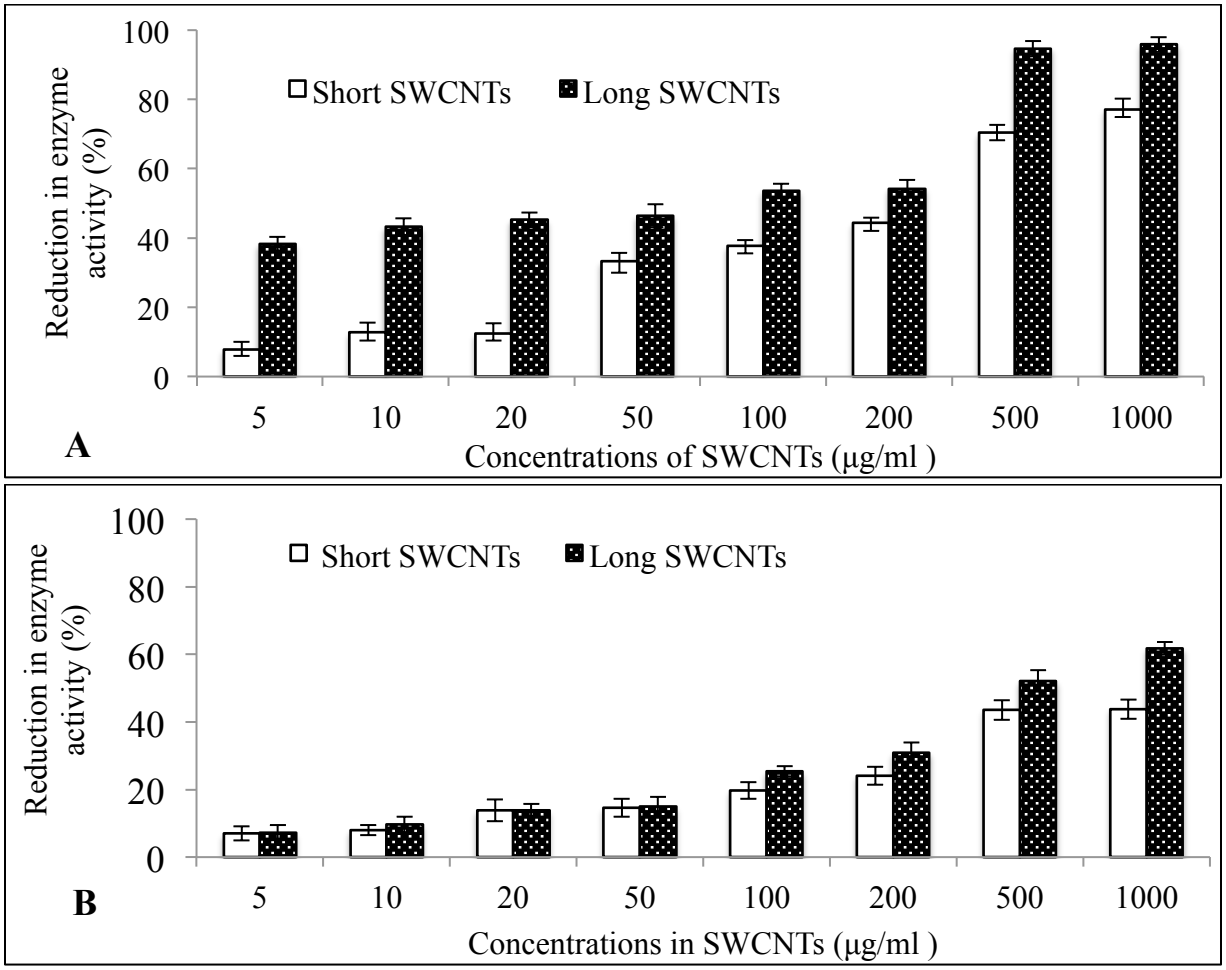

Figure 3-3: Effect of SWCNTs on viability of *Escherichia coli* detected by the galactosidase enzyme assay. (A) Starting *E. coli* cell density 6.5 $\log_{10}$ CFU $Test^{-1}$, (B) Starting *E. coli* cell density 9.0 $\log_{10}$ CFU $Test^{-1}$.

In treatments at low initial *E. coli* density, there was a limited effect of SWCNTs on beta galactosidase activity at the treatments of 5, 10, and 20 μg/ml (Fig. 3-3A). Reductions in viability increased when with increasing concentrations of short SWCNTs. A similar trend was observed in treatments with long SWCNTs, with the exception that reductions were more moderate between 5 and 200 μg/ml. Greater viability reductions were observed using both short and long SWCNT concentrations of 500 and 1000 μg/ml (> 70% reduction in viability). When comparing the effects of short and long SWCNTs on the viability of *E. coli*, long SWCNTs resulted in a greater viability reduction at all concentrations tested (F test, $p = 0.000$).

Decreasing viability with increasing SWCNT concentration was also observed at the high density of *E. coli* (Fig. 3-3B); however, viability reductions were less than those observed at the low *E. coli* density. For both short and long SWCNTs, viability reductions varied by concentration, with the exception of the 500 and 1000 μg/ml treatments with short SWCNTs. At treatment concentrations of 100, 200, 500, and 1000 μg/ml, long SWCNTs resulted in greater viability reductions than short SWCNTs (F test, $p < 0.05$).

3.3.1.3. LIVE/DEAD® BacLight™ assay

The LIVE/DEAD® BacLight™ assay was used as a membrane integrity-based viability assay. Using fluorescence spectroscopy to quantify green (viable) and red (non-viable) fluorescence, a decrease in viability was observed following treatment of the low density of bacteria with short and long SWCNTs (Fig. 3-4A). The reduction in viability of *E. coli* was significantly different between each short SWCNT concentration and the next higher concentration, except between 5 and 10 μg/ml and among 200, 500, and 1000 μg/ml treatments. Viability differed significantly between each long SWCNT concentration and the next higher

concentration, except between 5 and 10 μg/ml. Consistent with other methods of viability assessment, a greater reduction in viability was observed in treatments with long SWCNTs compared to that with short SWCNTs. The effects of short and long SWCNTs on *E. coli* cell viability at the high density is shown in Fig. 3-4B. Similarly, Reductions in viability increased with increasing concentrations of both short and long SWCNTs. Long SWCNTs resulted in greater reductions in viability relative to short SWCNTs at all treatment concentrations.

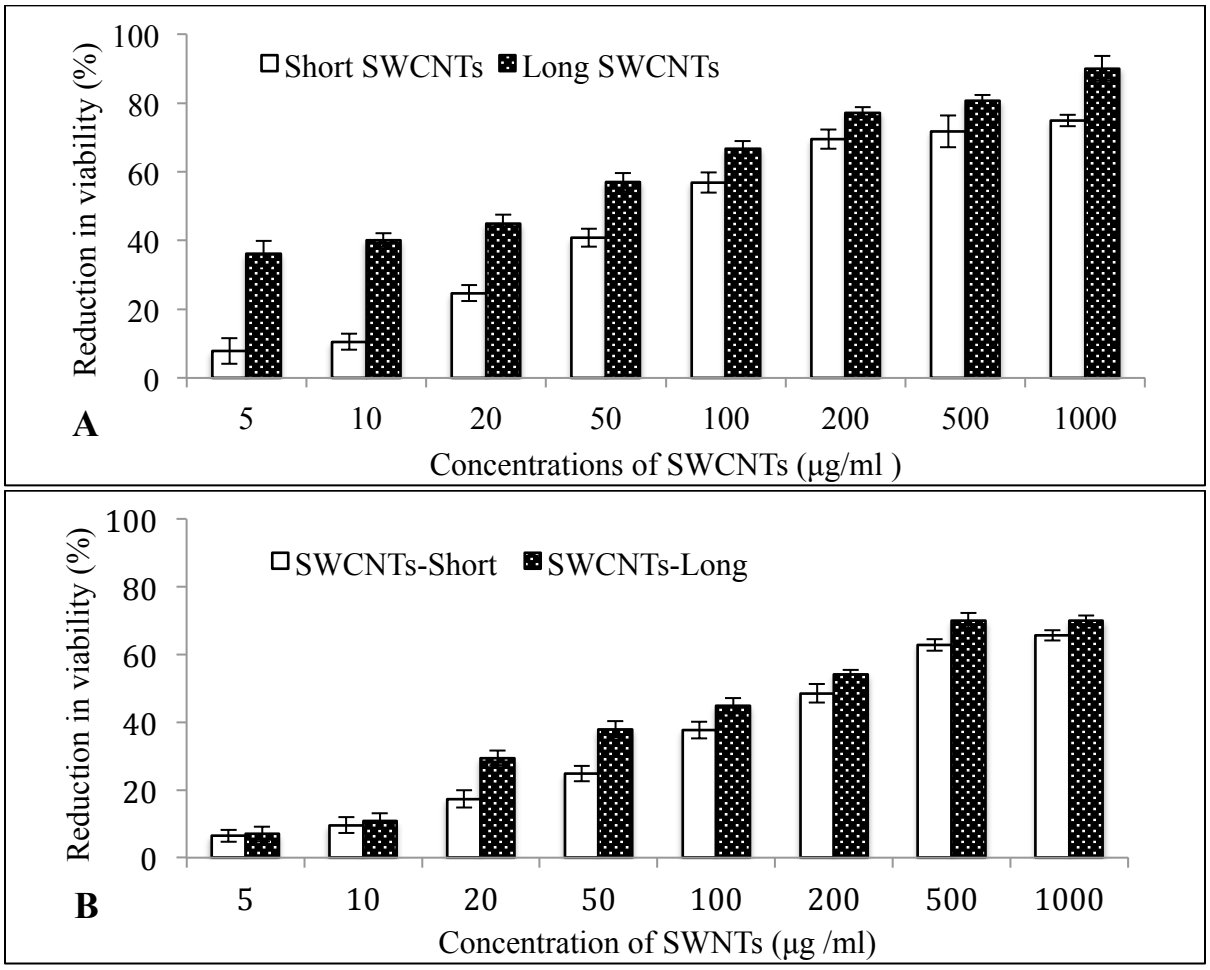

Figure 3-4: Effect of SWCNTs on viability of *Escherichia coli* detected by the LIVE/DEAD® BacLight™ assay. (A) Starting *E. coli* cell density 6.5 $\log_{10}$ CFU $Test^{-1}$, (B) Starting *E. coli* cell density 9.0 $\log_{10}$ CFU $Test^{-1}$.

3.3.1.4. RNA concentration

The effects of treatments on RNA concentration are presented in Fig. 3-5A and B. At both low and high densities of *E. coli*, total RNA levels decreased by more than 99.99% following treatment with SWCNTs at 1000 μg/ml concentration. Reductions were greater for long SWCNTs than short SWCNTs at all concentrations. For short SWCNTs, RNA concentration differed among treatments, with the exception of the 500 and 1000 μg/ml treatments, which had similar RNA concentrations (F test, $p > 0.05$). A similar trend was observed for treatments with long SWCNTs.

3.3.1.5. Cell integrity following exposure to SWCNTs

SEM revealed that the morphology of *E. coli* cells was altered following exposure to short and long SWCNTs at 500 μg/ml (Fig. 3-6A to C). Untreated cells were observed as rod shaped with an intact cell membrane. In contrast, cells exposed to short and long SWCNTs had an irregular morphology and were clustered together as aggregates (Fig. 3-6B and C). This suggests that SWCNTs cause cell damage and changes to morphology.

3.3.1.6. Effect of SWCNT impurities on E. coli viability

In order to confirm that the observed effect on *E. coli* viability was not due to chemical impurities that may have remained following SWCNT purification, SWCNTs were washed and the wash solution was used to treat *E. coli* cells. When compared to untreated controls, *E. coli* cells treated with the washing solution showed negligible reductions in viability, regardless of the concentration of SWCNTs from which the washing solution was derived (Table 3-2). The plate count and beta galactosidase assays showed similar reductions for washing solution treatments (F test, $p > 0.05$).

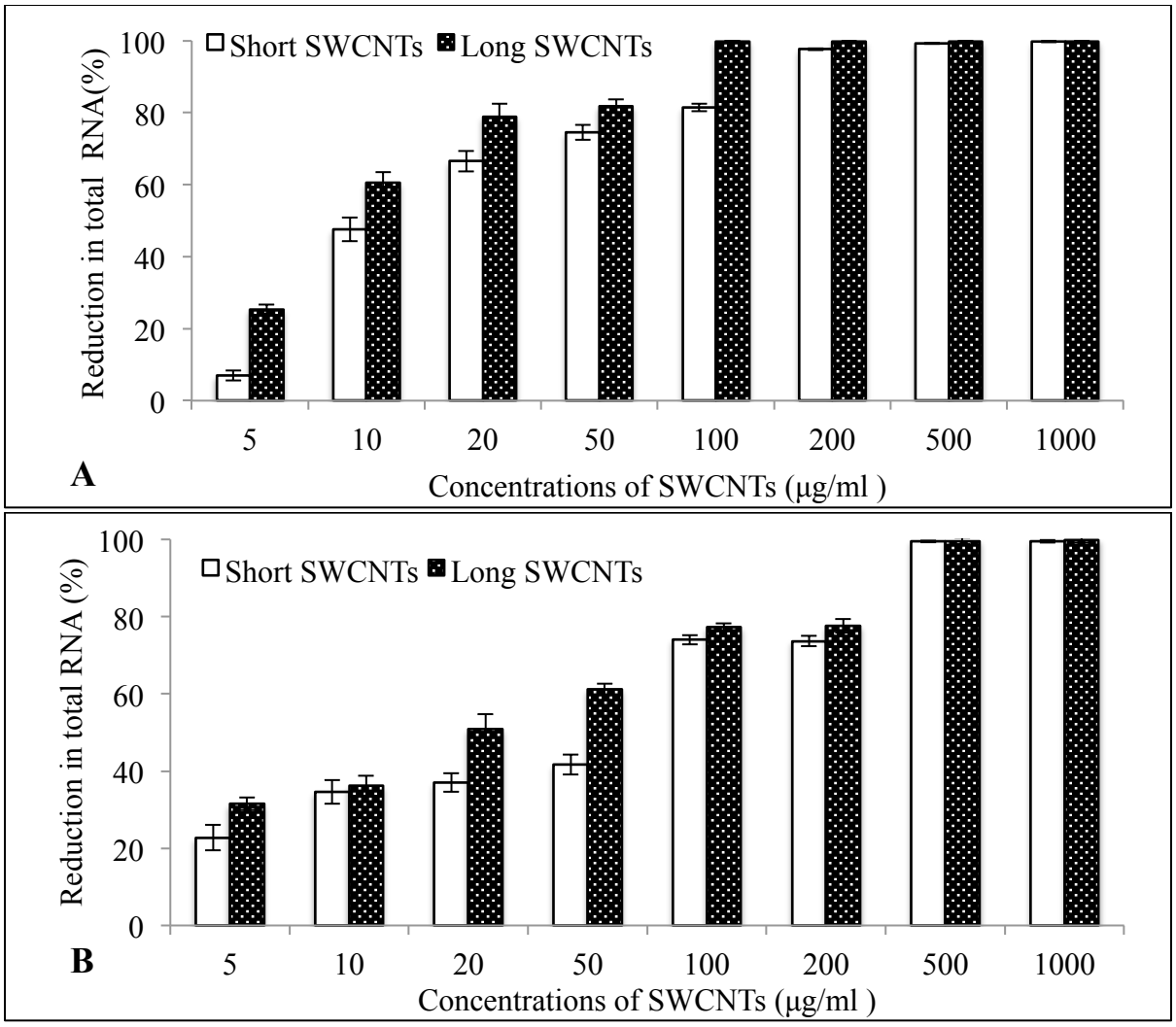

Figure 3-5: Effect of SWCNTs on viability of *Escherichia coli* detected by the RNA quantification. (A) Starting *E. coli* cell density 6.5 $\log_{10}$ CFU Test^{-1}, (B) Starting *E. coli* cell density 9.0 $\log_{10}$ CFU Test^{-1}.

Table 3-2: Effect of SWNT leachate on cell viability.

Concentration of SWCNTs (μg/ml) used to generate leachate	Live cell detected by the plate count method (%)	Live cell detected by the beta galactosidase enzyme assay method (%)
0	100	100
5	99.98 ± 0.02	99.88 ± 0.12
10	99.97 ± 0.01	99.95 ± 0.02
20	99.98 ± 0.01	99.95 ± 0.01
50	99.89 ± 0.09	99.91 ± 0.07
100	99.91 ± 0.09	99.93 ± 0.04
200	99.92 ± 0.07	99.90 ± 0.03
500	99.89 ± 0.10	99.88 ± 0.10
1000	99.85 ± 0.13	98.88 ± 0.06

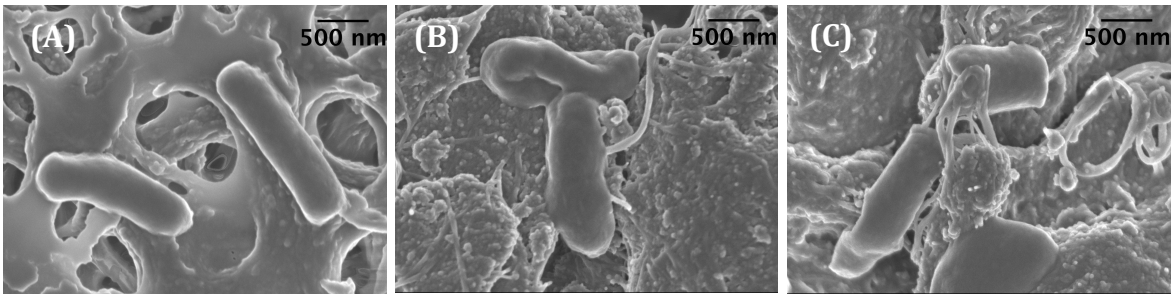

Figure 3-6: (A) SEM image of *Escherichia coli* cells incubated without SWCNTs, (B) SEM image of *E. coli* cells incubated with short SWCNTs (500 μg/ml), and (C) SEM images of *E. coli* cells incubated with long SWCNTs (500 μg/ml).

3.3.2. Discussion

Using a plate count, beta galactosidase assay, LIVE/DEAD® BacLight™ assay, and RNA quantification, results show that the viability of *E. coli* following exposure to SWCNTs is dependent on the density of *E. coli*. The high density (9 $\log_{10}$ CFU $test^{-1}$) was proportionally less affected by SWCNTs than the low density (6.5 $\log_{10}$ CFU $test^{-1}$), suggesting that *E. coli* exhibits density-dependent variability in susceptibility to SWCNTs. Liu et al. (2000) showed that *E. coli* undergo major regulatory and physiological changes when cell density increases from 10^8 to10^9 CFU/ml. These changes include an increased expression of RpoS, trehalose, and catalase, and a 10-fold reduced expression of the porin protein *OmpF*; all of which contribute to a significantly more resistant population at the higher cell density. Based on these findings, the density of bacteria should be considered in future studies that assess the toxicity of SWCNTs.

Toxicity was affected by SWCNT length, with long SWCNTs exhibiting greater toxicity. This is consistent with findings from previous studies (Chen et al., 2013; Parise et al., 2013; Yang et al., 2010). Yang et al. (2010) proposed that SWCNTs are more likely to contact bacterial cells than short SWCNTs, and Parise et al. (2013) provided evidence to support this proposal by showing that long SWCNTs are more likely to aggregate with bacteria, while short SWCNTs are more likely to self-aggregate. Chen et al. (2013) showed that long SWCNTs wrap around bacterial cells, which probably facilitates the greater aggregation.

In previous work with SWCNTs, it was assumed that purification steps removed toxic metals that are used in SWCNT production (Kang et al., 2007a). SWCNTs used in this study were similarly treated to remove contaminating metals. Results indicated that SWCNT washings were not toxic for *E. coli*, confirming that observed reductions in viability were due to SWCNTs and not metal residues remaining after purification.

A goal of this study was to examine alternatives to the plate count for assessing the viability of bacteria exposed to SWCNTs. LIVE/DEAD® BacLight™ and beta galactosidase assays were more conservative indicators of viability reductions than the plate count. The LIVE/DEAD® BacLight™ data are consistent with previous findings that estimates of viability reductions for bacteria exposed to SWCNTs are greater for culture-based methods than methods that are based on membrane permeability (Boulos et al., 1999). The more conservative estimates of viability reductions from LIVE/DEAD® BacLight™ and beta galactosidase assays suggest the possible presence of viable but non-culturable *E. coli* cells following SWCNT treatment. Further studies are required to test the validity of this hypothesis.

Estimates of viability reductions using total RNA were greater than those observed for other indicators. This could be due to the activation of RNase in *E. coli* cells that are under stress, as previously reported by Condon (2007). Therefore, it is appropriate to use more than one indicator when assessing the viability of *E. coli* after exposure to SWCNTs.

3.4. Summary

A plate count, beta galactosidase assay, LIVE/DEAD® BacLight™ assay, and RNA quantification assay, are useful for determining the effect of SWCNTs on the viability of *E. coli*. Although these four methods use different measures of cell viability, their results are quite agreeable. All assays show that SWCNTs are toxic for *E. coli* cells. Factors that influence the toxicity of SWCNTs to *E. coli* cells are length and density of SWCNTs and density of cells.

CHAPTER 4: MITIGATION OF BACTERICIDAL EFFECT OF CARBON NANOTUBE BY CELL ENTRAPMENT

4.1. Background

CNTs are one of the most widely used nanomaterials, in consumer products due to their large surface area to volume ratio, electrical properties, high tensile strength, and ultra lightweight. Common consumer products such as bicycle frames (MBC Swissland) and rims (ENVE composites and Zyvex technologies), tennis rackets (Babolat), hockey sticks (Easton), and plastic films (Unidym) incorporate CNTs as key components. According to Global Industry Analysts Inc., worldwide production of CNTs was about $1.9 billion in 2010 and is predicted to reach $7.7 billion in 2015 (GIA, 2012). With such massive growth, novel materials containing CNTs are entering the environment at an alarming rate, and research to understand the environmental and public health impact is struggling to keep pace. However, recent studies have shown that CNTs can negatively impact organisms, organs, cells, and biomacromolocules (Zhao and Liu, 2012).

CNTs can cause dermal toxicity (following skin contact) and possibly lung cancer (following inhalational exposure) in humans. The pathology is due to oxidative stress and immune-mediated responses including inflammation, granuloma formation, fibrosis, and apoptosis (Crouzier et al., 2010; Shvedova et al., 2008; Wang et al., 2010). CNTs negatively impact non-mammal animal species such as zebrafish, where bovine serum albumin-coated MWCNTs cause a delay in larval hatching and a lower survival rate (Cheng et al., 2009). They also adversely affect plant species (Khodakovskaya et al., 2009) and bacteria (Kang et al., 2008a; Vecitis et al., 2010).

The antibacterial effect of CNTs is dependent on factors such as solution buffering capacity, CNT concentration and length, species and density of bacteria, and exposure time (Zarubina et al., 2010). Although the precise mechanism of CNT toxicity for bacteria is unclear, direct contact appears to be important. Both gram-negative and gram-positive species show altered cell morphology, membrane damage, cell wall disruption, and cytoplasm leakage following exposure to CNTs (Kang et al., 2007a; Liu et al., 2010a; Obraztsova et al., 2009; Young et al., 2012). It appears that damage to bacterial cells is caused by a mesh of interacting CNTs rather than individual CNTs (Liu et al., 2010a).

The well-documented antibacterial properties of CNTs (Brady-Estevez et al., 2010; Kang et al., 2008a; Vecitis et al., 2010) have been exploited to enhance the effectiveness of products used for decontamination. For example, CNT embedded filters substantially reduce the levels of bacteria and viruses in water, and fungi and bacteria in air relative to standard filters (Brady-Estevez et al., 2010; Xu and Yao, 2011). Unfortunately, increasing levels of CNTs in environments such as soil and activated sludge can also cause reductions in populations of ecologically important bacterial species (Chung et al., 2011; Jin et al., 2013), upsetting the delicate balance of these ecosystems. Therefore, solutions are required to mitigate the potential negative effects of CNTs on beneficial bacteria in critical ecosystems. One proposed solution focused on the CNT: multiple walled CNTs were coated with a polystyrene-based polymer, which altered the surface environment and reduced toxicity for lung cells (Tabet et al., 2011). In contrast, the present study proposes a solution that focuses on protecting the bacterial cells by entrapment in porous polymeric matrices.

Entrapped microbial cells are used in food and pharmaceutical industries (alcohol fermentation and production of antibiotics) (Ellaiah et al., 2003; Kumaravel and Gopal,

2010; Srinivasulu et al., 2003) because of their enhanced resistance to environmental stresses, such as shear forces in mixing vessels, relative to free cells. Cells are typically entrapped in a hydrogel, which may be natural (alginate, carrageenan, and chitosan) or synthetic (polyacrylamide, polyacrylate, and polyurethane, PVA) (Aykut et al., 1988; Kumaravel and Gopal, 2010; Manohar et al., 2001; Pramanik et al., 2011). PVA and alginate are frequently used for entrapment because they are economical, nontoxic polymers, physically and chemically stable, and have a low mass transfer resistance (Albert et al., 2011).

The goal of this study was to investigate the effect of purified SWCNTs on the viability bacterial cells entrapped in PVA and alginate. *E. coli* ATCC 8739 was used as a model organism. The strain has been used extensively in the laboratory for antibacterial studies (Maria-Neto et al., 2012). A beta-D-galactosidase assay, the LIVE/DEAD® Baclight™ assay, and RNA quantification were used as surrogates of *E. coli* viability during treatments. The primary advantage of these approaches is that they can be used to monitor viability in situ without the need for harsh procedures to remove the bacterial cells from the entrapment matrix. Variables examined included SWCNT length and concentration, and initial density of entrapped *E. coli* cells. Free cells were included in the study for a comparative purpose. Regular and electron microscopies were used to monitor changes in the entrapment bead structure following exposure to SWCNTs.

4.2. Materials and Methods

4.2.1. Chemicals and cell culture

PVA, boric acid, sodium orthophosphate, sodium alginate, and calcium chloride were purchased from VWR international, Inc. (West Chester, Pennsylvania, USA). The PVA, which was used in this study, has a molecular weight of between 77,000 and 79,000 and a degree of

hydrolysis of 99.0% to 99.8%. The specific gravity and melting point of the PVA are 1.19-1.31 and 200°C, respectively. The melting, boiling, and flash points of sodium alginate are 300°C, 495.2°C (at 760 mm Hg), and 211.1°C, respectively.

4-methylumbelliferyl-β-D-galactoside (Mugal), isopropyl-β-D-thiogalactopyranoside (IPTG), and Xgal were purchased from Sigma Chemical Co. (MO, USA). *E. coli* ATCC 8739 was obtained from the Global Bioresource Center (American Type Culture Collection, VA, USA). The strain was plated onto NA and incubated overnight at 37°C. A single colony from the overnight incubation was used to prepare a liquid culture for the experiments. This liquid culture was incubated overnight at 37°C and shaken continuously at 1,500 rpm (Lab-line® orbital shaker 3590, IL, USA). Cells were harvested during stationary growth, pelletized at 4500× *g* for 15 min, and washed twice in PBS before being entrapped.

4.2.2. Single-walled carbon nanotubes

SWCNTs with a diameter of 1-2 nm, and a length of 0.5-2 μm (short SWCNTs) and 5-30 μm (long SWCNTs) were obtained from Cheap Tube Inc. (Brattlebro, VT, USA). They were purified as described in Chapter 3 to remove silica, cobalt, and amorphous carbon before being used in experiments. Characteristics of the purified CNTs are described in Chapter 3.

4.2.3. Cell entrapment

E. coli ATCC 8739 cells were entrapped in PVA according to Pramanik et al. (2011). For alginate entrapment, the procedure described by Konsoula and Liakopoulou-Kyriakides (2006) was modified. The modification involved hardening the alginate beads overnight.

4.2.4. Experimental setup, procedure, and design

Treatments were performed in 50 ml glass bottles using either 6.5 $\log_{10}$ CFU or 9.0 $\log_{10}$ CFU *E. coli* ATCC 8739 per test entrapped in PVA or alginate. The different starting *E. coli*

densities were tested because the work presented in Chapter 3 showed that the resistance of bacteria to SWCNTs is affected by initial cell density. The *E. coli* density was determined by plate count on NA at 37°C overnight. For both PVA and sodium alginate entrapped cell beads, 45 beads (3-4 mm diameter for each bead) were used in each experiment.

Entrapped bacterial cells were treated with 0, 5, 10, 20, 50, 100, 200, 500, or 1000 μg/ml SWCNTs. The mixture was stirred using a magnetic stirrer at 800 rpm for 90 min at room temperature. Following treatments, the viability of entrapped cells was determined using a galactosidase enzyme assay, the LIVE/DEAD® Baclight™ commercial viability assay, and by quantification of RNA.

4.2.4.1. Galactosidase assay

The galactosidase assay was modified from Fiksdal (1994). β-D galactosidase cleaves lactose into galactose and glucose. This assay measures the rate at which β-D galactosidase catalyzes the release of the fluorophore 4-methylumbelliferone (MU) from the substrate 4-methylumbelliferyl-β-D galactoside (MUGal). The fluorophore was quantified spectrophotometrically at an excitation wavelength of 360 nm and an emission wavelength of 460 nm. The modified procedure was carried out as described in Chapter 3, with the exception that the filtration step was not required.

4.2.4.2. LIVE/DEAD® Baclight™ assay

The L7012 LIVE/DEAD® Baclight™ bacterial viability assay (Invitrogen, Grand Island, NY, USA) was used with a microplate reader to determine the viability of *E. coli* ATCC 8739. The assay uses two fluorescent dyes, SYTO 9 and PI. SYTO 9, a green fluorescent dye, can penetrate both live and dead cells, while the red-fluorescent nucleic acid stain PI can only diffuse through damaged membranes. Viable cells with an intact membrane appear green, while

non-viable cells show red fluorescence. The percent viability of cells was determined based on the ratio of red and green fluorescence in samples.

The LIVE/DEAD® Baclight™ assay followed a protocol recommended by the kit manufacturer. Cells entrapped in hydrogels were released by submersing the beads in solvents before the LIVE/DEAD® Baclight™assay was performed. Alginate beads were immersed in a 0.3 M sodium citrate solution at pH 5.0 with shaking until complete dissolution was achieved (Roukas, 1996). The PVA beads were dissolved at 65-70°C in deionized water with continuous shaking for 10 min (Pramanik et al., 2011). The solvents were centrifuged at 14,000× *g* for 10 min and pellets were used in the LIVE/DEAD® Baclight™ assay.

4.2.4.3. RNA quantification

Alginate entrapped cells were dissolved in a 0.3 M sodium citrate solution at pH 5.0 (Roukas, 1996). PVA beads were cut and immersed in phosphate buffer (pH 6.8). The mixture was centrifuged at 2,383× *g* for 10 min to release the cells into the supernatant (Pramanik et al., 2011). After release from sodium alginate and PVA, cells were pelletized at 14,000× *g* for 10 min. Total RNA was extracted and purified using the GenElute™ Bacterial Total RNA Miniprep Kit (Qiagen, MD, USA). The total RNA concentration in ng/ml was determined from a 260 nm to 280 nm absorbance (A260/A280) value using a Nanodrop spectrophotometer (model 1000 uv/vis).

4.2.4.4. Microscopic evaluations

Following exposure of PVA and alginate beads to 500 μg/ml of short and long SWCNTs, they were examined microscopically under bright-field mode in order to evaluate the attachment of SWCNTs on the bead surface (BX61™, Olympus, PA, USA). PVA and alginate beads

exposed to 500 μg/ml of long SWCNTs were examined by SEM analysis. PVA beads were examined according to a procedure described by Chen et al. (1998b). Briefly, the beads were dehydrated in a graded series of ethanol and critical point dried using a Tousimis Autosamdri-810 critical point drier using liquid carbon dioxide as a transitional fluid. Alginate beads were rinsed in a $CaCl_2$ solution (0.1 M) for 15 min twice, and placed in a mixture of 2.5% glutaraldehyde and 0.1 M $CaCl_2$ for 1 hour. They were rinsed in 0.1 M $CaCl_2$ twice, and dehydrated by successive transfers through 30% ethanol in 0.07 M $CaCl_2$ (30 min), 50% ethanol in 0.05 M $CaCl_2$ (30 min), 70% ethanol in 0.03 M $CaCl_2$ (30 min), 90% ethanol in de-ionized water (30 min), and 100% ethanol (60 min). PVA and alginate beads were cut in half, attached to aluminum mounts by silver paint, and coated with gold using a Balzers SCD 030 sputter coater. Images of the bead specimens were taken using a JEOL JSM-6490LV scanning electron microscope.

4.2.5. Statistical analysis

One-way ANOVA and *t*-test were performed using Excel 2011 statistical tools. A *p*-value < 0.05 was used as a criterion for significance level. ANOVA was used to determine whether cell viability results (represented by galactosidase activity, live-dead assay result, and RNA quantity) from different conditions (entrapment matrix including no entrapment, SWCNT concentration, cell density, and type of SWCNTs) are statistically different. When ANOVA showed that different conditions provided significantly different viability results, *t*-test was performed.

4.3. Results and Discussion

Effects of SWCNTs on the viability of entrapped and free bacterial cells, determined by three different viability assays, are shown in Figs. 1–3. The viability of bacteria following exposure to SWCNTs for 90 min is expressed as a percentage of that in bacteria in time

matched controls without SWCNTs. The viability of entrapped and free bacteria in controls, determined by three different viability assays, did not differ significantly between 0 and 90 min.

4.3.1. Effect of entrapment on the viability of cells exposed to SWCNTs

The viability of the alginate and PVA entrapped cells decreased with increasing concentration of SWCNTs (Figs. 4-1 to 4-3). The viability decreases were less dramatic for entrapped cells compared to free cells. The viability results of the free cells and the entrapped cells were significantly different except for entrapped cells at the low SWCNTs concentrations (5 and 10 μg/ml) (Figs. 4-1 and 4-2). The RNA quantities of alginate and PVA entrapped cells exposed to short and long SWCNTs were statistically greater than that of the free cells except at 5 μg/ml of short SWCNTs (Fig. 4-3).

Studies reported that entrapped cells are protected from environmental stress such as high concentrations of alcohol or antibiotics (Chen et al., 1998b; Nishio, 1998). Results in Chapter 3 and a previous study indicated that the toxicity of SWCNTs is mainly from physical contact between cells and CNTs (Young et al., 2012). For entrapped cells, the matrices might act as a shield to protect the cells. The viability of entrapped cells (for both alginate and PVA) and was significantly higher than that of the free cells for every concentration of SWCNTs.

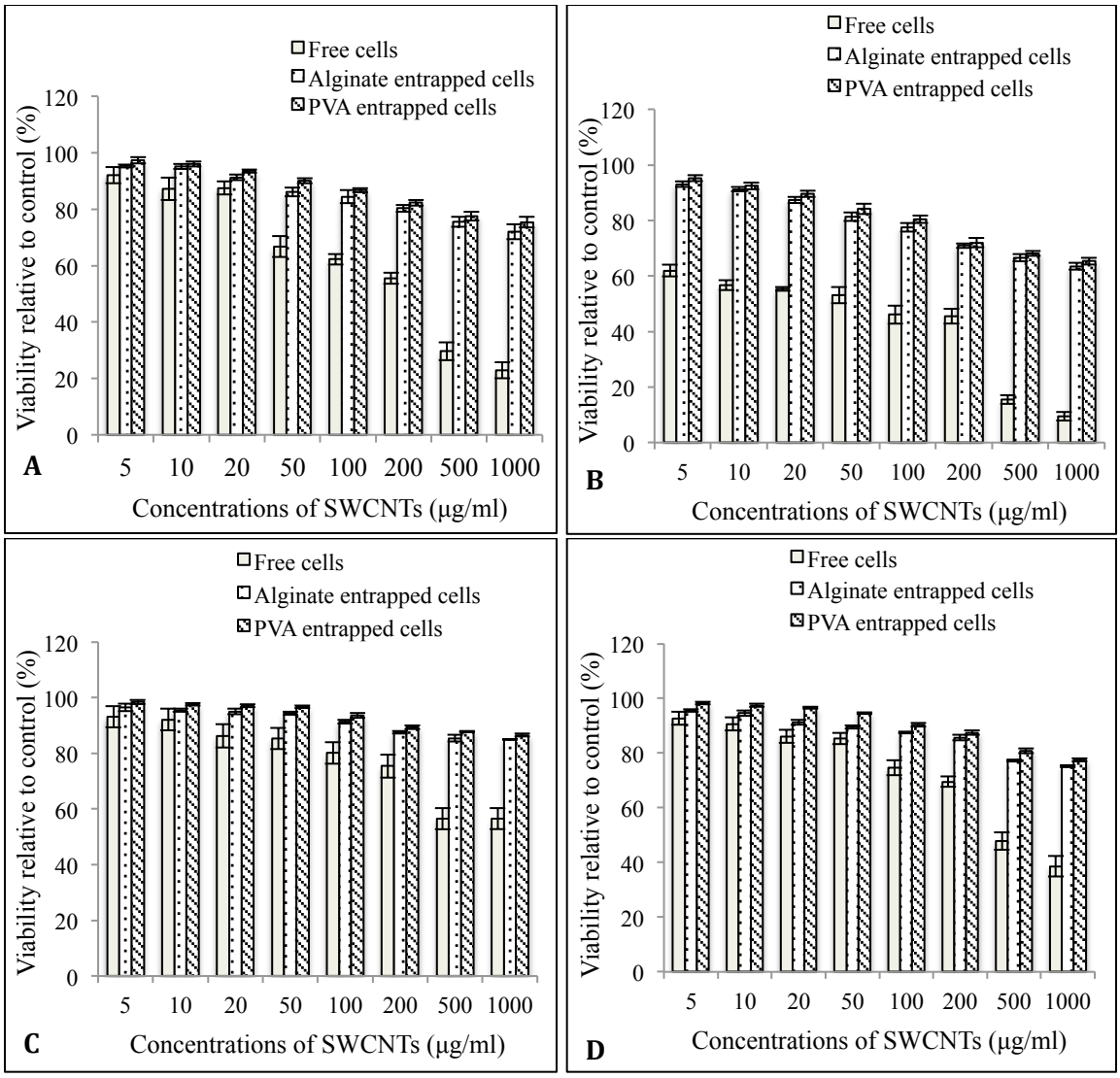

Figure 4-1: Effect of SWCNTs on viability of free *E. coli* and *E. coli* entrapped in alginate and PVA based on the galactosidase enzyme assay. (A) Initial *E. coli* cell density ~ 6.5 $\log_{10}$ CFU $test^{-1}$ and short SWCNTs, (B) Initial *E. coli* cell density ~ 6.5 $\log_{10}$ CFU $test^{-1}$ and long SWCNTs, (C) Initial *E. coli* cell density ~ 9.0 $\log_{10}$ CFU $test^{-1}$ and short SWCNTs, and (D) Initial *E. coli* cell density ~ 9.0 $\log_{10}$ CFU $test^{-1}$ and long SWCNTs.

Statistically the matrix type had no effect on the percent viability at all SWCNT concentrations for both short and long SWCNTs. In this study, physical separation provided by PVA and alginate reduced direct contact between the entrapped cells and SWCNTs, and then might inhibit the oxidative effects. Since the cells were uniformly distributed over the beads, most of the cells entrapped inside were protected.

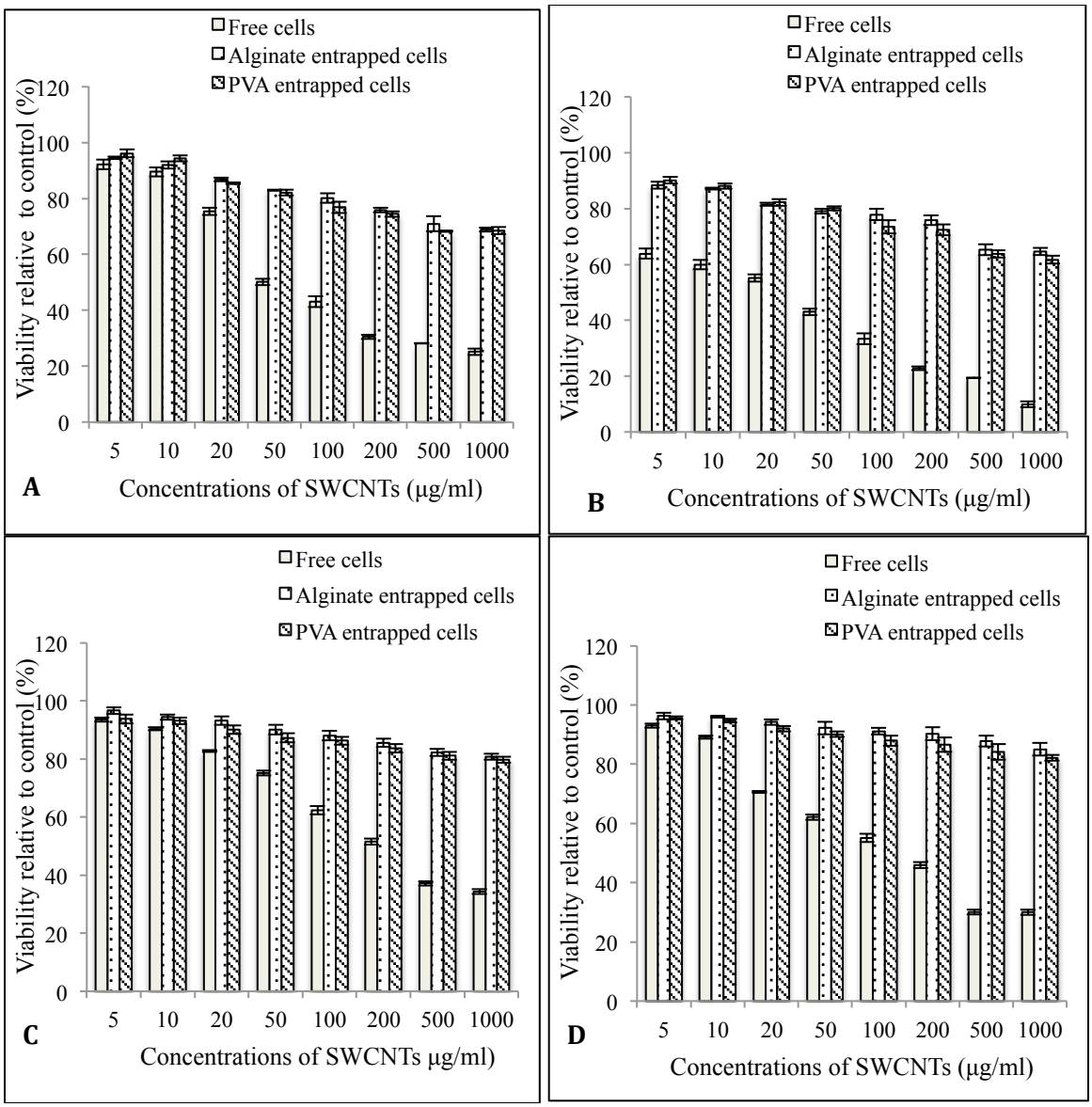

Figure 4-2: Effect of SWCNTs on viability of free *E. coli* and *E. coli* entrapped in alginate and PVA based on the LIVE/DEAD® Baclight™ assay. (A) Initial *E. coli* cell density ~ 6.5 $\log_{10}$ CFU test^{-1} and short SWCNTs, (B) Initial *E. coli* cell density ~ 6.5 $\log_{10}$ CFU test^{-1} and long SWCNTs, (C) Initial *E. coli* cell density ~ 9.0 $\log_{10}$ CFU test^{-1} and short SWCNTs, and (D) Initial *E. coli* cell density ~ 9.0 $\log_{10}$ CFU test^{-1} and long SWCNTs.

4.3.2. Effect of bacterial density on the viability of entrapped cells exposed to SWCNTs

The resistance of entrapped *E. coli* to SWCNTs was dependent on the initial cell density, with greater resistance observed at the higher density. The higher initial cell density led to more cells entrapped inside the beads; hence more cells were protected. Liu et al. (2000) reported that alterations of genetic and proteomic regulations and physiology of *E. coli* induced by increasing cell density led to more resistance to adverse conditions.

4.3.3. Effect of the SWCNT length on the viability of entrapped cells

In general, regardless of the initial cell density and the matrix, entrapped cells exhibited significantly higher reduction in viability when exposed to long SWCNTs compared to short SWCNTs. Long SWCNTs exhibited more bactericidal effect compared to the short SWCNTs in the treatments with free cells (Chapter 3). It might be because more cells on and close to the surface were damage after exposure to long SWCNTs than short SWCNTs. The cells inside the beads were protected in the same degree for both long and short SWCNTs treatment.

The length of SWCNTs influenced on the toxicity. Longer CNTs may increase the contact area between CNTs and bacteria wall by wrapping around the cells and consequently induce more damage than shorter CNTs (Chen et al., 2013). Yang et al. (2010) suggested that longer SWCNTs caused more aggregation that led to more toxicity to the cells. Since SWCNTs could penetrate into the beads through the matrix pores, the long SWCNTs might cause more damage to the cells on the outer layer of the bead than the short SWCNTs. The long SWCNTs might penetrate deeper through the matrix (because of the length) and had more chance for contact with the cell inside the matrix. With large amounts of SWCNTs (500 and 1000 μg/ml), the pores on the surface of beads might be blocked and less or no SWCNTs could diffuse

into the beads. This led to no difference in cell viability between short and long SWCNTs at 500 and 1000 µg/ml.

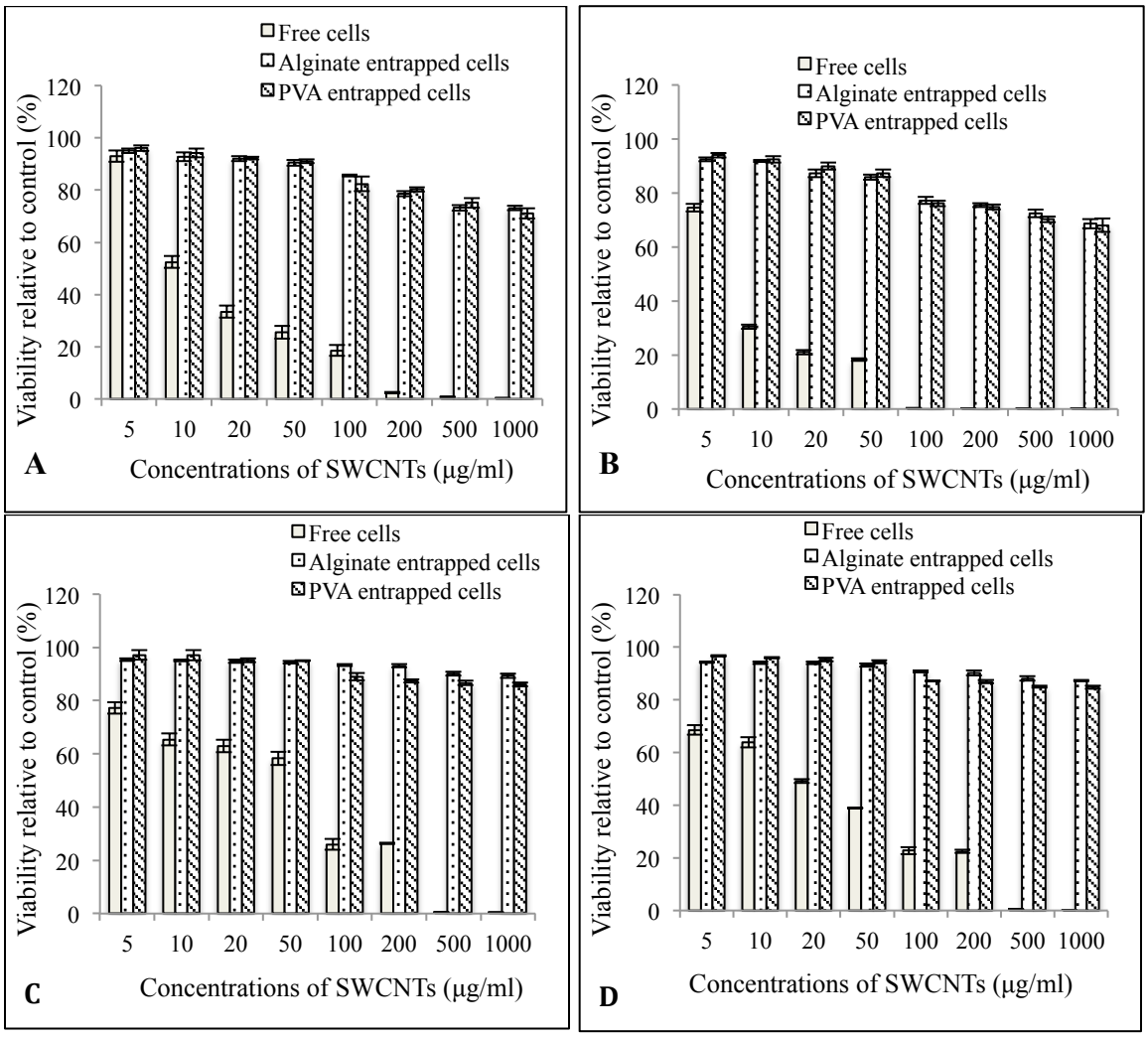

Figure 4-3: Effect of SWCNTs on viability of free *E. coli* and *E. coli* entrapped in alginate and PVA based on RNA quantity. (A) Initial *E. coli* cell density ~ 6.5 $\log_{10}$ CFU test^{-1} and short SWCNTs, (B) Initial *E. coli* cell density ~ 6.5 $\log_{10}$ CFU test^{-1} and long SWCNTs, (C) Initial *E. coli* cell density ~ 9.0 $\log_{10}$ CFU test^{-1} and short SWCNTs, and (D) Initial *E. coli* cell density ~ 9.0 $\log_{10}$ CFU test^{-1} and long SWCNTs.

4.3.4. The influence of the cell viability methods on the SWCNT toxicity results

Overall, after exposure to SWCNTs, the viability of the entrapped cells was higher than that of the free cells based on all three viability methods used including galactosidase enzyme

assay (Fig. 4-1), LIVE/DEAD® Baclight™ assay (Fig. 4-2), and RNA quantification (Fig. 4-3). The RNA quantity based viability differences between the entrapped and free cells are more obvious compared to those from the other two viability methods particularly at high SWCNT concentrations. The matrix might interfere with the galactosidase enzyme assay while the competition between SYTO9 and PI for nucleic binding might lead to the increase of false dead cells (Lehtinen et al., 2004).

4.3.5. Microscopic observations

Figure 4-4: Entrapment beads before and after exposure to 500 μg/ml of long SWCNTs. (A) PVA beads, and (B) alginate beads.

After exposure to SWCNTs, the PVA beads were much darker than the control while the alginate did not change the appearance (Fig. 4-4). The PVA matrix has porous structure scattering all over the beads (Fig. 4-5A) while alginate matrix is also porous but denser (Fig. 4-5B). As shown in Fig. 4-5C, SWCNTs adsorbed onto the outer surface and penetrated the PVA beads (10-200 μm deep). Very less SWCNTs were observed on the surface of as well as in the alginate beads (Fig. 4-5D).

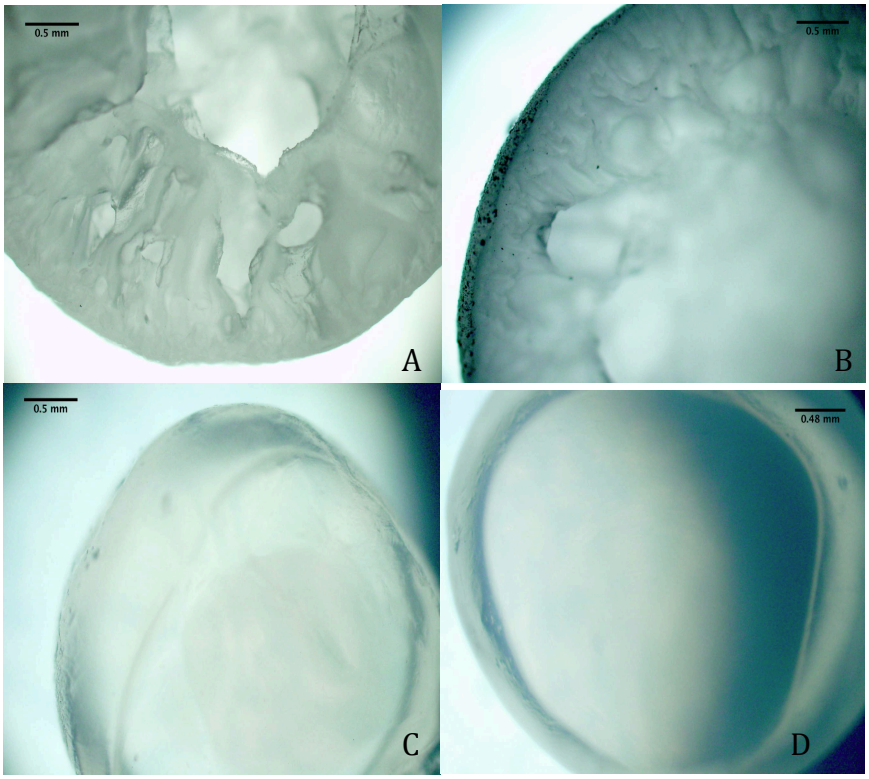

Figure 4-5: Microscopic images of the cross section of (A) PVA beads before exposure to long SWCNTs, (B) PVA beads after exposure to 500 µg/ml of long SWCNTs, (C) Alginate beads before exposure to long SWCNTs, and (D) Alginate beads after exposure to 500 µg/ml of long SWCNTs.

SEM images confirmed that SWCNTs penetrated into the PVA beads (Fig. 4-6) while no SWCNTs were observed inside the alginate beads. When the concentration of SWCNTs increased, the more SWCNTs penetrated into the PVA beads. The very dense or less porous microstructure of alginate could limit the diffusion of SWCNTs inside the matrix. Although the transport of SWCNTs into the PVA beads might be facilitated by the highly macroporous structure of the matrix, PVA may form crystalline coating around CNTs (Mansur et al., 2012) which might reduce the antibacterial effect of SWCNTs.

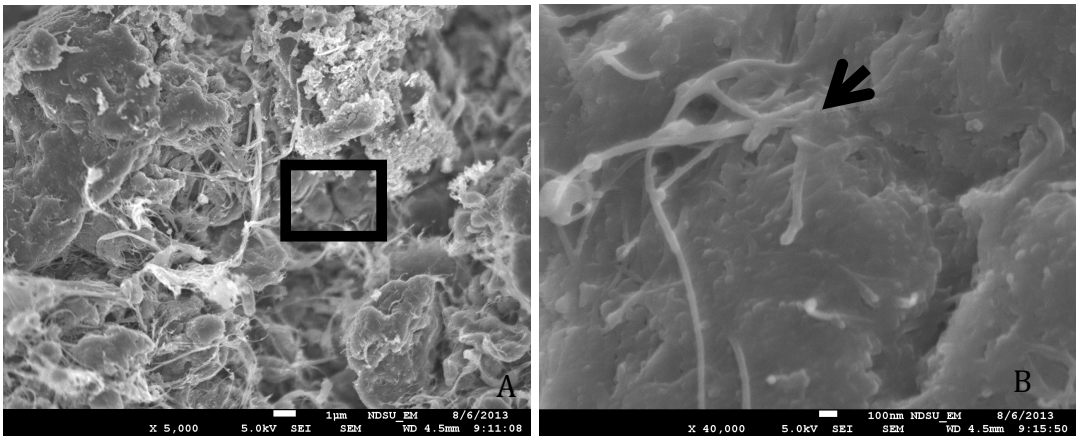

Figure 4-6: SEM images of outer layer of PVA beads after exposure to 500 µg/ml of long SWCNTs: (A) Bundle/Web of SWCNTs and (B) A close up image of the box in (A) showing SWCNT bundle/web (arrow).

4.4. Summary

The alginate and PVA entrapment mitigated the bactericidal effect of SWCNTs on the viability of cells. The three viability indictors used in this study provided consistent results. The bactericidal effect on entrapped cells was higher with increasing SWCNT concentration, lower initial cell density, and longer SWCNTs. Employing alginate and PVA matrices resulted in comparable protection of cell viability. Entrapped cells may be applied in treatment and remediation of water and wastewater contaminated with SWCNTs. This is the first report on nanomaterial toxicity mitigation by using cell entrapment.

CHAPTER 5: BACTERICIDAL EFFECT OF SINGLE WALL CARBON NANOTUBES ON ENTRAPPED CELLS IS FUNCTIONALITY DEPENDENT

5.1. Background

CNTs have been incorporated into many commercial products. Widely uses of CNTs in industries could potentially lead to CNTs releases to environment. The releases may be from disintegration of CNTs based products in landfills, incinerators, fire accidents and environments, and wastewater effluent from CNT related industries. When CNTs reach the environment, their transport through various matrices (air, water, soil, and sediment) may cause potential risks to various ecological receptors (Petersen et al., 2011). Microorganisms, especially bacteria, have an important role in ecosystems. Any negative effects on these essential bacteria by CNTs could lead to the environmental alteration. Many studies have been conducted on the bactericidal effect of CNTs (Brady-Estevez et al., 2008; Brady-Estevez et al., 2010; Nepal et al., 2008; Vecitis et al., 2010). Mostly, the toxicity was observed at high doses of CNTs. Kang et al (2007a, 2008, and 2009) reported the toxicity of CNTs on *E. coli*. CNTs exhibited the toxicity on *Vibrio fischeri* (Safekordi et al., 2012). Rodrigues et al. (2013) reported that soil microorganisms could be affected by the presence of single walled carbon nanotubes (SWCNTs), including microorganisms associated with the carbon and phosphorous cycling. The impacts varied among different microbial groups (Rodrigues et al., 2013).

Functionalized CNTs are one of the commonly used CNTs because of their potential for biomedical applications such as biosensors, drug and vaccine delivery devices, medical treatment, and tissue engineering (Kam and Dai, 2005; Kam et al., 2005a; Kam et al., 2005b; Vardharajula et al., 2012). The functionalization of CNTs alters their aggregation. Bare CNTs are hydrophobic but the functionalization can change their surface properties. In addition, the

functionalization can alter the biocompatibility. CNTs functionalized with polyethylene glycol were less toxic on soil microorganisms compared to bare CNTs (Tong et al., 2012). Amiri et al. (2012) reported that CNTs functionalized with lysine were more toxic than pristine CNTs. Some studies reported the enhancement of the antimicrobial activity of functionalized CNTs (f-CNTs) (Arias and Yang, 2009, Goyal et al., 2010) while another suggested that f-CNTs had no negative effect on cells (Roy et al., 2012). This discrepancy is the results of the differences in CNT size, functionalization, cell type, and buffer in experiments.

Even though the toxicity mechanism is not clear, direct contact between CNTs and bacteria seems to be a requirement. Membrane damage, morphology changes, stressed and inactive cells were the characteristics of the cells after exposure to CNTs (Kang et al., 2008a; Kang et al., 2008b; Kang et al., 2007a; Obraztsova et al., 2009; Young et al., 2012). Arias and Yang (2009) suggested that the close contact between the cells and CNTs damaged the cells by the CNTs needle-like action. Liu et al. (2010a) indicated the importance of direct contact between CNTs and *E. coli* and *Bacillus subtilis* cells and the formation of CNT aggregation for the toxicity.

The risk associated with CNTs has raised concerns and therefore finding methods to minimize the negative effects of CNTs is vital. Since direct contact between CNTs and cells is the main toxicity mechanism, Tabet et al. (2011) attempted to reduce the CNT effect on the lung cells by coating CNTs with polymer. In the study presented in Chapter 4, cells are entrapped in hydrogels, PVA and alginate and exposed them to pristine SWCNTs. Both PVA and alginate entrapment could lessen the bactericidal effect of SWCNTs on cells. The entrapment matrix acted as a shield to minimize the transport of SWCNTs into the beads so that the cells inside were not negatively affected. SWCNTs were only found at the outer layers of the beads. The

presence of SWCNTs at the outer layer of the beads was the results of the limited transport of the SWCNTs into the porous beads. SWCNTs with no functionalization, which mainly consist of pure carbon, are known to be chemically inert and therefore interact only physically with the beads. One of the most predominant CNTs in use is functionalized CNTs. The derived groups on the CNT surface may interact (attract or repel) with the entrapment matrix. Therefore, the impact of f-CNTs on entrapped cells may be different from that of pristine CNTs.

The goal of this study is to investigate the effects of SWCNTs with different surface functional groups, hydroxyl (-OH) and carboxylic (-COOH), on the viability of free *E. coli* cells and entrapped *E. coli* cells in PVA and alginate matrices. Covalent functionalization offers more secure conjunction of functional molecules (Zhang et al., 2010). Hydroxyl functionalized single wall carbon nanotubes (SWCNT-OHs) and carboxylic functionalized single wall carbon nanotubes (SWCNT-COOHs) are the common oxidized covalent functionalized CNTs because functional groups on oxidized CNTs provide great propensity for reacting with other compounds (Prato et al., 2008). The concentration of functionalized SWCNTs (f-SWCNTs), f-SWCNT length, and density of initial bacterial cells were variables examined. The effects of f-SWCNTs on the viability of free cells and entrapped cells were studied by using beta-D-galactosidase enzyme assay, plate count, LIVE/DEAD® Baclight™ assay, and RNA content analysis. The interaction between f-SWCNTs and matrices was examined by a regular microscopy.

5.2. Materials and Methods

5.2.1. Materials

The materials used in this study were the same as those listed in Chapter 4 except for SWCNTs. Two types of functionalized SWCNTs, SWCNT-OHs and SWCNT-COOH, with a

diameter of 1-2 nm, and a length of 0.5-2 μm (short f-SWCNTs) and 5-30 μm (long f-SWCNTs) were obtained from Cheap Tube Inc. (Brattlebro, VT, USA).

PVA, boric acid, sodium orthophosphate, sodium alginate, and calcium chloride were obtained from VWR international Inc. (West Chester, Pennsylvania, USA). 4-methylumbelliferyl-β-D-galactoside (Mugal), isopropyl-β-D-thiogalactopyranoside (IPTG), and Xgal were from Sigma Chemical Co. (MO, USA). *E. coli* ATCC 8739 was purchased from the Global Bioresource Center (American Type Culture Collection, VA, USA).

5.2.2. Media and culture conditions

E. coli ATCC 8739 was grown onto NA plates at 37°C. A single colony from the overnight incubation was grown in a liquid culture at 37°C under aerobic condition. The details of the procedure are described previously (Chapters 3 and 4).

5.2.3. Cell entrapment

A known amount of *E. coli* densities was entrapped in PVA and sodium alginate. The PVA entrapment followed the method of Pramanik et al. (2011). For alginate entrapment, a procedure by (Konsoula and Liakopoulou-Kyriakides, 2006) was modified and followed. The modification was to harden the alginate beads overnight.

5.2.4. Experimental setup, procedure, and design

All experiments were conducted in 50 ml glass bottles. Two different starting densities of *E. coli* ATCC 8739 (6.5 $\log_{10}$ CFU and 9.0 $\log_{10}$ CFU per test) for both free cells and entrapped cells were used in the experiments. The procedure to prepare these two cell densities is described in Chapter 3. f-SWCNT concentrations of 5, 10, 20, 50, 100, 200, 500, and 1000 μg/ml were used to determine the effects of f-SWCNTs on free cells and entrapped cells. The exposure experiment, which lasted 90 minutes, was conducted at room temperature with 800 rpm

mixing. The viability of free cells and entrapped cells after exposure to f-SWCNTs was quantified by using the galactosidase enzyme assay, LIVE/DEAD® Baclight™ assay, and RNA quantification. The detailed procedures of these three indicators were the same as those described in Chapters 3 and 4.

5.2.5. Microscopic evaluations

The surface and cross section of PVA and alginate beads after exposure to 500 μg/ml of short and long f-SWCNTs were observed by using a microscope (BX61™, Olympus, PA, USA) under a bright field mode.

5.2.6. Statistical analysis

The viability data of free and entrapped cells were analyzed by ANOVA and *t*-test at 5% significance level using Microsoft Excel 2011. ANOVA was first used to determine whether cell viability results (represented by galactosidase activity, live/dead baclight assay results, and RNA quantity) from different conditions (entrapment matrix including no entrapment, f-SWCNT concentration, cell density, and type of f-SWCNTs) are statistically different. When ANOVA showed that different conditions provided significantly different viability results, *t*-test was performed to obtain a *p*-value.

5.3. Results and Discussion

5.3.1. Effect of functionalized SWCNTs on free cell viability

5.3.1.1. Hydroxyl functionalized single wall carbon nanotubes

The effect of SWCNT-OHs on low density of *E. coli* cell viability is shown in Figs. 5-1A 5-2A, and 5-3A. The viability of free cells exposed to SWCNT-OHs slightly decreased with increasing of both short and long SWCNT-OH concentrations. There was no significant

difference in cell viability between each SWCNT-OH concentration and the next higher concentration for both short and long SWCNT-OHs.

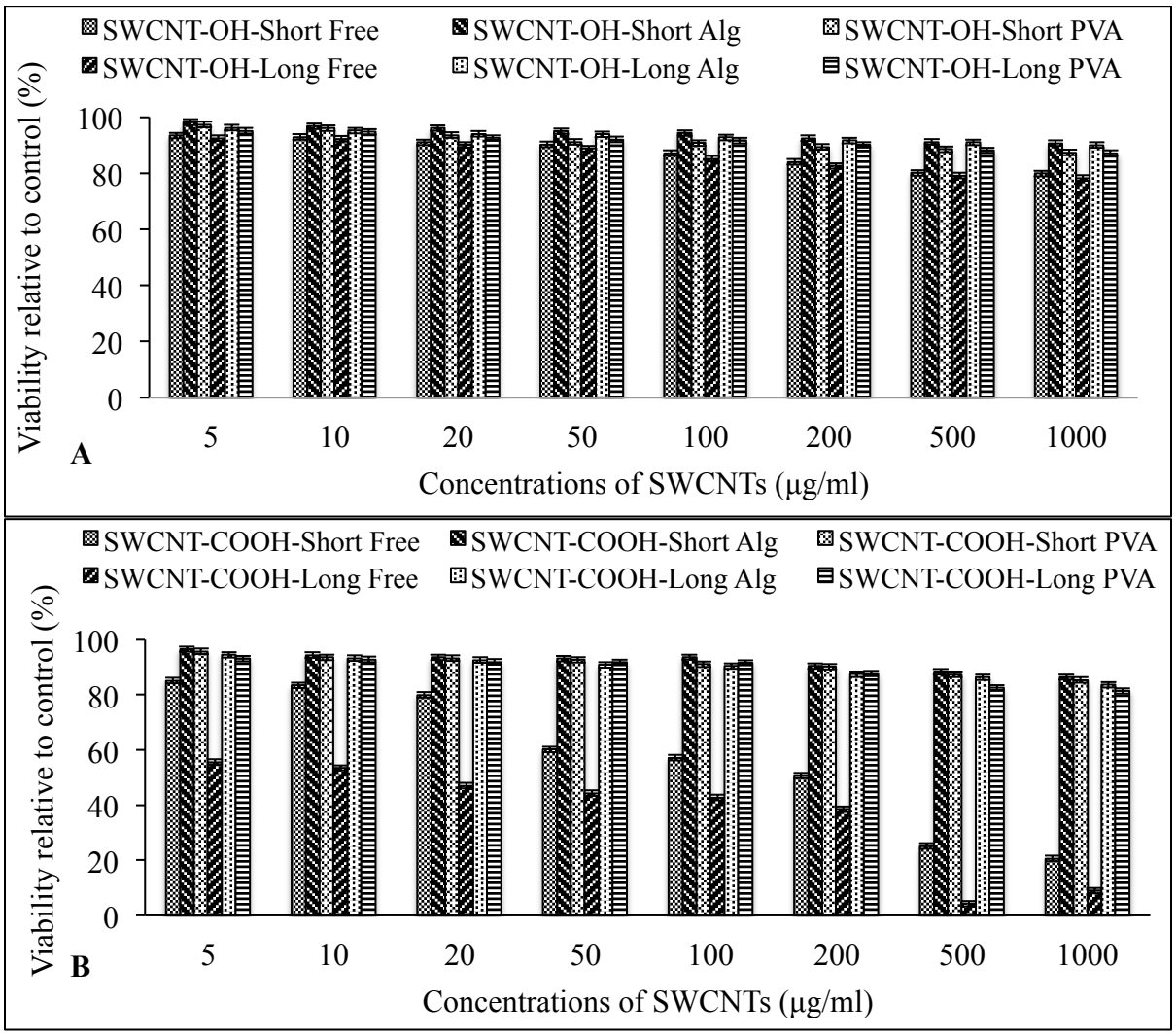

Figure 5-1: Effect of f-SWCNTs on viability of free and entrapped *E. coli* detected by the galactosidase enzyme assay - starting cell density of 6.5 $\log_{10}$ CFU test^{-1}. (A) SWCNT-OHs and (B) SWCNT-COOHs.

Arias and Yang (2009) reported similar results when *Salmonella* cells were exposed to short SWCNT-OHs (1 to 5 µm length). They suggested that high ionic strength of PBS might limit the direct contact between the cells and f-SWCNTs resulting in less effect on cell viability compared to pristine SWCNTs. There was no significant difference in the cell viability between

short and long SWCNT-OHs for all SWCNT-OH concentrations. The viability trend provided by the LIVE/DEAD® Baclight™ assay and RNA quantity were similar to that observed by the enzyme assay (Fig. 5-3A).

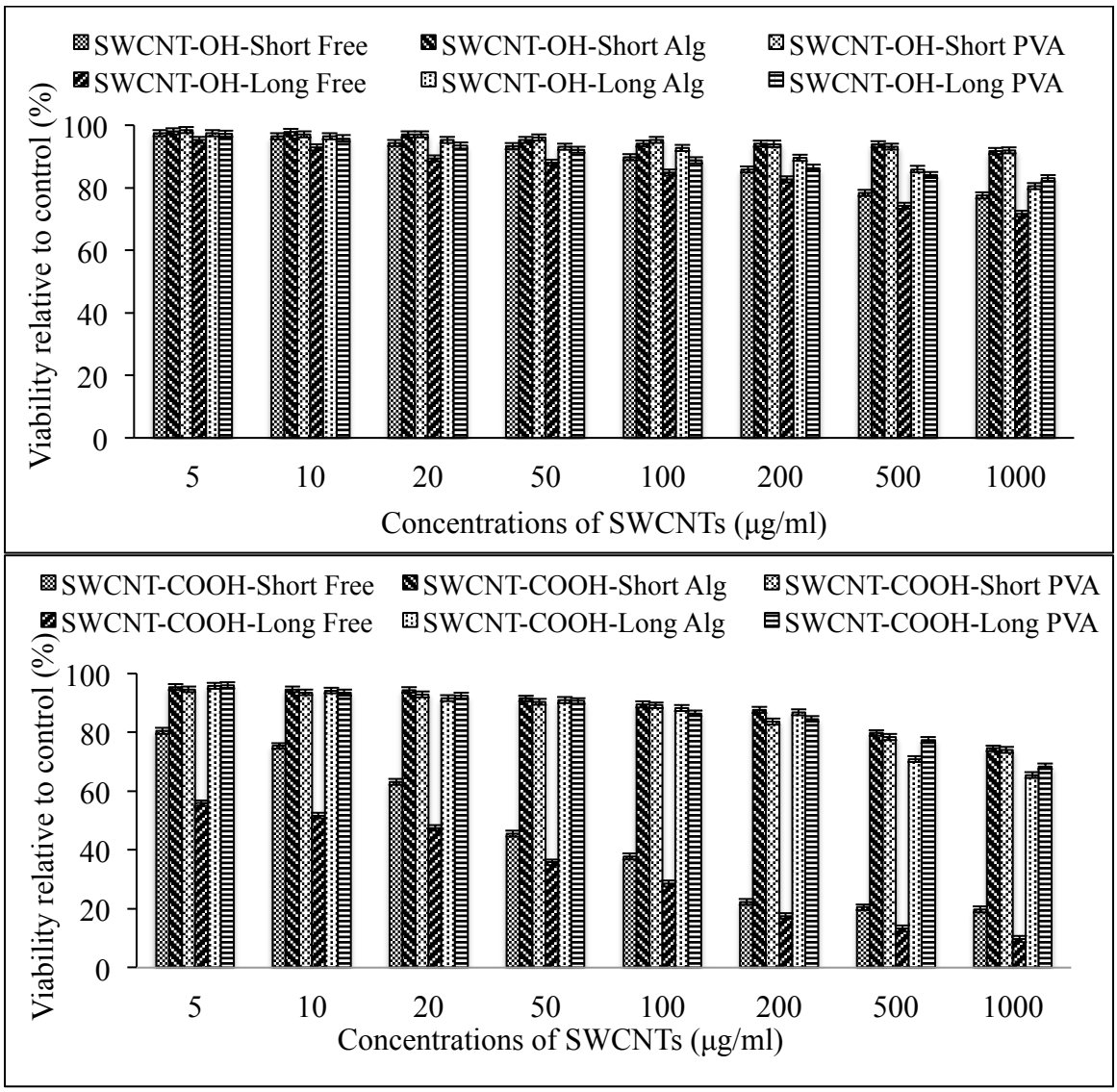

Figure 5-2: Effect of f-SWCNTs on viability of free and entrapped *E. coli* detected by the LIVE/DEAD® Baclight™ assay - starting cell density of 6.5 $\log_{10}$ CFU $test^{-1}$. (A) SWCNT-OHs and (B) SWCNT-COOHs.

The reduction in the viability of free cells exposed to SWCNT-OHs was less for the high initial cell density. However, the enzyme activity, membrane integrity, and RNA quantity based

viability results provided by the high initial cell density were not statistically different compared to the low initial cell density for both short and long SWCNT-OHs (Figs. 5-4A, 5-5A, and 5-6A) except the RNA quantity at high SWCNT-OH concentrations (500 and 1000 μg/ml). The viability of cells decreased with increasing short and long SWCNT-OH concentrations. Long SWCNT-OHs again did not exhibit more bactericidal effect compared to short SWCNT-OHs.

5.3.1.2. Carboxylic functionalized single wall carbon nanotubes

The -COOH functional group enhanced the bactericidal effect of SWCNTs on *E. coli* cells at the low cell density. The reduction in viability of free cells exposed to both short and long SWCNT-COOHs increased with increasing concentration of SWCNT-COOHs. The effects on enzyme activity (Fig. 5-1B), membrane integrity (Fig. 5-2B), and RNA quantity (Fig. 5-3B) were agreeable. Arias and Yang (2009) reported that SWCNT-COOHs did not exhibit the bactericidal effect on *Salmonella* cells in PBS. The reason of this discrepancy might be from the different bacteria strains and experimental conditions that were used in this study.

Increasing solubility of SWCNTs because of the carboxylic group (Usrey and Strano, 2009) might increase the contact area between the cells and f-SWCNTs and in turn caused more damage to the cells. Chen et al. (2012) reported the agglomeration of SWCNT-COOHs in long bundles and ropes due to the increase in interaction between SWCNT-COOHs via hydrogen bonding (between -COOH groups). The more agglomeration with increasing SWCNT-COOH concentration might decrease the contact area of SWCNT-COOHs and the cells resulting in its comparable effects between 500 and 1000 μg/ml of short SWCNT-COOHs. For long SWCNT-COOHs, this observation is also applicable.

The percent viability of free cells exposed to short SWCNT-COOHs was much higher than that exposed to long SWCNT-COOHs. As discussed above, this was not the case for

SWCNT-OHs as comparable limited bactericidal effects were observed between the two lengths. These results suggest that for f-SWCNTs that exhibited substantial bactericidal effect, increasing in their length led to more effect. The same trend was observed with pristine SWCNTs (Yang et al., 2010).

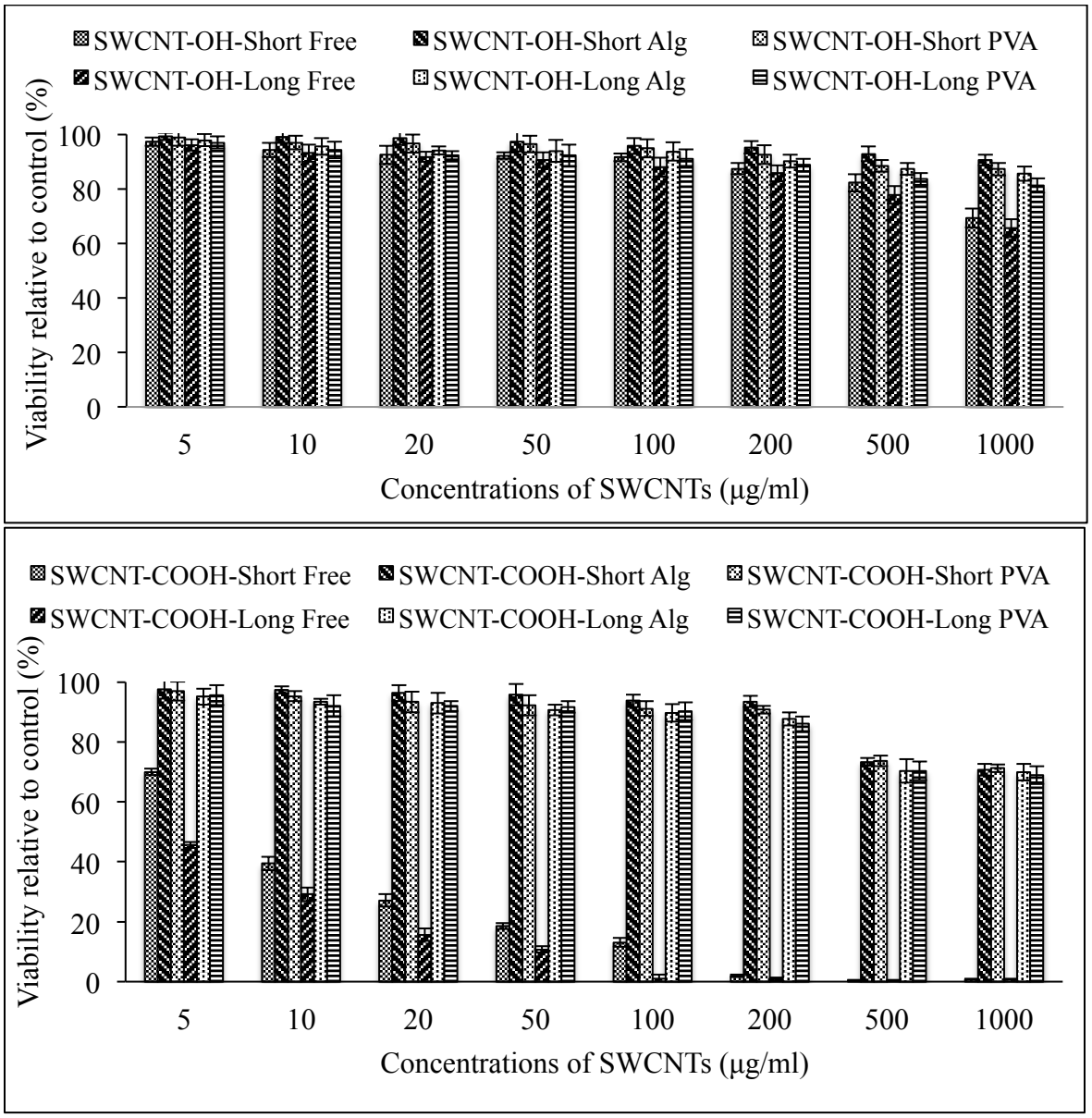

Figure 5-3: Effect of f-SWCNTs on viability of free and entrapped *E. coli* based on RNA quantification - starting cell density of 6.5 $\log_{10}$ CFU $test^{-1}$. (A) SWCNT-OHs and (B) SWCNT-COOHs.

At the high cell density, the viability of free cells exposed to short and long SWCNT-COOHs also dropped with increasing SWCNT-COOH concentrations (Figs. 5-4B, 5-5B, and 5-6B). The viability of the high cell density population was higher than that of the low cell density population. The increase in the number of cells enhanced the resistance of the population (Liu et al., 2000). As expected, long SWCNT-COOHs caused more bactericidal effect on the cells than short SWCNT-COOHs.

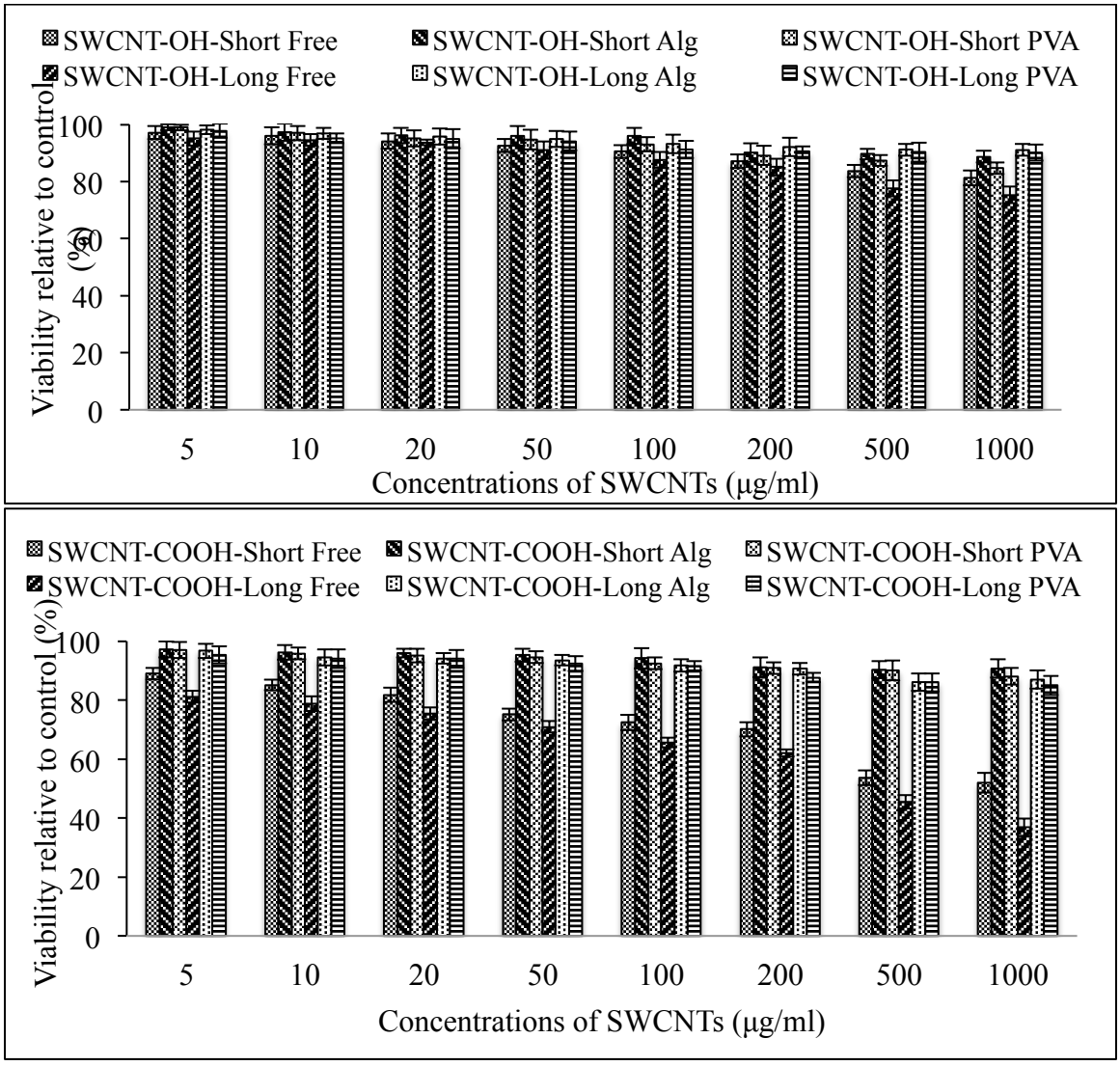

Figure 5-4: Effect of f-SWCNTs on viability of free and entrapped *E. coli* detected by the galactosidase enzyme assay - starting cell density of 9.0 $\log_{10}$ CFU $test^{-1}$. (A) SWCNT-OHs and (B) SWCNT-COOHs.

5.3.1.3. Hydroxyl functionalized single wall carbon nanotubes versus carboxylic functionalized single wall carbon nanotubes

The viability of free cells exposed to short and long SWCNT-OHs was much greater compared to that exposed to both short and long SWCNT-COOHs. Both SWCNT-OHs and SWCNT-COOHs have the same specific surface areas ($407 m^2/g$). Zeta potential values at pH of 7.4 were -30 to -35 and -45 to -47 mV for SWCNT-COOHs and SWCNT-OHs, respectively (Rosenzweig et al., 2013). The slightly higher zeta potential values of SWCNT-OHs suggested that, with the same specific surface, SWCNT-OHs are more stable in water compared to SWCNT-COOHs leading to lower tendency to form agglomerates associated with cytotoxicity (Coccini et al., 2010).

The mean adsorption energy per water molecule is larger for -COOH group than -OH group leading to a longer-range influence on the water nucleation process with -COOH group compared to that with -OH group (Collignon et al., 2005). However, while -OH group is saturated with 3 water molecules, -COOH group needs only 2 water molecules (Collignon et al., 2005). -COOH groups may also create the hydrogen bonding (Chen et al., 2012). This leads to an increase in agglomeration and in turn an increase in the toxicity effects on cells.

5.3.2. Effect of entrapment on the viability of cells exposed to f-SWCNTs

5.3.2.1. Hydroxyl functionalized single wall carbon nanotubes

Even the effects of SWCNT-OHs on the viability of the free and entrapped cells were limited; the cell viability protection by alginate and PVA entrapment was evident. For the low cell density, the mitigation effect of entrapment was observed clearly at high SWCNT-OH concentrations from 100 to 1000 μg/ml. Statistically, the matrix type had no effect on the viability at all f-SWCN concentrations for both short and long SWCNT-OHs.

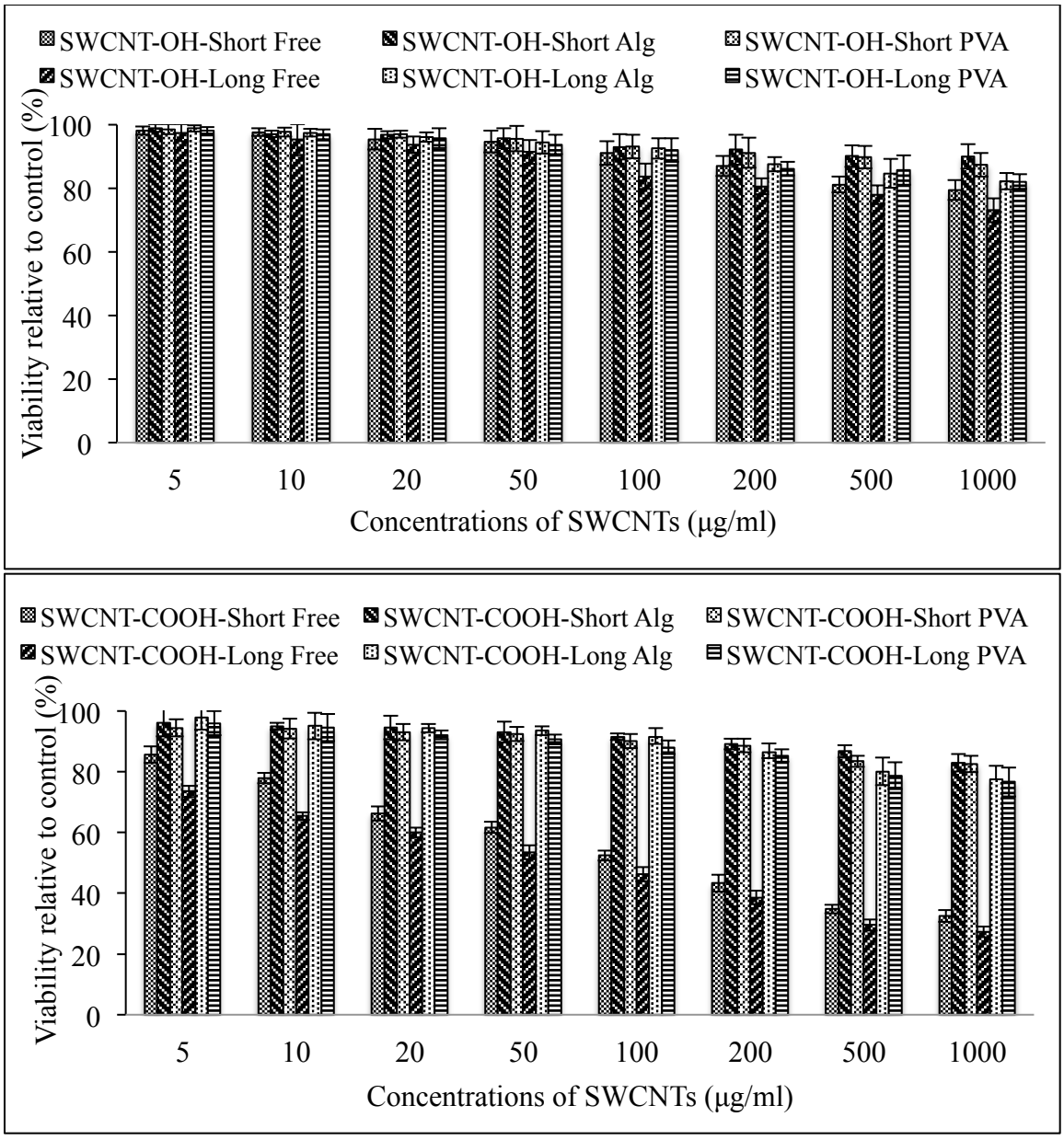

Figure 5-5: Effect of f-SWCNTs on viability of free and entrapped *E. coli* detected by the LIVE/DEAD® Baclight™ assay - starting cell density of 9.0 $\log_{10}$ CFU $test^{-1}$. (A) SWCNT-OHs and (B) SWCNT-COOHs.

Again, for exposure to both short and long SWCNT-OHs, both alginate and PVA entrapped cells showed higher viability than free cells at the high initial cell density. The effect of SWCNT-OHs on the viability of free cells was very minimal for low SWCNT-OH concentrations ranging from 5 to 200 μg/ml. As a result, the cell protection by the

entrapment was not definite. There was no significant difference in percent cell viability between the alginate and PVA entrapment for both short and long SWCNT-OHs.

5.3.2.2. Carboxylic functionalized single wall carbon nanotubes

Alginate and PVA entrapment lessened the toxicity effect of SWCNT-COOHs. The viability of entrapped cells in both alginate and PVA was significantly greater than that of free cells for both low and high cell densities. The viability of entrapped cells with alginate and PVA decreased with increasing concentrations of short and long SWCNT-COOHs. However, the decrease was very gradual and much less than that of the free cells.

For PVA entrapment, there was no significant difference in entrapped cell viability between each SWCNT-COOH concentration and the next higher concentration for both short and long SWCNT-COOHs. For the PVA beads, the affinity between -COOH groups of f-SWCNTs and phosphate (-POOH) groups bonded to PVA might interfere with the diffusion of SWCNT-COOHs into the beads. Additionally, PVA may form the crystalline coating around CNTs (Mansur et al., 2012); therefore this might reduce the antibacterial effects of SWCNT-COOHs.

Strong and stable calcium alginate gels with most of -OH and -COOH groups having high affinity to Ca^{2+} might limit the diffusion of SWCNT-COOHs into the beads. Therefore, SWCNT-COOHs had limited or no contact with the cells that were entrapped deep inside. Additionally, the effects of long and short SWCNT-COOHs did not statistically differ because of the diffusion limitation of SWCNT-COOHs into the beads. This trend was observed with all the viability methods used in this study including the galactosidase enzyme assay, LIVE/DEAD® Baclight™ assay, and RNA quantification. There was no significant difference in the viability of entrapped cells in alginate and PVA for all treatments.

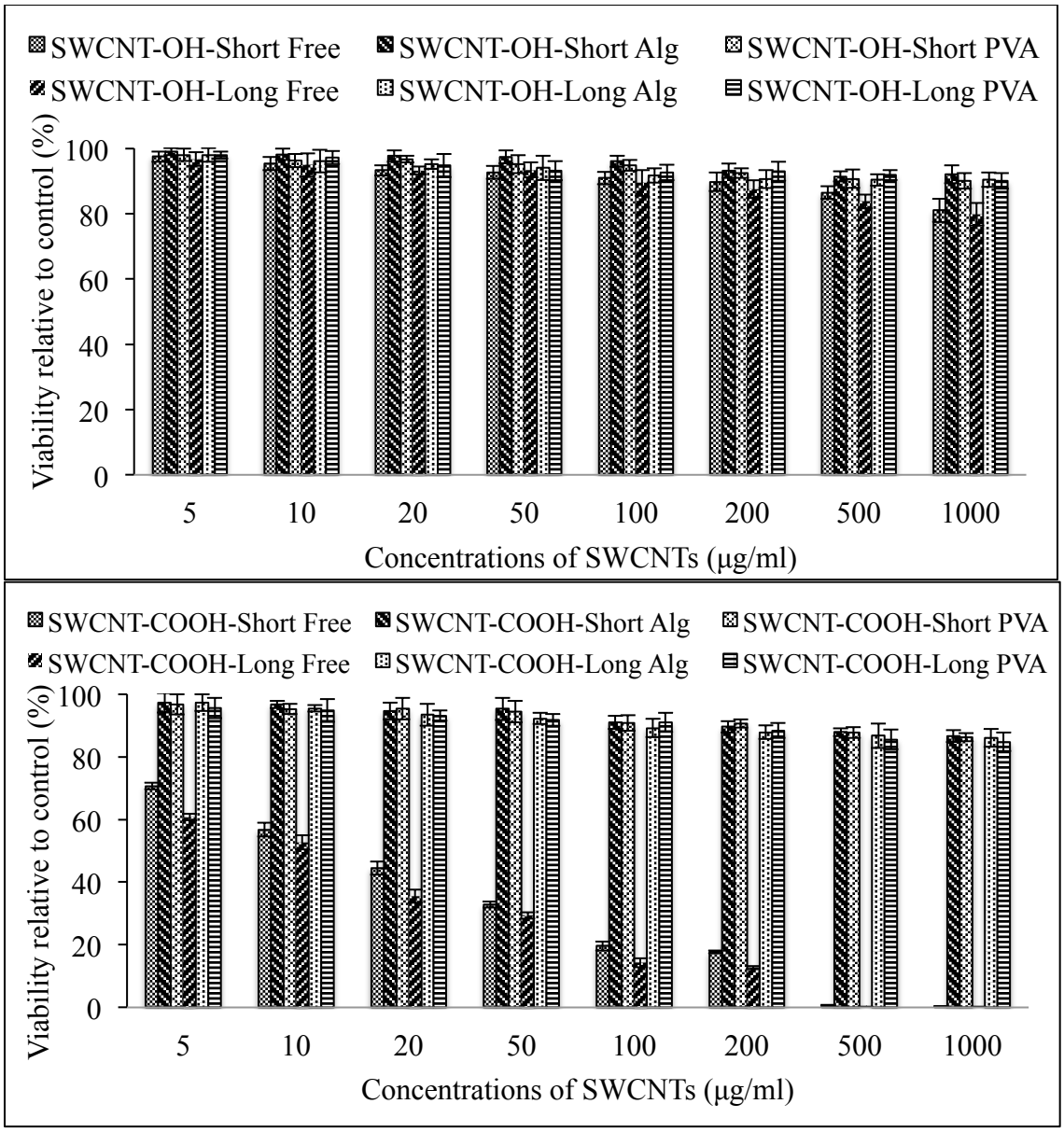

Figure 5-6: Effect of f-SWCNTs on viability of free and entrapped *E. coli* based on RNA quantification - starting cell density of 9.0 $\log_{10}$ CFU $test^{-1}$. (A) SWCNT-OHs and (B) SWCNT-COOHs.

5.3.2.3. Hydroxyl functionalized single wall carbon nanotubes versus carboxylic functionalized single wall carbon nanotubes

Regardless of the length of f-SWCNTs, the viability of free cells and entrapped cells in alginate exposed to SWCNT-OHs was slightly higher than that exposed to SWCNT-COOHs. Fig.

5-7 shows that there were more SWCNT-COOHs than SWCNT-OHs attached to the surface of the PVA beads. Therefore, SWCNT-COOHs had more contact opportunity to the entrapped cells than SWCNT-OHs. The entrapped cells close to the PVA bead surface were likely more affected by SWCNT-COOHs than SWCNT-OHs.

Regardless of the functional groups, there are no difference in the protection ability between PVA and alginate. As mentioned above, the hydrogen bonds between -POOH group of PVA and functional groups of CNTs may help in minimizing the transport of f-SWCNTs into the beads. Alginate is a linear copolymer of α-L-guluronate and β-D-mannuronate. Alginate displays an affinity toward multivalent cations such as Ca^{+2}. Alginate binds to those ions selectively and cooperatively and forms ionically cross-linked alginate gels (Draget et al., 1997). Calcium ions are located in electronegative cavities, like eggs in an egg-box. The ionic interactions make alginate gels strong and stable. The affinity of hydroxyl and carboxyl groups to Ca^{+2} in the egg box structure of calcium alginate might limit the interactions between f-SWCNTs and alginate gel, minimizing the diffusion of f-SWCNTs into the beads.

5.3.3. Microscopic observations

The macro-porous structure and the very dense porous structure were observed at the surface of PVA and alginate beads, respectively. After exposure to f-SWCNTs, the surface of PVA beads were covered by f-SWCNTs while less f-SWCNTs were detected on the surface of alginate beads (Figs. 5-7 and 5-8). This might be explained by the high affinity between -COOH or -OH groups of f-SWCNTs to -POOH group of PVA beads. However, cross section bead images showed that most f-SWCNTs were kept in the outer layer the beads. Therefore, there was no significant difference in the ability to lessen the bactericidal effects of f-SWCNTs between PVA and alginate.

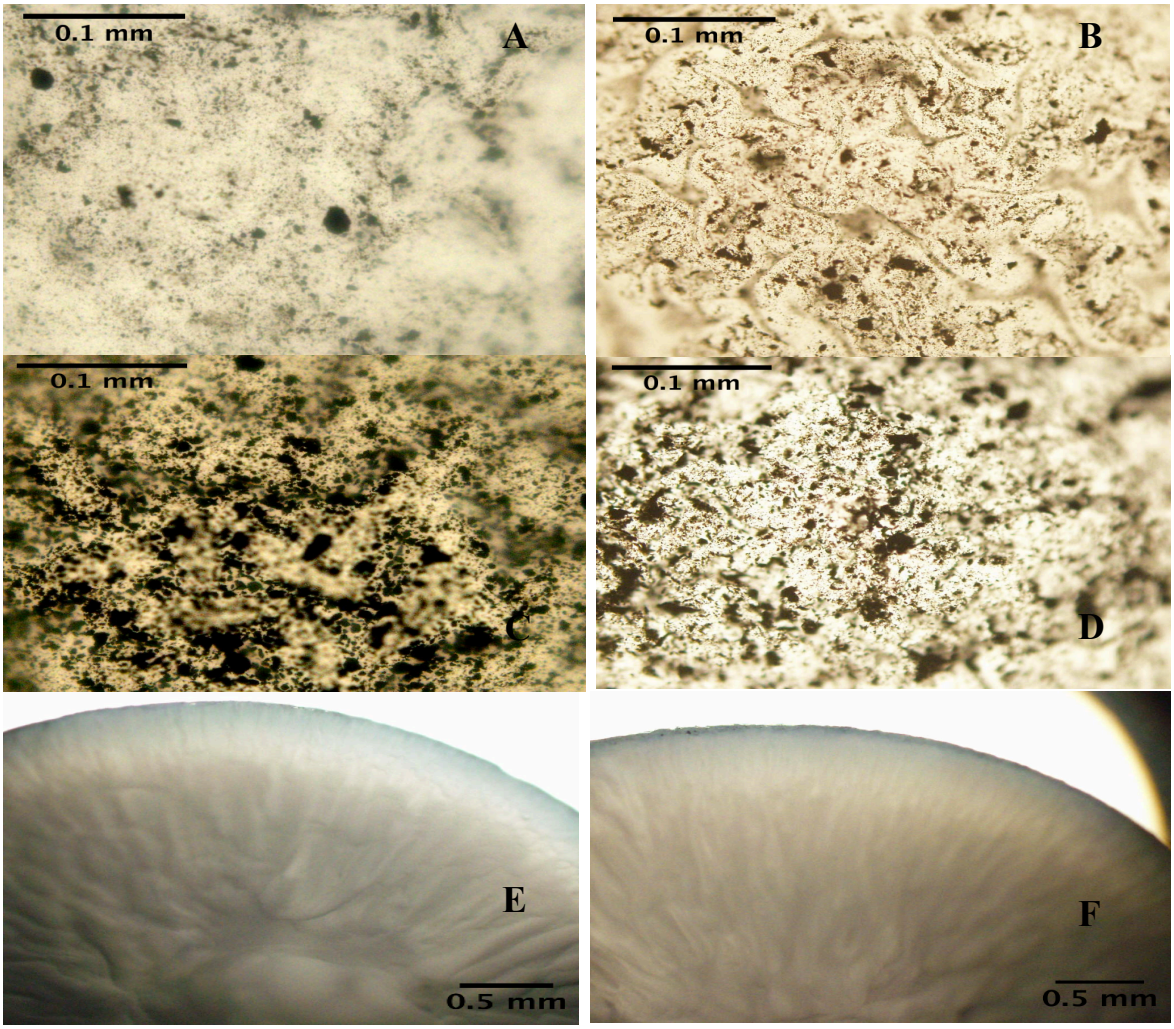

Figure 5-7: Microscopic images of PVA beads (A) Bead surface after exposure to 500 µg/ml of short SWCNT-OHs, (B) Bead surface after exposure to 500 µg/ml long SWCNT-OHs, (C) Bead surface after exposure to 500 µg/ml of short SWCNT-COOHs, (D) Bead surface after exposure to 500 µg/ml long SWCNT-COOHs, (E) Bead cross-section before exposure to 500 µg/ml of short SWCNT-COOHs, and (F) Bead cross-section after exposure to 500 µg/ml of short SWCNT-COOHs.

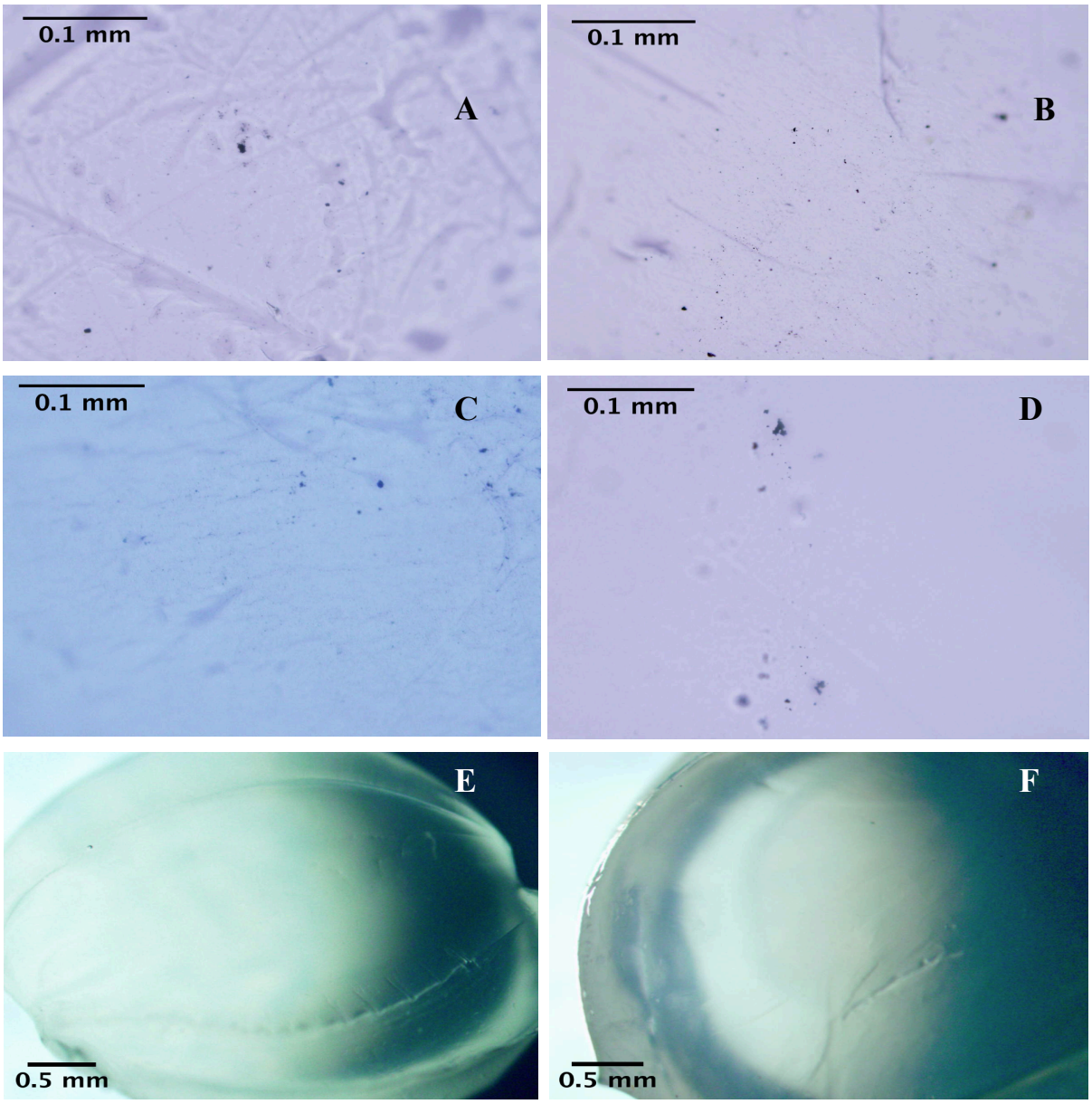

Figure 5-8: Microscopic images of alginate beads (A) Bead surface after exposure to 500 µg/ml of short SWCNT-OHs, (B) Bead surface after exposure to 500 µg/ml long SWCNT-OHs, (C) Bead surface after exposure to 500 µg/ml of short SWCNT-COOHs, (D) Bead surface after exposure to 500 µg/ml long SWCNT-COOHs, (E) Bead cross-section before exposure to 500 µg/ml of short SWCNT-COOHs, and (F) Bead cross-section after exposure to 500 µg/ml of short SWCNT-COOHs.

5.4. Summary

SWCNT-OHs and SWCNT-COOHs exhibited the bactericidal effect on the viability of *E. coli* cells. The chemical behavior of functional groups of CNTs resulted in different levels of antibacterial effects. SWCNT-COOHs caused more damage to the cells than SWCNT-OHs. Effect of length of f-SWCNTs on the cell viability depended on the functional group. While there was no difference in the impact of short and long SWCNT-OHs, the long SWCNT-COOHs was more toxic than the short SWCNT-COOHs. The alginate and PVA entrapment provided similar levels of protection of the cell viability against f-SWCNTs. This study provides more understanding on how the entrapment can limit the bactericidal effect of functionalized CNTs.

CHAPTER 6: ALTERATIONS OF GENE AND PROTEIN EXPRESSIONS OF ESCHERICHIA COLI EXPOSED TO CARBON NANOTUBES

6.1. Background

CNTs are an ideal material for many prominent commercial applications. Several commercial products in microcopy, transparent conductive films, composite materials, and energy storage contain CNTs. Varieties in lengths, width, aspect ratios, dispersion, surface coating and functionalization of CNTs enhance their applications, but may also contribute to their cytotoxicity.

Although many studies have been carried on the cytotoxicity of CNTs (Arias and Yang, 2009; Kang et al., 2008a; Kang et al., 2008b; Kang et al., 2007a; Rodrigues et al., 2013), very little is known about the molecular response by bacterial cells to CNT insults. CNTs induced DNA damage, and increased mutations in mouse embryonic stem cells (Zhu et al., 2007). Sargent et al. (2012) showed that CNTs cause abnormal mitosis. Pacurari et al. (2011) found that 7 genes out of 63 lung cancer biomarker genes, including *Arpgap19, Nos2, Shh, Wif1, Mt3, Ccdc99,* and *Msx2,* changed the expression after a 7 day exposure to CNTs. The cellular signaling and gene expression changed in human small airway epithelial cells after exposed to CNTs (Snyder-Talkington et al., 2013). CNTs induced differential protein expression in Calu-3 cells (Li et al., 2013) and intestinal epithelial cells (Lai et al., 2013).

Comprehensive analyses of differential gene and protein expressions can be utilized to explain complex bactericidal effects of CNTs. Few studies have investigated CNTs effects on gene expression on bacteria. Kang et al. (2008a) reported that CNTs caused greater than 2 fold up-regulation of genes involved in *sox*RS and *oxy*R systems, regulators of *E. coli* responding to oxidative stress. Berdjeb et al. (2013) reported that CNTs also caused increased expression of

rpoS, groEL, and *dnaK* genes in the marine bacteria, *Vibrio splendidus*. There have been no studies on the protein expression dynamics in bacteria exposed to CNTs.

Most organisms react to the environmental stress with a programmed series of responses. Typically, stress response mechanisms are then triggered in order to adapt to the new environment. Phage shock protein (Psp) system, an extracytoplasmic stress response system, that is responsible for repairing damage to the inner membrane, was first discovered in *E. coli* (Brissette et al., 1990), and is commonly found in Gram-negative bacteria (Joly et al., 2010; Kobayashi et al., 2007). The Psp system was first discovered in *E. coli* (Brissette et al., 1990). The Psp is essential during macrophage infection by *Salmonella enterica* (Eriksson et al., 2003) and *Shigella flexneri* (Lucchini et al., 2005), and is over-expressed in *E. coli* during biofilm formation of (Beloin et al., 2004) and in response to environmental and intracellular stresses (Weiner and Model, 1994).

The Psp system contains the genes coding for *PspA, PspB, PspC, PspD,* and *PspE;* and four single-gene units for *PspF, PspG*, and *ArcA* and *ArcB* (Huvet et al., 2011). In *E. coli*, *PspA* binds and inhibits PspF under non-stress conditions. The *PspB* and *PspC* which are activated under stress conditions, and then disrupt the PspA-PspF inhibitor complex resulting in *PspF* release. *PspA* is an effector of the response that is likely involved in maintaining the proton motive force (Kleerebezem et al., 1996; Kobayashi et al., 2007). The system is induced by heat, ethanol, osmotic shock, defect in protein transport across the cytoplasmic membrane, and overproduction of some integral membrane proteins including secretins (Darwin, 2005; Joly et al., 2010; Model et al., 1997). Cell membrane integrity has been linked to Psp expression (Adams et al., 2003; Adams et al., 2002).

Membrane perturbation has been proposed as a primary mechanism of CNT toxicity, and, therefore, Psp gene expression may be altered. The objective of this study was to investigate the impact of CNTs on the expression of genes and proteins in *E. coli* Psp system. Changes in *pspA*, *pspB* and *pspC* expressions were determined using quantitative reserve transcriptase PCR (RT-PCR). Protein expression was determined by using sodium dodecyl sulfate polyacrylamide gel electrophoresis (SDS-PAGE), western blot, and 2D electrophoresis. *E. coli* was used as a model organism because it is frequently used to assess the impact of CNTs on bacteria (Kang et al., 2007a, 2008; Arias and Yang, 2009). The benefits of using *E. coli* include the Profiling of *Escherichia coli* Chromosome database (http://www.shigen.nig.ac.jp/ecoli/pec/), Coli Genetic Stock Centre (Maloy and Hughes, 2007), and EcoProDB (http://eecoli.kaist.ac.kr/main.html), which provide a wealth of genetic and proteomic information on *E. coli*.

6.2. Materials and Methods

6.2.1. Bacterial strain and growth conditions

E. coli ATCC 8739 was obtained from the Global Bioresource Center (American Type Culture Collection, VA, USA). A single colony from the overnight incubation was used to prepare a liquid culture for the experiments. This liquid culture was in turn incubated overnight at 37°C and shaken continuously at 1,500 rpm (Lab-line® orbital shaker 3590, IL, USA). The cells were harvested during the stationary growth phase by pelleting at 4500× *g* for 15 min. Pellets were washed twice in a PBS before they were used in experiments.

6.2.2. Single-walled carbon nanotubes

Pristine SWCNTs and functionalized SWCNTs including hydroxyl functionalized single wall carbon nanotubes (SWCNT-OHs) and carboxylic functionalized single wall carbon nanotubes (SWCNT-COOHs) with a diameter of 1-2 nm, and a length of 0.5-2 μm (short

SWCNTs) and 5-30 μm (long SWCNTs) were obtained from Cheap Tube Inc. (Brattlebro, VT, USA). The pristine SWCNTs were purified to remove silica, cobalt, and amorphous carbon before being used in experiments. The purification procedure of SWCNTs is described in Chapter 3. Most of metal residues and amorphous carbon were removed by the purification as presented in Chapter 3.

6.2.3. Experimental setup and procedure

Glasses bottles (50 ml) were used for incubation experiments. A starting *E. coli* ATCC 8739 density of 6.5 $\log_{10}$ CFU per test was used. To determine the effects of SWCNTs on gene and protein expression, the working SWCNT concentrations of 10 and 100 μg/ml were tested. A control incubation bottle (no SWCNTs) was operated in parallel. The mixture of cells and SWCNTs was stirred using a magnetic stirrer at 75× *g* for 90 min at room temperature. Cells were harvested and washed twice in PBS before being used in the experiments.

6.2.4. Sample preparations for gene and protein analyses

6.2.4.1. RNA isolation and cDNA synthesis

Total RNA was extracted and purified by using the GenElute^{TM} Bacterial Total RNA Miniprep Kit (Quiagen, MD, USA). The RNA concentration in ng/ml was determined by using a Nanodrop spectrophotometer (model 1000 uv/vis) based on a 260 nm to 280 nm absorbance ratio (A260/A280). To generate cDNA, 2 μg of total RNA was mixed with random primers. The mixture was first heated for 5 min at 70°C and then cooled down to 4°C using a thermo-cycler. The reverse transcriptase master mix was then added. The reverse transcription program included the following thermal conditions: 60 min at 37°C, 10 min at 70°C, and cool down at 4°C. Controls in which no reverse transcriptase was added, were also included. The cDNA was kept at -20°C before using it in qPCR.

6.2.4.2. Protein isolation

Proteins were extracted according to the protocol by Mario Lebendiker (http://wolfson.huji.ac.il/purification/TagProteinPurif/Lysis_Bacterial_Cells.html) with some modifications as follows. After sonication in lysis buffer, the sample was put in nitrogen liquid for 1 min and then in water bath of 65°C for 5 min. This freezing and thawing step was repeated 5 times.

6.2.5. Quantitative PCR and data analysis

The SYBR qPCR assay was performed as described by Horne and Pruss (2006). Unlabeled cDNA, iQ SYBR Green Supermix (Bio-Rad), and primers specific for *psp*A (For: 5'-TGCCAACATCAACGCTCTGT-3' and Rev: 3'-CGGCGAGTCAGCTGTTTCTT-5'), *psp*B (For: 5'- GCGCGCTATTTCTGGCTATTC-3' and Rev: 3'-CTTTGCGACAATTCACTGCGA-5'), and *psp*C (For: 5'-TTTGCGCTTGATCCAATGCC -3' and Rev: 3'-GTTTCACTTGCCGCCAGTTC-5') were included. RT-PCR data were analysed by using a comparative threshold cycle (C_T) method and *gap*C as an endogenous reference.

6.2.6. SDS-PAGE and data analysis

Proteins were separated using SDS-PAGE, using the procedure described in the Mini-Protean tetra cell instruction manual (Bio-Rad). Prior to electrophoresis, protein aliquots were incubated in SDS reducing buffer for 4 min at 95°C. Electrophoresis was performed at 4°C on ice using a mini-protean tetra unit (Bio-Rad). The gel was run at 150 mA. Separated proteins in the unit were fixed and stained with the Biosafe Coomassie stain (Bio-Rad).

6.2.7. Western blots and data analysis

Proteins were separated by SDS-PAGE and transferred on to a PVDF membrane using a wet/tank blot system (Bio-Rad). Western blotting was performed as described by Novus Biologicals (http://www.novusbio.com) using polyclonal rabbit anti-PspA (1:10,000), polyclonal rabbit anti-PspB (1:5,000), and polyclonal rabbit anti-PspC (1:5,000) as primary antibodies (all provided by J. Tommassen, Institute for Biodynamics and Biocomplexity, Utrecht University, The Netherlands). Goat anti-rabbit-horseradish peroxidase (1:10,000) was used as a second antibody (Bio-Rad). Proteins were detected using the Immun-Blot Opti-4CN colorimetric kit (Bio-Rad). Images of membranes were captured using an Alpha Innotech FluorChem® Imaging System. Relative band intensities of Western blots were calculated using ImageJ 1.48o, which was obtained from the National Institute of Health (http://rsb.info.nih.gov/ij/).

6.2.8. Two dimensional electrophoresis and image analysis

Two dimensional (2D) gel electrophoresis of whole cell proteins followed the procedure described in ReadyPrep 20D Starter Kit (Bio-Rad). Extracted protein was used to analyze the alternation in proteome of *E. coli* ATCC 8739 exposed to 10 and 100 μg/ml of pristine SWCNTs (short and long), SWCNT-OHs (short and long), and SWCNT-COOHs (short and long). This fraction was loaded onto precast immobilized pH gradient strips with a pH gradient of 3.0 to 10.0 for separation in the first dimension. The strips then were loaded onto the 8-16% Tris-HCl ready gel precast gels (Bio-Rad) to separate the proteins in the second dimension. Proteins were stained by using the Biosafe Coomassie stain and silver stain Plus kit (Bio-Rad). Gel images were acquired immediately using an Alpha Innotech FluorChem® Imaging system and analyzed using Delta2d obtained from Decodon (http://www.decodon.com).

6.3. Results and Discussion

6.3.1. Proteomic profiles of *Escherichia coli* ATCC 8739 exposed to SWCNTs

Whole cell proteins were examined in *E. coli* ATCC 8739 following exposure to 10 and 100 μg/ml of pristine SWCNTs, SWCNT-OHs, and SWCNT-COOHs. Both short and long of each type were experimented. More than 150 protein spots were visualized on the silver stained 2-DE gel (Fig. 6-1A-M). Most of the protein spots tended to be in the area corresponding to pH 4 to 7, which is agreement with previous study in *E. coli* (Marisch et al., 2013). The alterations in the quantity and intensity of protein spots were observed when comparing the 2-D patterns of the control (no exposure to CNTs) and 12 treatments (Table 6-1). Fewer proteins were observed at the higher CNT concentration (100 μg/ml).

Regulation in bacteria under the stress condition is complex (Reid et al., 2008), and protein composition of a cell is continually adjusted in order to meet the challenges of the changing environment (Renzone et al., 2005). After exposure to 10 μg/ml of CNTs, changes in the protein expression level may help the cells respond to the stress conditions. Cell death at the higher CNT concentration (100 μg/ml) may explain the reduction in number of proteins detected. Bacteria undergo change in gene expression and protein expression in response to stress (Storz et al., 2000). Phage shock proteins (Psp) are stress proteins in *E. coli*. The expression of *pspA* is shown in Fig. 6-2 A to G. Proteins were stained by using Bio-Safe Coomassie. The location of *pspA* was determined based on a 2D electrophoresis map reported by Champion et al. (2003). While the intensity of two protein spots representing *pspA* of cells exposed to 10 μg/ml of short and long pristine SWCNTs, SWCNT-OHs, and SWCNT-COOHs for both short and long was higher than that of the control, the intensity was lower in cells exposed to 100 μg/ml, with the exception of cells treated with short and long SWCNT-OHs.

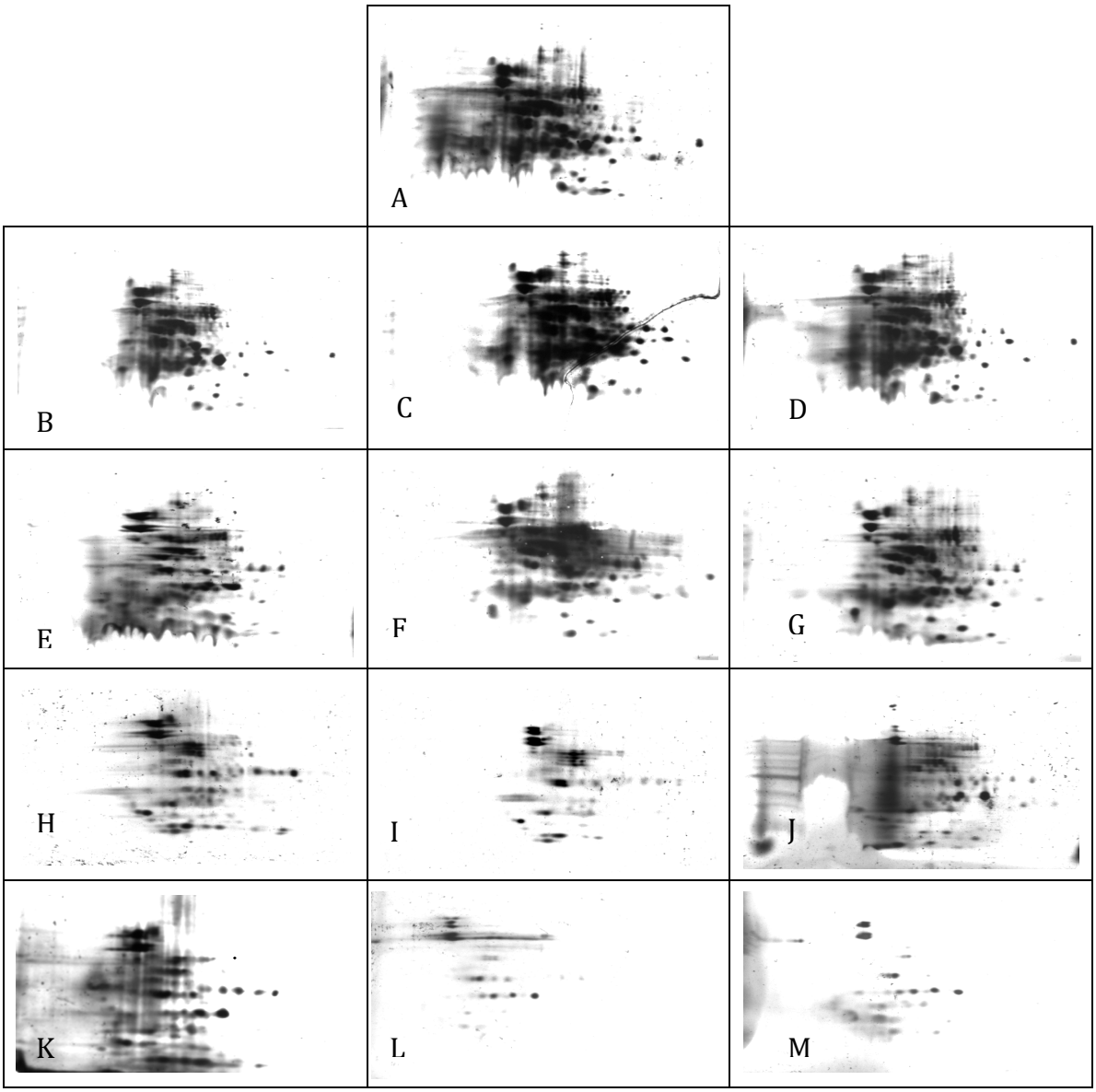

Figure 6-1: 2D-Electrophoresis analysis of protein in *E. coli* cells exposed to (A) No SWCNTs (control), (B-G) 10 μg/ml of SWCNTs, and (H-M) 100 μg/ml of SWCNTs. (B) Short pristine SWCNTs, (C) Long pristine SWCNTs, (D) Short SWCNT-OHs, (E) Long SWCNT-OHs, (F) Short SWCNT-COOHs, (G) Long SWCNT-COOHs, (H) Short pristine SWCNTs, (I) Long pristine SWCNTs, (J) Short SWCNT-OHs, (K) Long SWCNT-OHs, (L) Short SWCNT-COOHs, and (M) Long SWCNT-COOHs.

Table 6-1: Regulations of the protein expressions in *E. coli* cells due to exposure to SWCNTs.

Control vs. Treatment		Number of spots				
		No difference	Up-regulated	Down-regulated	Only in control	Only in treatment
10 μg/ml	Short SWCNTs	25	64	52	39	0
	Long SWCNTs	13	53	71	43	8
	Short SWCNT-OHs	30	75	62	13	3
	Long SWCNT-OHs	20	79	65	27	5
	Short SWCNT-COOHs	24	64	66	26	7
	Long SWCNT-COOHs	12	73	80	15	12
100 μg/ml	Short SWCNTs	8	2	62	98	10
	Long SWCNTs	4	3	46	121	6
	Short SWCNT-OHs	2	2	64	109	3
	Long SWCNT-OHs	4	2	74	89	11
	Short SWCNT-COOHs	2	11	29	138	0
	Long SWCNT-COOHs	2	2	37	139	0

pspA plays a role in maintaining proton motive force and is involved in alteration of cell membrane integrity (Adams et al., 2002; Weiner and Model, 1994). The toxicity mechanisms of CNTs were proposed including direct contact between CNTs and cells, and then alteration of the cell membrane integrity (Kang et al., 2008a; Kang et al., 2008b; Kang et al., 2007). As a result, cells may express *pspA* as part of stress response to the low CNT concentration, but not to the higher concentration of CNTs, because of a possibility for more immediate cell death.

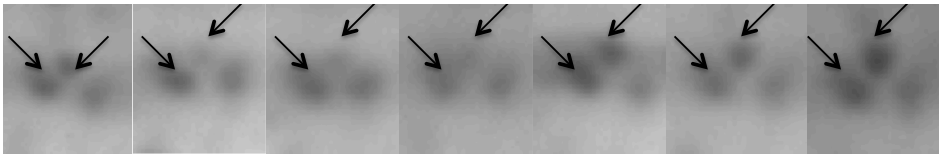

Figure 6-2: 2D-Electrophoresis analysis of *pspA* protein in *E. coli* cells exposed to (A) No SWCNTs (control), (B) Short pristine SWCNTs (C) Long pristine SWCNTs, (D) Short SWCNT-OHs, (E) Long SWCNT-OHs, (F) Short SWCNT-COOHs, and (G) Long SWCNT-COOHs.

6.3.2. Identification of altered phage shock proteins related to CNTs exposure by Western blots.

Previous studies have shown that a reduction in membrane potential induces the phage shock proteins expression, including *pspA* (Jovanovic et al., 2010; Jovanovic et al., 2006). The Western blots showed that *pspA* expression of *E. coli* cells exposed to 10 μg/ml of CNTs was higher than that of the control (Fig. 6-3). The data also showed 1.27, 1.35, 3.10, 4.05, 5.35, and 5.65-fold increases in *pspA* expression level of cells exposed to 10 μg/ml of short SWCNT-OHs, long SWCNT-OHs, pristine short SWCNTs, pristine long SWCNT, short SWCNT-COOHs, and long SWCNT-COOHs, respectively. These results indicated that the phage shock pathway of *E. coli* is induced following exposure to 10 μg/ml of CNTs exposure.

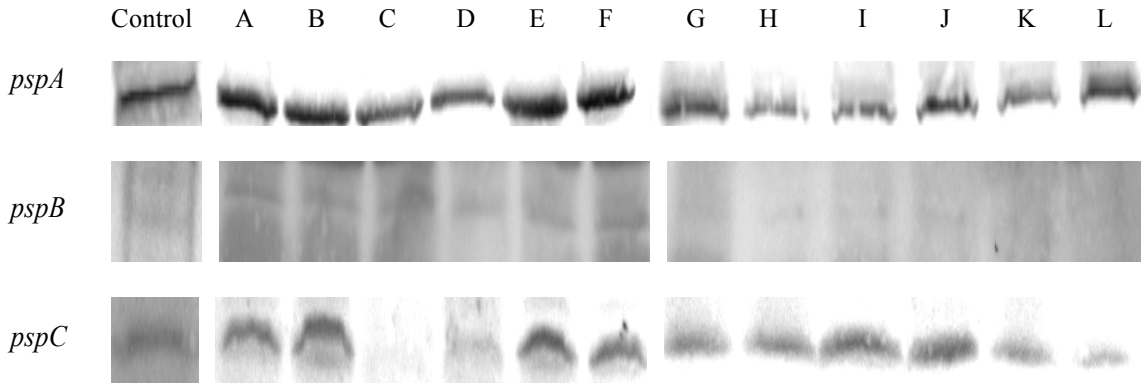

Figure 6-3: Western blot analysis of *pspA*, *pspC*, and *pspB* protein levels of *E. coli* cells exposed to (A) No SWCNTs (control), (B-G) 10 μg/ml of SWCNTs, and (H-M) 100 μg/ml of SWCNTs. (B) Short pristine SWCNTs, (C) Long pristine SWCNTs, (D) Short SWCNT-OHs, (E) Long SWCNT-OHs, (F) Short SWCNT-COOHs, (G) Long SWCNT-COOHs, (H) Short pristine SWCNTs, (I) Long pristine SWCNTs, (J) Short SWCNT-OHs, (K) Long SWCNT-OHs, (L) Short SWCNT-COOHs, and (M) Long SWCNT-COOHs.

Expression was the greatest for the cells exposed to short and long SWCNT-COOHs, and lowest for the cells exposed to SWCNT-OHs. This is in agreement with previous studies assessing viability reductions in CNT-treated *E. coli* in Chapters 4 and 5. The phage shock proteins may be involved in the recovery from stresses. SWCNT-OHs have limited effects on the viability of cells compared to SWCNTs and SWCNT-COOHs for both short and long ones. The percent viability of cells relative to control detected by the beta galactosidase enzyme assay was 94.9-95.4%, 63.8-65.0%, and 52.7-56.7% for SWCNT-OHs, SWCNTs, and SWCNT-COOHs, respectively. The results are also consistent with the 2D-electrophoresis data.

pspC may have a central role in transducing the stress signal to *pspA* and activates the expression of the phage shock pathway (Brissette et al., 1990; Jovanovic et al., 2010). Fig. 6-3 shows the expression level of *pspC* in the *E. coli* cells exposed to CNTs. The expression of *pspC* in cells after exposure to short and long pristine SWCNTs and SWCNT-COOHs was substantially higher than that in cells exposed to both short and long SWCNT-OHs and the control. The results showed that SWCNT-OHs did not trigger the expression of *pspC*. Based

on the expression levels of *pspA*, the environmental stresses caused by both short and long SWCNT-OHs may not induce the *psp* operon within the 90 min incubation.

The expression levels of *pspB* for bacterial cells exposed to CNTs are presented in Fig. 6-3. The expression was weak for all treatments with CNTs. Weiner et al. (1991) reported that *pspB* and *pspC* acted together to release of the negative regulation of *pspA*. However, the expression of *pspC* or the complex *pspB-C*, but not *pspB* alone, induced the *psp* operon. *pspB* is not absolutely required for the induction of the psp genes via the *pspC* dependent pathway (Weiner et al., 1991). Results in this study suggested that *pspB* may not be needed in response to CNT exposure. Compared the effects of short and long CNTs on the protein expression, the protein levels of bacterial cells exposed to long CNTs were higher than those exposed to short CNTs.

There was greater expression of *pspA* in the cells exposed t 100 μg/ml than 10 μg/ml of CNTs. A similar trend was observed with *pspC* except for short and long SWCNT-OHs. No significant difference was detected in *pspB* expression among treatments ($p > 0.05$). These results suggest that regardless of the CNT length, *pspA* and *pspC* are part of the stress response pathway for cells exposed to 100 μg/ml of SWCNT-OHs but not 100 μg/ml pristine SWCNTs and SWCNT-COOHs. In contrast, *pspB* is not involved in the response of *E. coli* to CNT insult.

6.3.3. Identification of altered phage shock proteins A, B and C transcription responses to CNTs exposure.

Expression of *pspA, pspC, and pspB* genes was determined using a RT-PCR approach (Fig. 6-4). For the treatment with 10 μg/ml CNTs, the *pspA* expression was highest in the cells exposed to short (85 fold higher) and long (58 fold higher) SWCNT-COOHs. While the expression levels of *pspA* protein in treatment with short and long SWCNT-OHs were the

lowest, *pspA* gene expression in the cells exposed to SWCNT-OHs was higher than pristine SWCNTs regardless of the length. Similarly, *pspC* protein expression detected by western blots was very weak, but the mRNA level expression ratio was the highest. The exposure time and the CNT type may have influences on the *psp* operon activities. Expression of *pspB* was low compared to *pspA* and *pspC*.

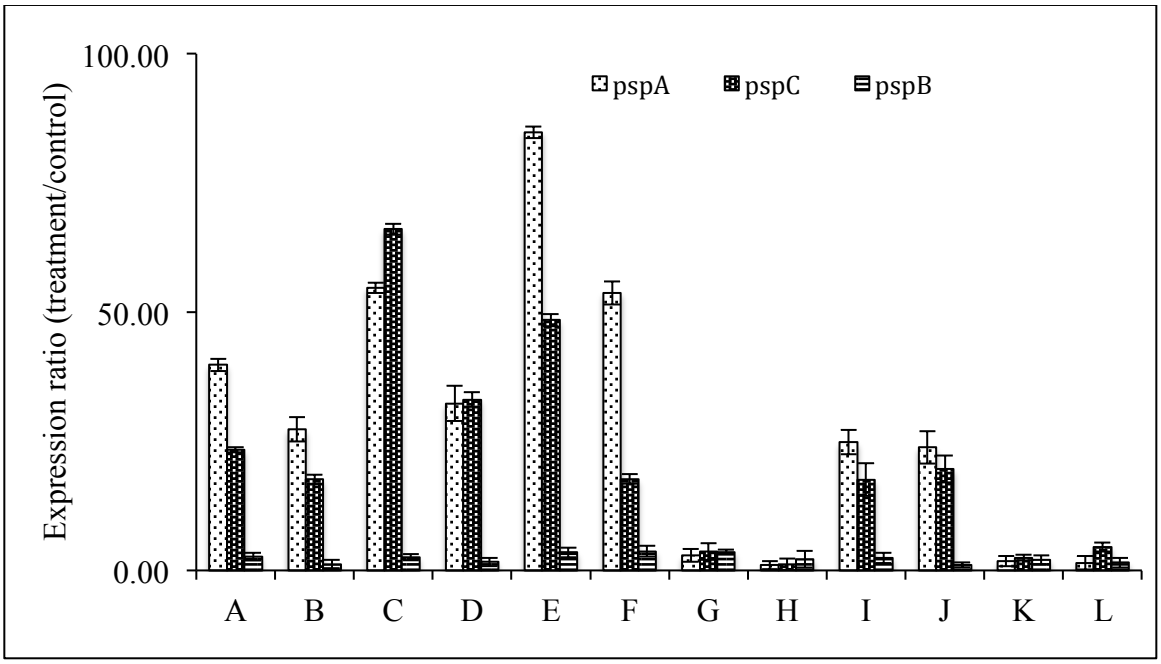

Figure 6-4: The expression levels of *psp* genes of *E. coli* cells determined by qPCR. Error bars indicate standard deviations. (A-F) Exposed to 10 μg/ml of SWCNTs, and (G-L) Exposed to 100 μg/ml of SWCNTs. (A) Short pristine SWCNTs, (B) Long pristine SWCNTs, (C) Short SWCNT-OHs, (D) Long SWCNT-OHs, (E) Short SWCNT-COOHs, (F) Long SWCNT-COOHs, (G) Short pristine SWCNTs, (H) Long pristine SWCNTs, (I) Short SWCNT-OHs, (J) Long SWCNT-OHs, (K) Short SWCNT-COOHs, and (L) Long SWCNT-COOHs.

Interestingly, when comparing short and long of pristine SWCNTs, SWCNT-OHs, and SWCNT-COOHs, expression of *pspA* and *pspC* genes were not correlated with the protein expressions. With the exception of *pspC* in cells treated with SWCNT-OHs, *pspA* and *pspC* proteins expression was lower in cells exposed to short CNTs than long CNTs. In contrast, the *pspA* and *pspC* gene expression in cells exposed to short CNTs were greater than that in cells

exposed to long CNTs. These observations can be explained by negative feedback regulation of *pspA* and *pspC* (Elderkin et al., 2005). Additionally, many genes involved in the expression of the *psp* operon such as *pspG, pspF, ArcA,* or *ArcB* may contribute to the differences in transcriptions and translations of *psp* genes.

The expressions of *pspA* and *pspC* decreased with increasing CNT concentration for both CNT lengths. *pspA* and *pspC* of the cells exposed to 100 μg/ml levels were not significantly different from the control, with the exception of short and long SWCNT-OHs. The functional group, length and concentration of CNTs did not influence the expression of *pspB*.

6.4. Summary

The alterations in gene and protein expression were observed after *E. coli* cells were exposed to CNTs. The concentration and type of CNTs influenced protein and gene expression levels. Regardless of the length, while 10 μg/ml of pristine SWCNTs and SWCNT-COOHs triggered the *psp* pathway via up-regulated *pspA* and *pspC*, *E. coli* cells exposed to 10 μg/ml of SWCNT-OHs did not show any evidence of this pathway activation. In contrast, these genes were activated when the cells were exposed to 100 μg/ml of SWCNT-OHs, and no up-regulated genes were observed from the cells exposed to pristine SWCNTs and SWCNT-COOHs. Only *pspA* and *pspC* were involved in the stress response to CNT exposure. This study provides greater understanding of underlying mechanisms on how CNTs affect bacterial cells and how multiple relevant genes are involved in responses to CNTs.

CHAPTER 7: CONCLUSIONS AND RECOMMENDATIONS FOR FUTURE WORK

7.1. Conclusions

The toxicity of carbon nanotubes is a current and debatable subject. This study investigated different methods for detecting the viability of bacterial cells exposed to SWCNTs. These viability methods were later used to examine the effects of length, concentration, and functional groups of SWCNTs on the viability of bacteria at two different initial cell densities. Molecular and cellular aspects of the toxicity of SWCNTs on bacteria were examined. The study also proposed cell entrapment as a means to mitigate the SWCNT cytotoxicity.

This study, using *E. coli* as a model organism, shows that four methods including a plate count, galactosidase assay, RNA quantification, and LIVE/DEAD® Baclight™ assay were reliable for assessing the viability of *E. coli* exposed to SWCNTs. Although these four methods rely on different principles to indicate cell viability, their results were agreeable. Therefore, the non-cultural based methods including the galactosidase assay, RNA quantification, and LIVE/DEAD® Baclight™ assay can serve as alternatives to the cultural based method, a plate count, which is more time consuming.

The degree of toxicity of SWCNTs on free *E. coli* cells depended on the functional group. The toxicity was in the following order: SWCNT-COOHs > SWCNTs > SWCNT-OHs. The effect on the cell viability varied with the length of SWCNTs. While there was no difference in the impact of short and long SWCNT-OHs, long SWCNT-COOHs and pristine SWCNTs were more toxic than their short counterparts. In addition, the concentrations of SWCNTs and bacterial cells influenced the toxicity of SWCNTs. The viability of cells exposed to SWCNTs decreased with increasing SWCNT concentrations. When exposed to SWCNTs, cells at a higher initial density exhibited more viability compared to those at a low initial density.

The alginate and PVA entrapments mitigated the bactericidal effects of SWCNTs and f-SWCNTs. The viability of the entrapped cells exposed to SWCNTs and f-SWCNTs was higher than that of the free cells. The bactericidal effect on the entrapped cells by SWCNTs was greater at higher SWCNT concentrations and a lower initial cell density, and for long SWCNTs but was not dependent on the functional group of SWCNTs. PVA and calcium alginate matrices present comparable protection of cell viability against both pristine and functionalized SWCNTs.

The profiling of the protein expressions of *E. coli* exposed to SWCNTs was examined. The protein expressions in *E. coli* depended on the length, type and concentrations of SWCNTs. The gene expressions were also investigated. The expression of the psp operon including *pspA, pspB,* and *pspC* in *E. coli* exposed to SWCNTs was reported for the first time. The expressions of these genes depended on the concentration and type of SWCNTs. The psp operon of cells was induced through the expressions of *pspA* and *pspC* when exposed to 10 μg/ml of pristine SWCNTs and SWCNT-COOHs but not 100 μg/ml. On the contrary, the operon was induced at 100 μg/ml of SWCNT-OHs rather than 10 μg/ml. *pspB* did not involve in the psp operon regulation under the presence of SWCNTs. At the high concentration of CNTs (100 μg/ml), several proteins were shut down.

This study reported multiple methods for determining the viability of cells exposed to SWCNTs. This provides alternative means that can be used under different conditions to detect the impact of nanomaterials on free and entrapped bacterial cells. The study helps in understanding how the entrapment can limit the bactericidal effect of functionalized SWCNTs. It proved that the length, functional group, concentrations of SWCNTs and bacterial cells had significant influence on the toxicity. The comprehensive profiling of gene and protein expressions reported in this study will enhance understandings on the toxicity mechanisms of

SWCNTs on bacteria and how the cells adapt to the toxicity at the molecular level. Particularly, the alteration of the psp operon expressions indicated that SWCNTs perturbed cell membrane and produced oxidative stress. The toxicity mechanisms proposed included bacteria-SWCNT contact, disturbance of cell membrane, and oxidative stress. Based on these mechanisms, cell entrapment in the hydrogels, PVA and alginate, provided a shield to protect the cells from the direct contact with SWCNTs, hence prohibited the cell membrane perturbation and oxidative stress.

7.2. Recommendations for Future Work

When bacterial cells are exposed to SWCNTs, they may resist toxicity via regulatory and physical changes. One avenue for study would be genes and proteins potentially contributing to resistance, such as *ompF, rpoS*, and trehalose. The σ-factor σ^{54} controls *psp* expression; therefore, determining the expression of both σ^{54} and the psp operon will provide a comprehensive understanding of the regulation of the *psp* operon in the presence of SWCNTs.

This study did not address other potential applications of cell protection via entrapment in engineered and natural systems. Future studies could explore potential uses of entrapped bacteria for treating water and wastewater containing SWCNTs.

The type of CNTs influences the toxicity and adsorption properties. This study revealed the influence of length, diameter, and functionalization of CNTs on cell viability. Further research could examine how CNT chirality (chiral, zigzag, or armchair) affects toxicity. The effect of the adsorption of CNTs on cells or macromolecules (nucleic acids, proteins, and carbohydrates) should also be determined. Adsorption and absorption of CNTs on cells and the immobilized matrix will be affected by surface chemistry.

Finding a means to investigate the behavior of CNTs inside living cells at the molecular level is essential in biological applications. Attachment of fluorescent functional groups to CNTs may be a method to discover these processes. The primary data about CNTs functionalized with FITC, tracing their location on/in the cells, and their effects on the cell viability were reported in this study (Appendix).

REFERENCES

Adams, H., Teertstra, W., Demmers, J., Boesten, R., Tommassen, J. 2003. Interactions between phage-shock proteins in Escherichia coli. *Journal of Bacteriology*, 185, 1174-1180.

Adams, H., Teertstra, W., Koster, M., Tommassen, J. 2002. PspE (phage-shock protein E) of Escherichia coli is a rhodanese. *FEBS Letters*, 518, 173-176

Ajayan, P.M. and Ebbesen, T.W. 1997. Nanometre-size tubes of carbon. *Reports on Progress in Physics*, 60, 1025-1062.

Akasaka, T. and Watari, F. 2009. Capture of bacteria by flexible carbon nanotubes. *Acta Biomaterialia*, 5, 607-612.

Al-Hakami, S.M., Khalil, A.B., Laoui, T., Atieh, M.A. 2013. Fast disinfection of *Escherichia coli* bacteria using carbon nanotubes interaction with microwave radiation. *Bioinorganic Chemistry and Applications*, 2013, 1-10.

Alazzam, A., Mfoumou, E., Stiharu, I., Kassab, A., Darnel, A., Yasmeen, A., Sivakumar, N., Bhat, R., Al Moustafa, A.-E. 2010. Identification of deregulated genes by single wall carbon-nanotubes in human normal bronchial epithelial cells. *Nanomedicine : Nanotechnology, Biology, and Medicine*, 6, 563-569.

Albert, M., Kiefer, M.V., Sun, W., Haller, D., Fraker, D.L., Tuite, C.M., Stavropoulos, S.W., Mondschein, J.I., Soulen, M.C. 2011. Chemoembolization of colorectal liver metastases with cisplatin, doxorubicin, mitomycin C, ethiodol, and polyvinyl alcohol. *Cancer*, 117, 343-352.

Allen, B.L., Kichambare, P.D., Gou, P., Vlasova, II, Kapralov, A.A., Konduru, N., Kagan, V.E., Star, A. 2008. Biodegradation of single-walled carbon nanotubes through enzymatic catalysis. *Nano Letters*, 8, 3899-3903.

Amarnath, S., Mohammad. A., Vidyanand Nanjundiah, A., Sood, K. 2012. β-Galactosidase leakage from *Escherichia coli* points to mechanical damages likely cause of carbon nanotube toxicity. *Soft Nanoscience Letters*, 2, 41-45.

Amiri, A., Zardini, H.Z., Shanbedi, M., Maghrebi, M., Baniadam, M., Tolueinia, B. 2012. Efficient method for functionalization of carbon nanotubes by lysine and improved antimicrobial activity and water-dispersion. *Materials Letters*, 72, 153-156.

Arias, L.R. and Yang, L. 2009. Inactivation of bacterial pathogens by carbon nanotubes in suspensions. *Langmuir*, 25, 3003-3012.

Ariga, O., Andoh, Y., Fujishita, Y., Watari, T., Sano, Y. 1991. Production of thermophilic α-amylase using immobilized transformed *Escherichia coli* by addition of glycine. *Journal of Fermentation and Bioengineering*, 71, 397-402.

Artukovic, E., Kaempgen, M., Hecht, D.S., Roth, S., Gruner, G. 2005. Transparent and flexible carbon nanotube transistors. *Nano Letters*, 5, 757-776.

Aykut, G., Hasirci, V.N., Alaeddinoglu, G. 1988. Immobilization of yeast cells in acrylamide gel matrix. *Biomaterials*, 9, 168-172.

Banerjee, S., Hemraj-Benny, T., Balasubramanian, M., Fischer, D.A., Misewich, J.A., Wong, S.S. 2004. Ozonized single-walled carbon nanotubes investigated using NEXAFS spectroscopy. *Chemical Communications,* 7, 772-773.

Batley, G.E. and McLaughlin, M.J. 2010. Fate of Manufactured Nanomaterials in the Australian Environment. RO Niche Manufacturing Flagship Report. Retrieved March, 2010, from http://www.environment.gov.au/node/21212.

Baughman, R.H., Zakhidov, A.A., de Heer, W.A. 2002. Carbon nanotubes-the route toward applications. *Science*, 297, 787-792.

Beloin, C., Valle, J., Latour-Lambert, P., Faure, P., Kzreminski, M., Balestrino, D., Haagensen, J.A., Molin, S., Prensier, G., Arbeille, B., Ghigo, J.M. 2004. Global impact of mature biofilm lifestyle on Escherichia coli K-12 gene expression. *Molecular Microbiology*, 51, 659-674.

Berdjeb, L., Pelletier, E., Pellerin, J., Gagne, J.P., Lemarchand, K. 2013. Contrasting responses of marine bacterial strains exposed to carboxylated single-walled carbon nanotubes. *Aquatic Toxicology*, 144, 230-241.

Bhattacharyya, S., Guillot, S., Dabboue, H., Tranchant, J.F., Salvetat, J.P. 2008. Carbon nanotubes as structural nanofibers for hyaluronic acid hydrogel scaffolds. *Biomacromolecules*, 9, 505-509.

Blaise, C., Gagné, F., Férard, J., Eullaffroy, P. 2008. Ecotoxicity of selected nano-materials to aquatic organisms. *Environmental Toxicology*, 23, 591-598.

Bouchard, D., Zhang, W., Powell, T., Rattanaudompol, U.S. 2012. Aggregation kinetics and transport of single-walled carbon nanotubes at low surfactant concentrations. *Environmental Science and Technology*, 46, 4458-4465.

Boulos, L., Prevost, M., Barbeau, B., Coallier, J., Desjardins, R. 1999. LIVE/DEAD BacLight®: application of a new rapid staining method for direct enumeration of viable and total bacteria in drinking water. *Journal of Microbiological Methods*, 37, 77-86.

Bower, C., Zhu, W., Jin, S., Zhou, O. 2000. Plasma-induced alignment of carbon nanotubes. *Applied Physics Letters*, 77, 830-832.

Bradley, K., Gabriel, J.C.P., Gruner, G. 2003. Flexible nanotube electronics. *Nano Letters,* 3, 1353-1355.

Brady-Estevez, A.S., Schnoor, M.H., Kang, S., Elimelech, M. 2010. SWNT-MWNT hybrid

filter attains high viral removal and bacterial inactivation. *Langmuir*, 26, 19153-19158.

Brady-Estevez, A.S., Kang, S., Elimelech, M. 2008. A single-walled-carbon-nanotube filter for removal of viral and bacterial pathogens. *Small*, 4, 481-484.

Brissette, J.L., Russel, M., Weiner, L., Model, P. 1990. Phage shock protein, a stress protein of Escherichia coli. *Proceedings of the National Academy of Sciences of the United States of America*, 87, 862-866.

Brodelius, P. and Nilsson, K. 1980. Entrapment of plant cells in different matrices. *FEBS Letters*, 122, 312-316.

Buzea, C., Pacheco, I., Robbie, K. 2007. Nanomaterials and nanoparticles: sources and toxicity. *Biointerphases*, 2, MR17-MR71.

Canas, J.E., Long, M.Q., Nations, S., Vadan, R., Dai, L., Luo, M.X., Ambikapathi, R., Lee, E.H., Olszyk, D. 2008. Effects of functionalized and nonfunctionalized single-walled carbon nanotubes on root elongation of select crop species. *Environmental Toxicology and Chemistry*, 27, 1922-1931.

Carmichael, R.D., Jones, A., Pickard, M.A. 1986. Semicontinuous and continuous production of chloroperoxidase by *Caldariomyces fumago* immobilized in *k*-carrageenan. *Applied and Environmental Microbiology*, 51, 276-280.

Cavallo, D., Fanizza, C., Ursini, C.L., Casciardi, S., Paba, E., Ciervo, A., Fresegna, A.M., Maiello, R., Marcelloni, A.M., Buresti, G., Tombolini, F., Bellucci, S., Iavicoli, S. 2012. Multi-walled carbon nanotubes induce cytotoxicity and genotoxicity in human lung epithelial cells. *Journal of Applied Toxicology*, 32, 454-464.

Chae, H.G., Minus, M.L., Rasheed, A., Kumar, S. 2007. Stabilization and carbonization of gel spun polyacrylonitrile/single wall carbon nanotube composite fibers. *Polymer*,

48, 3781-3789.

Champion, K.M., Nishihara, J.C., Aldor, I.S., Moreno, G.T., Andersen, D., Stults, K.L., Vanderlaan, M. 2003. Comparison of the *Escherichia coli* proteomes for recombinant human growth hormone producing and nonproducing fermentations. *Proteomics*, 3, 1365-1373.

Chen, J., Hamon, M.A., Hu, H., Chen, Y., Rao, A.M., Eklund, P.C., Haddon, R.C. 1998a. Solution properties of single-walled carbon nanotubes. *Science*, 282, 95-98.

Chen, C. Y. and Jafvert, C. T. 2010. Photoreactivity of carboxylated single-walled carbon nanotubes in sunlight: Reactive oxygen species production in water. *Environmental Science and Technology*, 44, 6674-6679.

Chen, K., Lee, S., Chin, S., Houng, J. 1998b. Simultaneous carbon-nitrogen removal in wastewater using phosphorylated PVA-immobilized microorganisms. *Enzyme and Microbial Technology*, 23, 311-320.

Chen, J., Liu, H., Weimer, W.A., Halls, M.D., Waldeck, D.H., Walker, G.C. 2002. Noncovalent engineering of carbon nanotube surfaces by rigid, functional conjugated polymers. *Journal of the American Chemical Society*, 124, 9034-9035.

Chen, K. L., Smith, B. A., Ball, W. P., Fairbrother, D. H. 2010. Assessing the colloidal properties of engineered nanoparticles in water: Case studies from fullerene C60 nanoparticles and carbon nanotubes. *Environmental Chemistry,* 7, 10-27.

Chen, H., Wang, B., Gao, D., Guan, M., Zheng, L., Ouyang, H., Chai, Z., Zhao, Y., Feng, W. 2013. Broad-spectrum antibacterial activity of carbon nanotubes to human gut bacteria. *Small*, 9, 2735-2746.

Chen, C., Xie, X.X., Zhou, Q., Zhang, F.Y., Wang, Q.L., Liu, Y.Q., Zou, Y., Tao, Q., Ji,

X.M., Yu, S.Q. 2012. EGF-functionalized single-walled carbon nanotubes for targeting delivery of etoposide. *Nanotechnology*, 23, 1-12.

Cheng, J.P., Chan, C.M., Veca, L.M., Poon, W.L., Chan, P.K., Qu, L.W., Sun, Y.P., Cheng, S.H. 2009. Acute and long-term effects after single loading of functionalized multi-walled carbon nanotubes into zebrafish (Danio rerio). *Toxicology and Applied Pharmacology*, 235, 216-225.

Cheng, J., Flahaut, E., Cheng, S.H. 2007. Effect of carbon nanotubes on developing zebrafish (Danio rerio) embryos. *Environmental Toxicology and Chemistry*, 26, 708-716.

Cherukuri, P., Gannon, C.J., Leeuw, T.K., Schmidt, H.K., Smalley, R.E., Curley, S.A., Weisman, R.B. 2006. Mammalian pharmacokinetics of carbon nanotubes using intrinsic near-infrared fluorescence. *Proceedings of the National Academy of Sciences of the United States of America*, 103, 18882-18886.

Chhowalla, M., Teo, K.B.K., Ducati, C., Rupesinghe, N.L., Amaratunga, G.A.J., Ferrari, A.C., Roy, D., Robertson, J., Milne, W.I. 2001. Growth process condition of vertically aligned carbon nanotubes using plasma enhanced chemical vapor deposition. *Journal of Applied Physics*, 90, 5308-5317.

Cho, K., Wang, X., Nie, S., Chen, Z.G., Shin, D.M. 2008. Therapeutic nanoparticles for drug delivery in cancer. *Clinical Cancer Research,* 14, 1310-1316.

Choudhary, V. and Gupta, A. 2011. Polymer/Carbon Nanotube Nanocomposites. In S. Yellamplli (Ed.), *Carbon Nanotubes – Polymer Nanocomposites*. Retrieved from http://www.intechopen.com/books.

Chun, G.T. and Agathos, S.N. 1993. Dynamic response of immobilized cells to pulse addition of L-valine in cyclosporin A biosynthesis. *Journal of Biotechnology*, 27, 283-294.

Chung, H., Son, Y., Yoon, T.K., Kim, S., Kim, W. 2011. The effect of multi-walled carbon nanotubes on soil microbial activity. *Ecotoxicology and Environmental Safety*, 74, 569-575.

Coccini, T., Roda, E., Sarigiannis, D.A., Mustarelli, P., Quartarone, E., Profumo, A., Manzo, L. 2010. Effects of water-soluble functionalized multi-walled carbon nanotubes examined by different cytotoxicity methods in human astrocyte D384 and lung A549 cells. *Toxicology*, 269, 41-53.

Collignon, B., Hoang, P., Picaud, S., Rayez, J. 2005. Clustering of water molecules on model soot particles: an ab initio study. *Computing Letters*, 1, 277-287.

Condon, C. 2007. Maturation and degradation of RNA in bacteria. *Current Opinion in Microbiology*, 10, 271-278.

Constantinides, A. and Mehta, N. 1991. Periodic operation of immobilized live cell bioreactor for the production of candicidin. *Biotechnology and Bioengineering*, 37, 1010-1020.

Crouzier, D., Follot, S., Gentilhomme, E., Flahaut, E., Arnaud, R., Dabouis, V., Castellarin, C., Debouzy, J.C. 2010. Carbon nanotubes induce inflammation but decrease the production of reactive oxygen species in lung. *Toxicology*, 272, 39-45.

Dai, H., Rinzler, A.G., Nikolaev, P., Thess, A., Colbert, D.T., Smalley, R.E. 1996. Single-wall nanotubes produced by metal-catalyzed disproportionation of carbon monoxide. *Chemical Physics Letters*, 260, 471-475.

Dalili, M. and Chau, P.C. 1988. Production of actinomycin D with immobilized *Streptomyces parvullus* under nitrogen and carbon starvation conditions. *Biotechnology Letters*, 10, 331-336.

Darwin, A.J. 2005. The phage-shock-protein response. *Molculer Microbioloy*, 57, 621-628.

Davoren, M., Herzog, E., Casey, A., Cottineau, B., Chambers, G., Byrne, H.J., Lyng, F.M. 2007. In vitro toxicity evaluation of single walled carbon nanotubes on human A549 lung cells. *Toxicology in Vitro*, 21, 438-448.

Delogu, L.G., Venturelli, E., Manetti, R., Pinna, G.A., Carru, C., Madeddu, R., Murgia, L., Sgarrella, F., Dumortier, H., Bianco, A. 2012. Ex vivo impact of functionalized carbon nanotubes on human immune cells. *Nanomedicine (London, England)*, 7, 231-243.

Delzeit, L., McAninch, I., Cruden, B. A., Hash, D., Chen, B., Han, J., Meyyappan, M. 2002. Growth of multiwall carbon nanotubes in an inductively couple plasma reactor. *Journal of Applied Physics*, 91, 6027-6033.

Deo, Y.M. and Gaucher, G.M. 1984. Semicontinuous and continuous production of penicillin-G by *Penicillium chrysogenum* cells immobilized in κ-carrageenan beads. *Biotechnology and Bioengineering*, 26, 285-295.

Deo, Y.M. and Gaucher, G.M. 1985. Effect of nitrogen supplementation on the longevity of antibiotic production by immobilized cells of *Penicillium urticae*. *Applied Microbiology and Biotechnology*, 21, 220-227.

Ding, L., Stilwell, J., Zhang, T., Elboudwarej, O., Jiang, H., Selegue, J.P., Cooke, P.A., Gray, J.W., Chen, F.F. 2005. Molecular characterization of the cytotoxic mechanism of multiwall carbon nanotubes and nano-onions on human skin fibroblast. *Nano Letters*, 5, 2448-2464.

Donaldson, K., Aitken, R., Tran, L., Stone, V., Duffin, R., Forrest, G., Alexander, A. 2006. Carbon nanotubes: a review of their properties in relation to pulmonary toxicology and workplace safety. *Toxicology Science*, 92, 5-22.

Dong, X., Tang, Y., Wu, M., Vlahovic, B., Yang, L. 2013. Dual effects of single-walled

carbon nanotubes coupled with near-infrared radiation on Bacillus anthracis spores: inactivates spores and stimulates the germination of surviving spores. *Journal of Biological Engineering*, 7, 19-30.

Draget, K.I., Skjak-Braek, G., Smidsrod, O. 1997. Alginate based new materials. *International Journal of Biological Macromolecules*, 21, 47-55.

Dresselhaus, M.S., Dresselhaus, G., Jorio, A., Souza Filho, A.G., Pimenta, M.A., Saito, R. 2002. Single nanotube Raman spectroscopy. *Accounts of Chemical Research*, 35, 1070-1078.

Elderkin, S., Bordes, P., Jones, S., Rappas, M., Buck, M. 2005. Molecular determinants for PspA-mediated repression of the AAA transcriptional activator PspF. *Journal of Bacteriology*, 187, 3238-3248.

Eletski AV. 1997. Carbon nanotubes. *Physics-Uspekhi*. 40, 899-924.

Ellaiah, P., Srinivasulu, B., Adinarayana, K. 2003. Studies on neomycin production using immobilized cells of S marinensis NUV-5 in various reactor configurations: a technical note. *AAPS PharmSciTech*, 4, 136-141.

Endo, M., Hayashi, T., Kim, Y.A., Terrones, M., Dresselhaus. S. 2004. Applications of carbon nanotubes in the twenty-first century. *Philosophical Transactions of the Royal Society of London. Series A: Mathematical, Physical and Engineering Sciences*, 362, 2223-2238.

Environmental Protection Agency (EPA). 2010. Control of nanoscale materials under the toxic substances control Act. Retrieved March, 2010, from http://www.epa.gov/oppt/nano/.

Eriksson, S., Lucchini, S., Thompson, A., Rhen, M., Hinton, J.C. 2003. Unravelling the biology of macrophage infection by gene expression profiling of intracellular Salmonella enterica. *Molecular Microbiology*, 47, 103-118.

Escobar, M.; Goyanes, S.; Corcuera, M. A.; Eceiza, A.; Mondragon, I.; Rubiolo, G. H.;

Candal, R. J. 2009. Purification and functionalization of carbon nanotubes by classical and advanced oxidation processes. *Journal of Nanoscience and Nanotechnology*, 9, 6228-6233.

Fan, C. L., Li, W., Li, X., Zhao, S. J., Zhang, L., Mo, Y. J., Cheng, R. M. 2007. Efficient photo-assisted Fenton oxidation treatment of multi-waited carbon nanotubes. *Chinese Science Bulletin*, 52, 2054-2062.

Federici, F., Petruccioli, M., Miller, M.W. 1990. Enhancement and stabilization of the production of glucoamylase by immobilized cells of *Aureobasidium pullulans* in a fluidized-bed reactor. *Applied Microbiology and Biotechnology,* 33, 407-409.

Fiksdal, L., Pommepuy, M., Caprais, M.P., Midttun, I. 1994. Monitoring of fecal pollution in coastal waters by use of rapid enzymatic techniques. *Applied and Environmental Microbiology*, 60, 1581-1584.

Frackowiak*,* E. and Beguin, F. 2002. Electrochemical storage of energy in *carbon* nanotubes and nanostructured carbons. *Carbon,* 40*,* 1775-1787.

Fraczek, A., Menaszek, E., Paluszkiewicz, C., Blazewicz, M. 2008. Comparative in vivo biocompatibility study of single- and multi-wall carbon nanotubes. *Acta Biomaterialia*, 4, 1593-1602.

Francis, D. and Kadish, K.M. 2012. Handbook of Carbon Nano Materials. Volume 3: Medicinal and Bio-Related Applications. World Scientific Publishing Co. Pte.Ltd., Singapore.

Galazzo, J.L. and Bailey J.E. 1990. Growing *Saccharomyces cerevisiae* in calcium-alginate beads induces cell alterations which accelerate glucose conversion to ethanol. *Biotechnology and Bioengineering*, 36, 417-426.

Gao, B., Bower, C., Lorentzen, J.D., Fleming, L., Kleinhammes, A., Tang, X.P., McNeil,

L.E., Wu, Y., Zhou, O. 2000. Enhanced saturation lithium composition in ball-milled single-walled carbon nanotubes. *Chemical Physics Letters*, 327, 69-75.

George, I., Petit, M., Servais, P. 2000. Use of enzymatic methods for rapid enumeration of coliforms in freshwaters. *Journal of Applied Microbiology*, 88, 404-413.

George, I., Petit, M., Theate, C., Servais, P. 2001. Use of rapid enzymatic assays to study the distribution of faecal coliforms in the Seine river (France). *Water Science and Technology*, 43, 77-80.

Ghosh, M. and Nanda, G. 1991. Immobilized *Aspergillus sydowii* produces xylanase. *Biotechnology Letters*, 13, 807-808.

Gottschalk, F., Sonderer, T., Scholz, R.W., Nowack, B. 2009. Modeled environmental concentrations of engineered nanomaterials (TiO(2), ZnO, Ag, CNT, Fullerenes) for different regions. *Environmental Science and Technololgy*, 43, 9216-9222.

Gottschalk, F., Sonderer, T., Scholz, R.W., Nowack, B. 2010. Possibilities and limitations of modeling environmental exposure to engineered nanomaterials by probabilistic material flow analysis. *Environmental Toxicology and Chemistry*, 29, 1036-1048.

Goyal, D., Zhang, X.J., Rooney-Varga, J.N. 2010. Impacts of single-walled carbon nanotubes on microbial community structure in activated sludge. *Letters in Applied Microbiology*, 51, 428-435.

Groboillot, A., Boadi, D.K., Poncelet, D., Neufeld, R.J. 1994. Immobilization of cells for application in the food industry. *Critical Reviews in Biotechnology*, 14, 75-107.

Grozeva, L., Tchorbanov, B., Aleksieva, P. 1993. Production of casein hydrolysates by extracellular acid proteinases of immobilized *Humicola lutea* cells. *Applied Microbiology and Biotechnology*, 39, 512-514.

Guo, T., Nikolaev, P., Thess, A., Colbert, D.T., Smalley, R.E. 1995. Catalytic growth of single-walled nanotubes by laser vaporization. *Chemical Physics Letters*, 243, 49-54.

Gwon, Y.H., Ha, J.K., Cho, K.K., Kim, H.S. 2012. Physical and electrochemical properties of synthesized carbon nanotubes [CNTs] on a metal substrate by thermal chemical vapor deposition. *Nanoscale Research Letters*, 7, 1-5.

Han, J.H., Lee, E.J., Lee, J.H., So, K.P., Lee, Y.H., Bae, G.N., Lee, S.B., Ji, J.H., Cho, M.H., Yu, I.J. 2008. Monitoring multiwalled carbon nanotube exposure in carbon nanotube research facility. *Inhalation Toxicology*, 20, 741-749.

Handy, R., Al-Bairuty, G., Al-Jubory, A., Ramsden, C., Boyle, D., Shaw, B., Henry, T. 2011. Effects of manufactured nanomaterials on fishes: a target organ and body systems physiology approach. *Journal of Fish Biology*, 79, 821-853.

Handy, R., Henry, T., Scown, T., Johnston, B., Tyler, C. 2008. Manufactured nanoparticles: their uptake and effects on fish--a mechanistic analysis. *Ecotoxicology (London, England)*, 17, 396-409.

Hashimoto, S. and Furukawa, K. 1987. Immobilization of activated sludge by PVA-boric acid method. *Biotechnology and Bioengineering*, 30, 52-59.

Hecht, D.S., Hu, L., Irvin, G. 2011. Emerging transparent electrodes based on thin films of carbon nanotubes, graphene, and metallic nanostructures. *Advanced Materials*, 23, 1482-1513.

Hemraj-Benny, T., Bandosz, T.J., Wong, S.S. 2008. Effect of ozonolysis on the pore structure, surface chemistry, and bundling of single-walled carbon nanotubes. *Journal of Colloid and Interface Science*, 317, 375-382.

Hirlekar, R., Yamagar, M., Garse, H., Vij, M. Kadam, V. 2009. Carbon nanotubes and its

applications: A review. *Asian Journal of Pharmceutical and Clinical Research,* 2, 17-27.

Hirsch, A. 2002. Functionalization of single-walled carbon nanotubes. *Angewandte Chemie International Edition,* 41, 1853-1859.

Holbrook, R.D., Kline, C.N., Filliben, J.J. 2010. Impact of source water quality on multiwall carbon nanotube coagulation. *Environmental Science and Technology*, 44, 1386-1391.

Horne, S.M. and Pruss, B.M. 2006. Global gene regulation in Yersinia enterocolitica: effect of FliA on the expression levels of flagellar and plasmid-encoded virulence genes. *Archives of Microbiology*, 185, 115-126.

Hu, Z.C. 1993. Characterization of immobilized enzymes in polyurethane foams in a dynamic bed reactor. *Applied Microbiology and Biotechnology*, 39, 289-295.

Hu, Z.C., Korus, R.A., Levinson, W.E., Crawford, R.L. 1994. Adsorption and biodegradation of pentachlorophenol by polyurethane-immobilized Flavobacterium. *Environmental Science and Technology*, 28, 491-496.

Hu, H., Yu, A., Kim, E., Zhao, B., Itkis, M.E., Bekyarova, E., Haddon, R.C. 2005. Influence of the zeta potential on the dispersability and purification of single-walled carbon nanotubes. *The Journal of Physical Chemistry B*, 109,11520-11524.

Huang, W.J., Taylor, S., Fu, K.F., Lin, Y., Zhang, D.H., Hanks, T.W., Rao, A.M., Sun, Y.P. 2002. Attaching proteins to carbon nanotubes via diimide-activated amidation. *Nano Letters*, 2, 311-314.

Huczko, A., Lange, H., Calko, E., Grubek-Jaworska, H., Droszcz, P. 2001. Physiological testing of carbon nanotubes: Are they asbestos-like? *Fullerene Science and Technology*, 9, 251-254.

Hung, C.P., Lo, H.F., Hsu, W.H., Chen, S.C., Lin, L.L. 2008. Immobilization of *Escherichia*

coli novablue gamma-glutamyltranspeptidase in Ca-alginate-kappa-carrageenan beads. *Applied Biochemistry and Biotechnology*, 150, 157-170.

Huvet, M., Toni, T., Sheng, X., Thorne, T., Jovanovic, G., Engl, C., Buck, M., Pinney, J.W., Stumpf, M.P. 2011. The evolution of the phage shock protein response system: Interplay between protein function, genomic organization, and system function. *Molecular Biology and Evolution*, 28, 1141-1155.

Hwang, G.L. and Hwang, K.C. 2001. Carbon Nanotubes Reinforced Ceramics. *Journal of Materials Chem*istry, 11, 1722-1725.

Hwang, K. C. 1995. Efficient cleavage of carbon graphene layers by oxidants. *Journal of the Chemical Society, Chemical Communications*, 2, 173-174.

Iijima, S. 1991. Helical microtubules of graphitic carbon. *Nature*, 354, 56-58.

Iijima, S., Ichihashi, T. 1993. Single-shell carbon nanotubes of 1-nm diameter. *Nature,* 363, 603-605.

Jaisi, D.P. and Elimelech, M. 2009. Single-walled carbon nanotubes exhibit limited transport in soil columns. *Environmental Science and Technology*, 43, 9161-9166.

Jaisi, D.P., Saleh, N.B., Blake, R.E., Elimelech, M. 2008. Transport of single-walled carbon nanotubes in porous media: Filtration mechanisms and reversibility. *Environmental Science and Technology*, 42, 8317-8323.

Javey, A., Guo, J., Wang, Q., Lundstrom, M., Dai, H. 2003. Ballistic carbon nanotube field-effect transistors. *Nature*, 424, 654-657.

Jin, L., Son, Y., Yoon, T.K., Kang, Y.J., Kim, W., Chung, H. 2013. High concentrations of single-walled carbon nanotubes lower soil enzyme activity and microbial biomass. *Ecotoxicology and Environmental Safety*, 88, 9-15.

Joly, N., Engl, C., Jovanovic, G., Huvet, M., Toni, T., Sheng, X., Stumpf, M.P., Buck, M. 2010. Managing membrane stress: the phage shock protein (Psp) response, from molecular mechanisms to physiology. *FEMS Microbiology Reviews*, 34, 797-827.

Johri, B.N., Alurralde, J.D., Klein, J. (1990). Lipase production by free and immobilized protoplasts of *Sporotrichum (Chrysosporium) thermophile* Apinis. *Applied Microbiology and Biotechnology*, 33, 367-371.

Jovanovic, G., Engl, C., Mayhew, A.J., Burrows, P.C., Buck, M. 2010. Properties of the phage-shock-protein (Psp) regulatory complex that govern signal transduction and induction of the Psp response in Escherichia coli. *Microbiology*, 156, 2920-2932.

Jovanovic, G., Lloyd, L.J., Stumpf, M.P., Mayhew, A.J., Buck, M. 2006. Induction and function of the phage shock protein extracytoplasmic stress response in *Escherichia coli*. *Journal of Biological Chemistry*, 281, 21147-21161.

Juliana C.D., Augusto,J., Rodrigues, R. Moran, P., Gustavo P.V., Nunhez, J.R. 2013. Effect of immobilized cells in calcium alginate beads in alcoholic fermentation. *AMB Express*, 3, 31-38.

Kagan, V.E., Konduru, N.V., Feng, W., Allen, B.L., Conroy, J., Volkov, Y., Vlasova, II, Belikova, N.A., Yanamala, N., Kapralov, A., Tyurina, Y.Y., Shi, J., Kisin, E.R., Murray, A.R., Franks, J., Stolz, D., Gou, P., Klein-Seetharaman, J., Fadeel, B., Star, A., Shvedova, A.A. 2010. Carbon nanotubes degraded by neutrophil myeloperoxidase induce less pulmonary inflammation. *Nature Nanotechnology*, 5, 354-359.

Kam, N.W. and Dai, H. 2005. Carbon nanotubes as intracellular protein transporters: generality and biological functionality. *Journal of the American Chemical Society*, 127, 6021-6026.

Kam, N.W., Liu, Z., Dai, H. 2005a. Functionalization of carbon nanotubes via

cleavable disulfide bonds for efficient intracellular delivery of siRNA and potent gene silencing. *Journal of the American Chemical Society*, 127, 12492-12493.

Kam, N.W., O'Connell, M., Wisdom, J.A., Dai, H. 2005b. Carbon nanotubes as multifunctional biological transporters and near-infrared agents for selective cancer cell destruction. *Proceedings of the National Academy of Sciences of the United States of America*, 102, 11600-11605.

Kang, S., Herzberg, M., Rodrigues, D.F., Elimelech, M. 2008a. Antibacterial effects of carbon nanotubes: size does matter! *Langmuir*, 24, 6409-6413.

Kang, S.J., Kocabas, C., Ozel, T., Shim, M., Pimparkar, N., Alam, M.A., Rotkin, S.V., Rogers, J.A. 2007b. High-performance electronics using dense, perfectly aligned arrays of single-walled carbon nanotubes. *Nature Nanotechnology*, 2, 230-236.

Kang, S., Mauter, M.S., Elimelech, M. 2008b. Physicochemical determinants of multiwalled carbon nanotube bacterial cytotoxicity. *Environmental Science and Technology*, 42, 7528-7534.

Kang, S., Mauter, M.S., Elimelech, M. 2009. Microbial cytotoxicity of carbon-based nanomaterials: implications for river water and wastewater effluent. *Environmental Science and Technology*, 43, 2648-2653.

Kang, S., Pinault, M., Pfefferle, L.D., Elimelech, M. 2007a. Single-walled carbon nanotubes exhibit strong antimicrobial activity. *Langmuir*, 23, 8670-8673.

Kawakita, K., Hata, K., Sata, H., Saito, Y. 2006. Development of microfocused x-ray source by using carbon nanotube field emitter. *Journal of Vacuum Science and Technology B: Microelectronics and Nanometer Structures*, 24, 950-952.

Kierstan, M. and Bucke, C. 1977. The immobilization of microbial cells, subcellular

organelles, and enzymes in calcium alginate gels. *Biotechnology and Bioengineering*, 19, 387-397.

Khodakovskaya, M., Dervishi, E., Mahmood, M., Xu, Y., Li, Z.R., Watanabe, F., Biris, A.S. 2009. Carbon nanotubes are able to penetrate plant seed coat and dramatically affect seed germination and plant growth. *American Chemical Society Nano*, 3, 3221-3227.

Klaine, S.J. 2009. Considerations for research on the environmental fate and effects of nanoparticles. *Environmental Toxicology and Chemistry*, 28, 1787-1788.

Kleiner, K. and Hogan, J. 2003.How safe is nanotech? *New Scientist*, 177, 14-15.

Kleerebezem, M., Crielaard, W., Tommassen, J. 1996. Involvement of stress protein PspA (phage shock protein A) of Escherichia coli in maintenance of the protonmotive force under stress conditions. The *EMBO Journal*, 15, 162-171.

Kobayashi, R., Suzuki, T., Yoshida, M. 2007. Escherichia coli phage-shock protein A (PspA) binds to membrane phospholipids and repairs proton leakage of the damaged membranes. *Molecular Microbiology*, 66, 100-109.

Kohler A.R., Som C., Helland A., Gottschalk F. 2008. Studying the potential release of carbon nanotubes throughout the application life cycle. *Journal of Cleaner Production*, 16, 927-937.

Konsoula, Z. and Liakopoulou-Kyriakides, M. 2006. Thermostable α-amylase production by Bacillus subtilis entrapped in calcium alginate gel capsules. *Enzyme and Microbial Technology*, 39, 690-696.

Kreuter, J. 2007. Nanoparticles--a historical perspective. *International Journal of Pharmaceutics*, 331, 1-10.

Kumaravel, V. and Gopal, S.R. 2010. Immobilization of Bacillus amyloliquefaciens

MBL27 cells for enhanced antimicrobial protein production using calcium alginate beads. *Biotechnology and Applied Biochemistry*, 57, 97-103.

Kuo, W.C. and Shu, T.Y. 2004. Biological pre-treatment of wastewater containing sulfate using anaerobic immobilized cells. *Journal of Hazardous Materials*, 113, 147-155.

Kuznetsova, A., Popova, I., Yates, J. T., Bronikowski, M. J., Huffman, C. B., Liu, J., Smalley, R. E., Hwu, H. H., Chen, J. G. G. 2001. Oxygen-containing functional groups on single-wall carbon nanotubes: NEXAFS and vibrational spectroscopic studies. *Journal of the American Chemical Society*, 123, 10699-10704.

Lacerda, L., Raffab, S., Pratoc, M., Biancod, A., Kostarelosa, K. 2007. Cell-penetrating CNTs for delivery of therapeutics. *Nano Today*, 2, 38-43.

Lai, X., Blazer-Yost, B.L., Clack, J.W., Fears, S.L., Mitra, S., Ntim, S.A., Ringham, H.N., Witzmann, F.A. 2013. Protein expression profiles of intestinal epithelial co-cultures: effect of functionalised carbon nanotube exposure. *International Journal of Biomedical Nanoscience and Nanotechnology*, 3, 127-162.

Leenen, E.J., Dos, S.V., Grolle, K.C., Tramper, J., Wijffels, R.H. 1996. Characteristics of and selection criteria for support materials for cell immobilization in wastewater treatment. *Water Research*, 30, 2985-2996.

Leeuw, T., Reith, R., Simonette, R., Harden, M., Cherukuri, P., Tsyboulski, D., Beckingham, K., Weisman, R. 2007. Single-walled carbon nanotubes in the intact organism: near-IR imaging and biocompatibility studies in Drosophila. *Nano Letters*, 7, 2650-2654.

Lehtinen, J., Nuutila, J., Lilius, E.M. 2004. Green fluorescent protein-propidium iodide (GFP-PI) based assay for flow cytometric measurement of bacterial viability. *Cytometry A*, 60, 165-172.

Leung, W.C., Wong, M.F., Chua, H., Lo, W., Yu, P.H.F., Leung, C.K. 2000. Removal and recovery of heavy metals by bacteria isolated from activated sludge treating industrial effluents and municipal wastewater. *Water Science and Technology*, 41, 233-240.

Li, W., Bai, Y., Zhang, Y. K., Sun, M. L., Cheng, R. M., Xu, X. C., Chen, Y. W., Mo, Y.J. 2005. Effect of hydroxyl radical on the structure of multi-walled carbon nanotubes. *Synthetic Metals*, 155, 509-515.

Li, P., Lai, X., Witzmann, F., Blazer-Yost, B. 2013. Bioinformatic Analysis of Differential Protein Expression in Calu-3 Cells Exposed to Carbon Nanotubes. *Proteomes*, 1, 219-239.

Lin, D., Liu, N., Yang, K., Xing, B., Wu, F. 2010. Different stabilities of multiwalled carbon nanotubes in fresh surface water samples. *Environmental Pollution*, 158, 1270-1274.

Lin, D. and Xing, B. 2007. Phytotoxicity of nanoparticles: inhibition of seed germination and root growth. *Environmental Pollution*, 150, 243-250.

Liu, X., Ng, C., Ferenci, T. 2000. Global adaptations resulting from high population densities in Escherichia coli cultures. *Journal of Bacteriology*, 182, 4158-4164.

Liu, X., Hurt, R.H., Kane, A.B. 2010b. Biodurability of single-walled carbon nanotubes depends on surface functionalization. *Carbon*, 48, 1961-1969.

Liu, F., Liang, H.L., Xu, K.H., Tong, L.L., Tang, B. 2007. Supramolecular interaction of ethylenediamine linked beta-cyclodextrin dimer and berberine hydrochloride by spectrofluorimetry and its analytical application. *Talanta*, 74, 140-145.

Liu, S., Ng, A.K., Xu, R., Wei, J., Tan, C.M., Yang, Y., Chen, Y. 2010a. Antibacterial action of dispersed single-walled carbon nanotubes on Escherichia coli and Bacillus subtilis investigated by atomic force microscopy. *Nanoscale*, 2, 2744-2750.

Liu, X., O'Carroll, D.M., Petersen, E.J., Huang, Q., Anderson, C.L. 2009b. Mobility of

multiwalled carbon nanotubes in porous media. *Environmental Science and Technology*, 43, 8153-8158.

Liu, S., Wei, L., Hao, L., Fang, N., Chang, M., Xu, R., Yang, Y., Chen, Y. 2009a. Sharper and faster "nano darts" kill more bacteria: a study of antibacterial activity of individually dispersed pristine single-walled carbon nanotube. *American Chemical Society Nano*, 3, 3891-3902.

Liu, Y.J., Zhang, A.N., Wang, X.C. 2009. Biodegradation of phenol by using free and immobilized cells of *Acinetobacter* sp. XA05 and *Sphingomonas* sp. FG03. *Biochemical Engineering Journal*, 44, 187-192.

Lordi, V.; Yao, N., Wei, J. 2001. Method for supporting platinum on single-walled carbon nanotubes for a selective hydrogenation catalyst. *Chemistry of Materials*, 13, 733-737.

Lucchini, S., Liu, H., Jin, Q., Hinton, J.C., Yu, J. 2005. Transcriptional adaptation of Shigella flexneri during infection of macrophages and epithelial cells: insights into the strategies of a cytosolic bacterial pathogen. *Infection and Immunity*, 73, 88-102.

Luongo, L. and Zhang, X. 2010. Toxicity of carbon nanotubes to the activated sludge process. *Journal of Hazardous Materials*, 178, 356-362.

Mahmoud, K.A. and Luong, J.H. 2008. Impedance method for detecting HIV-1 protease and screening for its inhibitors using ferrocene-peptide conjugate/Au nanoparticle/single-walled carbon nanotube modified electrode. *Analytical Chemistry*, 80, 7056-7062.

Maloy, S.R. and Hughes, K.T. 2007. Strain collections and genetic nomenclature. *Methods in Enzymology*, 421, 3-8.

Mamouni, J., Tang, Y., Wu, M., Vlahovic, B., Yang, L. 2011. Single-walled carbon nanotubes coupled with near-infrared laser for inactivation of bacterial cells. *Journal of*

Nanoscience and Nanotechnology, 11, 4708-4716.

Manohar, S., Kim, C.K., Karegoudar, T.B. 2001. Enhanced degradation of naphthalene by immobilization of Pseudomonas sp. strain NGK1 in polyurethane foam. *Applied Microbiology and Biotechnology*, 55, 311-316.

Mansur, H.S., Pereira, M.M., Costa, H.S., Mansur, A.A.P. 2012. Mechanical behavior of nanostructured hybrids based on poly(vinyl alcohol)/bioactive glass reinforced with functionalized carbon nanotubes. *Journal of Nanomaterials*, 123, 1-9.

Maria-Neto, S., Candido Ede, S., Rodrigues, D.R., de Sousa, D.A., da Silva, E.M., de Moraes, L.M., Otero-Gonzalez Ade, J., Magalhaes, B.S., Dias, S.C., Franco, O.L. 2012. Deciphering the magainin resistance process of Escherichia coli strains in light of the cytosolic proteome. *Antimicrob Agents Chemother*, 56, 1714-1724.

Marisch, K., Bayer, K., Scharl, T., Mairhofer, J., Krempl, P.M., Hummel, K., Razzazi-Fazeli, E., Striedner, G. 2013. A comparative analysis of industrial Escherichia coli K-12 and B strains in high-glucose batch cultivations on process-, transcriptome- and proteome level. *PLoS One*, 8, e70516, 1-16.

Mattison, N.T., O'Carroll, D.M., Kerry Rowe, R., Petersen, E.J. 2011. Impact of porous media grain size on the transport of multi-walled carbon nanotubes. *Environmental Science and Technology*, 45, 9765-9775.

Mauger, M. and Binh, V.T. 2006. Vertically aligned carbon nanotube arrays for giant field emission display. *Journal of Vacuum Science and Technology B*, 24, 997-1003.

Maynard, A.D., Baron, P.A., Foley, M., Shvedova, A.A., Kisin, E.R., Castranova, V. 2004. Exposure to carbon nanotube material: aerosol release during the handling of unrefined single-walled carbon nanotube material. *Journal of Toxicology and*

Environmental Health, Part A, 67, 87-107.

Meng, J., Meng, J., Duan, J., Kong, H., Li, L., Wang, C., Xie, S., Chen, S., Gu, N., Xu, H., Yang, X.D. 2008. Carbon nanotubes conjugated to tumor lysate protein enhance the efficacy of an antitumor immunotherapy. *Small*, 4, 1364-1370.

Merkulov, V.I., Lowndes, D.H., Wei, Y.Y, Eres, G., Voelkl, W. 2000. Patterned growth of individual and multiple vertically aligned carbon nanofibers. *Applied Physics Letters*, 76, 3555-3557.

Meyyappan, M., Delzeit, L., Cassell, A., Hash, David. 2003. Carbon nanotube growth by PECVD: A review. *Plasma Sources Science and Technology*, 12, 205-216.

Model, P., Jovanovic, G., Dworkin, J. 1997. The Escherichia coli phage-shock-protein (psp) operon. *Molecular Microbiology*, 24, 255-261.

Monteiro-Riviere, N.A., Nemanich, R.J., Inman, A.O., Wang, Y.Y., Riviere, J.E. 2005. Multi-walled carbon nanotube interactions with human epidermal keratinocytes. *Toxicology Letters*, 155, 377-384.

Morikawa, Y., Karube, I., Suzuki, S. 1980. Continuous production of bacitracin by immobilized living whole cells of *Bacillus* sp. *Biotechnology and Bioengineering*, 22, 1015-1023.

Mouchet, F., Landois, P., Puech, P., Pinelli, E., Flahaut, E., Gauthier, L. 2010. Carbon nanotube ecotoxicity in amphibians: assessment of multiwalled carbon nanotubes and comparison with double-walled carbon nanotubes. *Nanomedicine,* 5, 963-974.

Mueller, N.C. and Nowack, B. 2008. Exposure modeling of engineered nanoparticles in the environment. *Environmental Science and Technology*, 42, 4447-4453.

National Nanotechnology Initiative (NNI). 2008. What is Nanotechnology? Retrieved September 25, 2008, from

http://www.nano.gov/html/facts/whatIsNano.html.

Najafpour, G., Younesi, H., Ismail, K.S.K. 2004. Ethanol fermentation in an immobilized cell reactor using *Saccharomyces cerevisiae*. *Bioresource Technology*, 92, 251-260.

Nepal, D., Balasubramanian, S., Simonian, A.L., Davis, V.A. 2008. Strong antimicrobial coatings: single-walled carbon nanotubes armored with biopolymers. *Nano Letters*, 8, 1896-1901.

Nikolaev, P., Bronikowski, M.J., Bradley, R.K., Rohmund, F., Colbert, D.T., Smith, K.A., Smalley, R.E. 1999. Gas-phase catalytic growth of single-walled carbon nanotubes from carbon monoxide. *Chemical Physics Letters*, 313, 91-97.

Nishio, T., Yoshikura, T., Mishima, H., Inouye, Z., Itoh, H. 1998. Conditions for nitrification and denitrification by an immobilized heterotrophic nitrifying bacterium *Alcaligenes faecalis* OKK 17. *Journal of Fermentation and Bioengineering*, 86, 351-356.

Niyogi, S., Hamon, M.A., Hu, H., Zhao, B., Bhowmik, P., Sen, R., Itkis, M.E., Haddon, R.C. 2002. Chemistry of single-walled carbon nanotubes. *Accounts of Chemical Research*, 35, 1105-1113.

Nowack, B., David, R.M., Fissan, H., Morris, H., Shatkin, J.A., Stintz, M., Zepp, R., Brouwer, D. 2013. Potential release scenarios for carbon nanotubes used in composites. *Environment International*, 59, 1-11.

Njuguna, J. and Pielichowski, K. 2003. Polymer nanocomposites for aerospace application: Properties. *Advanced Engineering Materials,* 5, 769-778.

NSF. 2011. Nanotechnology research directions for societal needs in 2020: retrospective and outlook summary. National Science Foundation. In: Roco M, Mirkin C, Hersan M, eds. Science Policy Reports. New York: Springer.

O'Connell, M.J. 2006. Carbon nanotubes: properties and applications. Boca Raton, FL, Taylor and Francis Group.

O'Connell, M.J., Bachilo, S. M., Huffman, C. B., Moore, V. C., Strano, M. S., Haroz, E. H., Rialon, L.R., Boul, P.J., Noon, W.H., Kittrell, C., Huage, R.H., Weisman, R.B., Smalley, R. E. 2002. Band gap fluorescence from individual single-walled carbon nanotubes. *Science*, 297, 593-596.

Oberdorster, G., Ferin, J., Lehnert, B.E. 1994. Correlation between particle size, in vivo particle persistence, and lung injury. *Environmental Health Perspectives*, 102(Suppl. 5), 173-179.

Obraztsova, E.A., Lukashev, E.P., Zarubina, A.P., Parkhomenko, I.M., Yaminsky, I.V. 2009. Bactericidal action of single-walled carbon nanotubes. *Moscow University Physics Bulletin*, 64, 320-323.

Olivi, M., Zanni, E., De Bellis, G., Talora, C., Sarto, M., Palleschi, C., Flahaut, E., Monthioux, M., Rapino, S., Uccelletti, D., Fiorito, S. 2013. Inhibition of microbial growth by carbon nanotube networks. *Nanoscale*, 5, 9023-9029.

Ozkanca, R. 2002. beta-Galactosidase activity of Escherichia coli under long-term starvation, alterations in temperature, and different nutrient conditions in lake water. *International Microbiology*, 5, 127-132.

Park J.K. and Chang H.N. 2000. Microencapsulation of microbial cells. *Biotechnology Advances*, 18, 303-319.

Pacurari, M., Qian, Y., Porter, D.W., Wolfarth, M., Wan, Y., Luo, D., Ding, M., Castranova, V., Guo, N.L. 2011. Multi-walled carbon nanotube-induced gene expression in the mouse lung: association with lung pathology. *Toxicology and Applied Pharmacology*, 255, 18-31.

Panyam, J., Dali, M.M., Sahoo, S.K., Ma, W., Chakravarthi, S.S., Amidon, G.L., Levy, R.J., Labhasetwar, V. 2003. Polymer degradation and in vitro release of a model protein from poly(D,L-lactide-co-glycolide) nano- and microparticles. *Journal of Controlled Release*, 92, 173-187.

Parise, A., Thakor, H., Zhang, X. 2013. Activity inhibition on municipal activated sludge by single-walled carbon nanotubes. *Journal of Nanoparticle Research*, 16, 2159-2163.

Park, J.K. and Chang, H.N. 2000. Microencapsulation of microbial cells. *Biotechnology Advances*, 18, 303-319.

Parvin, B., Refi, I., Bunshi, F., Makoto, M., Tsukasa, A., Fumio, W. 2012. Phytotoxicity of multi-walled carbon nanotubes assessed by selected plant species in the seedling stage. *Applied Surface Science*, 262, 120-124.

Pasquini, L.M., Hashmi, S.M., Sommer, T.J., Elimelech, M., Zimmerman, J.B. 2012. Impact of surface functionalization on bacterial cytotoxicity of single-walled carbon nanotubes. *Environmental Science and Technology*, 46, 6297-6305.

Patlolla, A., Knighten, B., Tchounwou, P. 2010a. Multi-walled carbon nanotubes induce cytotoxicity, genotoxicity and apoptosis in normal human dermal fibroblast cells. *Ethnicity and Disease*, 20, 65-72.

Patlolla, A., Patlolla, B., Tchounwou, P. 2010b. Evaluation of cell viability, DNA damage, and cell death in normal human dermal fibroblast cells induced by functionalized multiwalled carbon nanotube. *Molecular and Cellular Biochemistry*, 338, 225-232.

Petersen, E., Zhang, L., Mattison, N., O'Carroll, D., Whelton, A., Uddin, N., Nguyen, T., Huang, Q., Henry, T., Holbrook, R., Chen, K. 2011. Potential release pathways, environmental fate, and ecological risks of carbon nanotubes. *Environmental Science and*

Technology, 45, 9837-9856.

Petrov, P., Stassin, F., Pagnoulle, C., Jerome, R. 2003. Noncovalent functionalization of multi-walled carbon nanotubes by pyrene containing polymers. *Chemical Communications*, 23, 2904-2905.

Philbrook, N., Walker, V., Afrooz, A., Saleh, N., Winn, L. 2011. Investigating the effects of functionalized carbon nanotubes on reproduction and development in Drosophila melanogaster and CD-1 mice. *Reproductive Toxicology (Elmsford, N.Y.)*, 32, 442-448.

Podila, R. and Brown, J.M. 2013. Toxicity of engineered nanomaterials: a physicochemical perspective. *Journal of Biochemical and Molecular Toxicology*, 27, 50-55.

Pramanik, S., McEvoy, J., Siripattanakul, S., Khan, E. 2011. Effects of cell entrapment on nucleic acid content and microbial diversity of mixed cultures in biological wastewater treatment. *Bioresource Technology*, 102, 3176-3183.

Prato, M., Kostarelos, K., Bianco, A. 2008. Functionalized carbon nanotubes in drug design and discovery. *Accounts of Chemical Research*, 41, 60-68.

Radomski, A., Jurasz, P., Alonso-Escolano, D., Drews, M., Morandi, M., Malinski, T., Radomski, M.W. 2005. Nanoparticle-induced platelet aggregation and vascular thrombosis. *British Journal of Pharmacology*, 146, 882-893.

Rajavel, K., Gomathi, R., Manian, S., Rajendra Kumar, R. 2014. In vitro bacterial cytotoxicity of CNTs: Reactive oxygen species mediate cell damage edges over direct physical puncturing. *Langmuir*, 30, 592-601.

Reid, A.N., Pandey, R., Palyada, K., Naikare, H., Stintzi, A. 2008. Identification of Campylobacter jejuni genes involved in the response to acidic pH and stomach transit. *Applied and Environmental Microbiology*, 74, 1583-1597.

Ren, Z.F., Huang, Z.P., Xu, J.W., Wang, J.H., Bush, P., Siegal, M.P., Provencio, P.N. 1998. Synthesis of large arrays of well-aligned carbon nanotubes on glass. *Science*, 282, 1105-1107.

Renzone, G., D'Ambrosio, C., Arena, S., Rullo, R., Ledda, L., Ferrara, L., Scaloni, A. 2005. Differential proteomic analysis in the study of prokaryotes stress resistance. *Annali Dell'Istituto Ssuperiore Di SanitÃ*, 41, 459-468.

Roberts, A.P., Mount, A.S., Seda, B., Souther, J., Qiao, R., Lin, S. 2007. In vivo biomodification of lipid-coated carbon nanotubes by Daphnia magna. *Environmental Science and Technology*, 41, 3025-3029.

Rodrigues, D., Jaisi, D., Elimelech, M. 2013. Toxicity of functionalized single-walled carbon nanotubes on soil microbial communities: implications for nutrient cycling in soil. *Environmental Science and Technology*, 47, 625-633.

Rompre, A., Servais, P., Baudart, J., de-Roubin, M.R., Laurent, P. 2002. Detection and enumeration of coliforms in drinking water: current methods and emerging approaches. *Journal of Microbiological Methods*, 49, 31-54.

Rodrigues, D.F. and Elimelech, M. 2010. Toxic effects of single-walled carbon nanotubes in the development of E. coli biofilm. *Environmental Science and Technology*, 44, 4583-4589.

Rosenzweig, S., Sorial, G.A., Sahle-Demessie, E., Mack, J. 2013. Effect of acid and alcohol network forces within functionalized multiwall carbon nanotubes bundles on adsorption of copper (II) species. *Chemosphere*, 90, 395-402.

Roukas, T. 1996. Continuous ethanol production from nonsterilized carob pod extract by immobilized Saccharomyces cerevisiae on mineral kissiris using a two-reactor system. *Applied Biochemistry and Biotechnology*, 59, 299-307.

Roy, M., Sonkar, S.K., Tripathi, S., Saxena, M., Sarkar, S. 2012. Non-toxicity of water soluble multi-walled carbon nanotube on Escherichia-coli colonies. *Journal of Nanoscience and Nanotechnology*, 12, 1754-1759.

Sadik, O.A. 2013. Anthropogenic nanoparticles in the environment. *Environmental Science: Processes and Impacts*, 15, 19-20.

Safekordi, A., Attar, H., Binaeian, E. 2012. Study on toxicity of manufactured nanoparticles to bacteria Vibrio fischeri using homemade luminometer. *The International Council for Central and East European Studies (ICCEES)'2012*, 60-65.

Saito, Y. and Uemura, S. 2000. Field emission from carbon nanotubes and its application to electron sources. *Carbon,* 38, 169-182.

Saleh, N.B., Pfefferle, L.D., Elimelech, M. 2010. Influence of biomacromolecules and humic acid on the aggregation kinetics of single-walled carbon nanotubes. *Environmental Science and Technology*, 44, 2412-2418.

Salkinoja-Salonen, M.S., Middeldorp, P.J.M., Briglia, M., Valo, R., Haggblom, M., McBain, A. 1989. Clean up of old industrial sites. *Advances in Applied Biotechnology,* Gulf Publishing Company, Houston, TX, USA. 4, 344-367.

Salvador-Morales, C., Flahaut, E., Sim, E., Sloan, J., Green, M.L., Sim, R.B. 2006. Complement activation and protein adsorption by carbon nanotubes. *Molecular Immunology*, 43, 193-201.

Sargent, L.M., Hubbs, A.F., Young, S.H., Kashon, M.L., Dinu, C.Z., Salisbury, J.L., Benkovic, S.A., Lowry, D.T., Murray, A.R., Kisin, E.R., Siegrist, K.J., Battelli, L., Mastovich, J., Sturgeon, J.L., Bunker, K.L., Shvedova, A.A., Reynolds, S.H. 2012. Single-walled carbon nanotube-induced mitotic disruption. *Mutation Research/Genetic*

Toxicology and Environmental Mutagenesis, 745, 28-37.

Saxena, R.K., Williams, W., Mcgee, J.K., Daniels, M.J., Boykin, E., Gilmour, M.I. 2007. Enhanced in vitro and in vivo toxicity of poly-dispersed acid-functionalized single-wall carbon nanotubes. *Nanotoxicology*, 1, 291-300.

Schierz, A. and Zanker, H. 2009. Aqueous suspensions of carbon nanotubes: Surface oxidation, colloidal stability and uranium sorption. *Environmental Pollution*, 157, 1088-1094.

Schindler, A., Brill, J., Fruehauf, N., Novak, J.P., Yaniv, Z. 2007. Solution-deposited carbon nanotube layers for flexible display applications. *Physica E: Low-Dimensional Systems and Nanostructures*, 37, 119-123.

Schwyzer, I., Kaegi, R., Sigg, L., Magrez, A., Nowack, B. 2011. Influence of the initial state of carbon nanotubes on their colloidal stability under natural conditions. *Environmental Pollution*, 159, 1641-1648.

Scott-Fordsmand, J., Krogh, P., Schaefer, M., Johansen, A. 2008. The toxicity testing of double-walled nanotubes-contaminated food to Eisenia veneta earthworms. *Ecotoxicology and Environmental Safety*, 71, 616-619.

Shen, C.X., Zhang, Q.F., Li, J., Bi, F.C., Yao, N. 2010. Induction of programmed cell death in Arabidopsis and rice by single-wall carbon nanotubes. *American Journal of Botany*, 97, 1602-1609.

Shvedova, A.A., Castranova, V., Kisin, E.R., Schwegler-Berry, D., Murray, A.R., Gandelsman, V.Z., Maynard, A., Baron, P. 2003. Exposure to carbon nanotube material: assessment of nanotube cytotoxicity using human keratinocyte cells. *Journal of Toxicology and Environmental Health Part A*, 66, 1909-1926.

Shvedova, A.A., Kisin, E., Murray, A.R., Johnson, V.J., Gorelik, O., Arepalli, S., Hubbs,

A.F., Mercer, R.R., Keohavong, P., Sussman, N., Jin, J., Yin, J., Stone, S., Chen, B.T., Deye, G., Maynard, A., Castranova, V., Baron, P.A., Kagan, V.E. 2008. Inhalation vs. aspiration of single-walled carbon nanotubes in C57BL/6 mice: inflammation, fibrosis, oxidative stress, and mutagenesis. *American Journal of Physiology-Lung Cellular and Molecular Physiology*, 295, L552-L565.

Simate, G.S., Iyuke, S.E., Ndlovu, S., Heydenrych, M., Walubita, L.F. 2012. Human health effects of residual carbon nanotubes and traditional water treatment chemicals in drinking water. *Environmental International*, 39, 38-49.

Simon-Deckers, A., Loo, S., Mayne-L'hermite, M., Herlin-Boime, N., Menguy, N., Reynaud, C., Gouget, B., Carriere, M. 2009. Size-, composition- and shape-dependent toxicological impact of metal oxide nanoparticles and carbon nanotubes toward bacteria. *Environmental Science and Technology*, 43, 8423-8429.

Smart, S.K., Cassady, A.I., Lu, G.Q., Martin, D.J. 2006. The biocompatibility of carbon nanotubes. *Carbon*, 44, 1034-1047.

Smidsrød, O. and Skjåk-Braek, G. 1990. Alginate as immobilization matrix for cells. *Trends in Biotechnology*, 8, 71-78.

Smith, C., Shaw, B., Handy, R. 2007. Toxicity of single walled carbon nanotubes to rainbow trout, (Oncorhynchus mykiss): respiratory toxicity, organ pathologies, and other physiological effects. *Aquatic toxicology (Amsterdam, Netherlands)*, 82, 94-109.

Snow, E.S., Campbell, P.M., Ancona, M.G., Novak, J.P. 2005. High-mobility carbon-nanotube thin-film transistors on a polymeric substrate. *Applied Physics Letters*, 86, 1-3.

Snow, E.S., Novak, J.P., Campbell, P.M., Park, D. 2003. Random networks of carbon nanotubes as an electronic material. *Applied Physics Letters*, 82, 2145-2147.

Snyder-Talkington, B.N., Schwegler-Berry, D., Castranova, V., Qian, Y., Guo, N.L. 2013. Multi-walled carbon nanotubes induce human microvascular endothelial cellular effects in an alveolar-capillary co-culture with small airway epithelial cells. *Particle and Fibre Toxicology*, 10, 35-49.

Sohn, J.I., Lee, S., Song, Y.H., Choi, S.Y., Cho., K.I., Nam, K.S. 2001. Patterned selective growth of carbon nanotubes and large field emission from vertically well-aligned carbon nanotube field emitter arrays. *Applied Physics Letters*, 78, 901-903.

Sreenivasan, K. (2004). Enhanced drug uptake and retention by surface phosphorylated polyvinyl alcohol. *Journal of Applied Polymer Science*, 94, 651-656

Srinivasulu, B., Adinarayana, K., Ellaiah, P. 2003. Investigations on neomycin production with immobilized cells of Streptomyces marinensis NUV-5 in calcium alginate matrix. *AAPS PharmSciTech*, 4, 449-454.

Stampoulis, D., Sinha, S., White, J. 2009. Assay-dependent phytotoxicity of nanoparticles to plants. *Environmental Science and Technology*, 43, 9473-9479.

Star, A., Stoddart, J.F., Steuerman, D., Diehl, M., Boukai, A., Wong, E.W., Yang, X., Chung, S.W., Choi, H., Heath, J.R. 2001. Preparation and Properties of Polymer-Wrapped Single-Walled Carbon Nanotubes. *Angewandte Chemie International Edition*, 40, 1721-1725.

Su, Y., Zhang, Y., Wei, H., Zhang, L., Zhang, Y. 2011. Magnetic-field-induced diameter-selective synthesis of single-walled carbon nanotubes. *Nanoscale*, 4, 1717-1721.

Sun, L.M., Zhang, C.L., Li, P. 2011. Characterization, antimicrobial activity, and mechanism of a high-performance (-)-epigallocatechin-3-gallate (EGCG)-CuII/polyvinyl alcohol (PVA) nanofibrous membrane. *Journal of Agricultural and Food Chemistry*, 59, 5087-

5092.

Tabet, L., Bussy, C., Setyan, A., Simon-Deckers, A., Rossi, M.J., Boczkowski, J., Lanone, S. 2011. Coating carbon nanotubes with a polystyrene-based polymer protects against pulmonary toxicity. *Particle and Fibre Toxicology*, 8, 1-13.

Tampion, J. and Tampion, M.D. 2011. Immobilized Cells: Principles and Applications (Vol 5). New York, NY, Cambridge University Press.

Tan, X.M., Lin, C., Fugetsu, B. 2009. Studies on toxicity of multi-walled carbon nanotubes on suspension rice cells. *Carbon*, 47, 3479-3487.

Tan, X.M. and Fugetsu, B. 2007. Multi-walled carbon nanotubes interact with cultured rice cells: Evidence of a self-defense response. *Journal of Biomedical Nanotechnology*, 3, 285-288.

Teo, K.V.K., Minoux, E., Hudanski, L., Peauger, F., Schnell, J.-P., Gangloff, L., Legagneux, P., Dieumegard, D., Amaratunga, G.A.J., Milneet, W.I. 2005. Microwave devices: Carbon nanotubes as cold cathodes. *Nature*, 437, 968-968.

Thess, A., Lee, R., Nikolaev, P., Dai, H., Petit, P., Robert, J., Xu, C., Lee, Y.H., Kim, S.G., Rinzler, A.G., Colbert, D.T., Scuseria, G.E., Tomanek, D., Fischer, J.E., Smalley, R.E. 1996. Crystalline ropes of metallic carbon nanotubes. *Science*, 273, 483-487.

Tinkle, S.S. 2008. Nanotechnology: collaborative opportunities for ecotoxicology and environmental health. *Environmental Toxicology and Chemistry*, 27, 1823-1824.

Tong, Z., Bischoff, M., Nies, L.F., Myer, P., Applegate, B., Turco, R.F. 2012. Response of soil microorganisms to As-produced and functionalized single wall carbon nanotubes (SWCNTs). *Environmental Science and Technology*, 46, 13471-13479.

Tryland, I. and Fiksdal, L. 1998. Enzyme characteristics of beta-D-galactosidase- and beta-D-glucuronidase-positive bacteria and their interference in rapid methods for

detection of waterborne coliforms and Escherichia coli. *Letters in Applied Microbiology*, 33, 246-250.

Ursini, C.L., Cavallo, D., Fresegna, A.M., Ciervo, A., Maiello, R., Buresti, G., Casciardi, S., Tombolini, F., Bellucci, S., Iavicoli, S. 2012. Comparative cyto-genotoxicity assessment of functionalized and pristine multiwalled carbon nanotubes on human lung epithelial cells. *Toxicology in Vitro,* 26*,* 831-840.

Usrey, M.L. and Strano, M.S. 2009. Adsorption of single walled carbon nanotubes onto silicon oxide surface gradients of 3-aminopropyltri(ethoxysilane) described by polymer adsorption theory. *Langmuir*, 25, 9922-9930.

Vaisman, L., Wagner, H.D., Marom, G. 2006. The role of surfactants in dispersion of carbon nanotubes. *Advances in Colloid and Interface Science*, 128, 37-46.

Van der Sluis, C., Mulder, A.N., Grolle, K.C., Engbers, G.H., ter Schure, E.G., Tramper, J., Wijffels, R.H. 2000. Immobilized soy-sauce yeasts: development and characterization of a new polyethylene-oxide support. *Journal of Biotechnology*, 80, 179-188.

Vander Wal, R. 2002. Fe-catalyzed single-walled carbon nanotube synthesis within a flame environment. *Combustion and Flame*, 130, 37-47.

Van Veen, J.A., Van Overbeek, L.S., Van Elsas, J.D. 1997. Fate and activity of microorganism introduced into soil. *Microbiology and Molecular Biology Reviews*, 61, 121-135.

Vardharajula, S., Ali, S.Z., Tiwari, P.M., Eroglu, E., Vig, K., Dennis, V.A., Singh, S.R. 2012. Functionalized carbon nanotubes: biomedical applications. *International Journal of Nanomedicine*, 7, 5361-5374.

Vecitis, C.D., Zodrow, K.R., Kang, S., Elimelech, M. 2010. Electronic-structure-dependent bacterial cytotoxicity of single-walled carbon nanotubes. *American Chemical Society*

Nano, 4, 5471-5479.

Walters, D. A., Ericson, L.M., Casavant, M.J., Liu, J., Colbert, D.T., Smith, K.A., Smalley R. E. 1999. Elastic strain of freely suspended single-wall carbon nanotube ropes. *Applied Physics Letters*, 74, 3803-3805.

Wang, Y., Li, Y., Fortner, J.D., Hughes, J.B., Abriola, L.M., Pennell, K.D. 2008. Transport and retention of nanoscale C60 aggregates in water-saturated porous media. *Environmental Science and Technology*, 42, 3588-3594.

Wang, L.Y., Mercer, R.R., Rojanasakul, Y., Qiu, A.J., Lu, Y.J., Scabilloni, J.F., Wu, N.Q., Castranova, V. 2010. Direct fibrogenic effects of dispersed single-walled carbon nanotubes on human lung fibroblasts. *Journal of Toxicology and Environmental Health-Part A-Current Issues*, 73, 410-422.

Wang, Y. H., Shan, H. W., Hauge, R. H., Pasquali, M., Smalley, R. E. 2007. A highly selective, one-pot purification method for single-walled carbon nanotubes. *The Journal of Physical Chemistry B*, 111, 1249-1252.

Wang, Z. W., Shirley, M. D., Meikle, S. T., Whitby, R. L. D., Mikhalovsky, S. V. 2009. The surface acidity of acid oxidized multi-walled carbon nanotubes and the influence of in-situ generated fulvic acids on their stability in aqueous dispersions. *Carbon*, 47, 73-79.

Wang, Q.H., Yan, M., Chang, R.P.H. 2001. Flat panel display prototype using gated carbon nanotube field emitters. *Applied Physics Letters*, 78, 1294-1296.

Warheit, D.B., Laurence, B.R., Reed, K.L., Roach, D.H., Reynolds,G.A.M., Webb, T.R. 2003. Comparative pulmonary toxicity assessment of single wall carbon nanotubes in rats. *Toxicological Sciences*, 77, 117-125.

Wei, B. Q., Vajtai, R., Ajayan, P. M. 2001. Reliability and current carrying capacity of

carbon nanotubes. *Applied Physics Letters,* 79, 1172-1174.

Weiner, L. and Model, P. 1994. Role of an Escherichia coli stress-response operon in stationary-phase survival. *Proceedings of the National Academy of Sciences of the United States of America*, 91, 2191-2195.

Welsher, K., Liu, Z., Daranciang, D., Dai, H. 2008. Selective probing and imaging of cells with single walled carbon nanotubes as near-infrared fluorescent molecules. *Nano Letters*, 8, 586-590.

Wick, P., Manser, P., Limbach, L.K., Dettlaff-Weglikowska, U., Krumeich, F., Roth, S., Stark, W.J., Bruinink, A. 2007. The degree and kind of agglomeration affect carbon nanotube cytotoxicity. *Toxicology Letters*, 168, 121-131.

Wijffels, R. H. 2001. Characterization of Immobilized Cells: Introduction. In R.H. Wijffels, R.M. Buitelaar, C. Bucke, J. Tramper, *Immobilized Cells: Basics and Applications*. Amsterdam, The Netherlands, Elservier Science B.V.

Wu, K.Y.A and Wisecarver, K.D. 1992. Cell immobilization using PVA crosslinked with boric acid. *Biotechnology and Bioengineering*, 39, 447-449.

Xu, Z.Q. and Yao, M.S. 2011. Effects of single-walled carbon nanotube filter on culturability and diversity of environmental bioaerosols. *Journal of Aerosol Science*, 42, 387-396.

Yang, C., Mamouni, J., Tang, Y., Yang, L. 2010. Antimicrobial activity of single-walled carbon nanotubes: length effect. *Langmuir*, 26, 16013-16019.

Yi, P. and Chen, K.L. 2011. Influence of surface oxidation on the aggregation and deposition kinetics of multiwalled carbon nanotubes in monovalent and divalent electrolytes. *Langmuir*, 27, 3588-3599.

Ying, Y. M., Saini, R. K., Liang, F., Sadana, A. K., Billups, W. E. 2003. Functionalization

of carbon nanotubes by free radicals. *Organic Letters*, 5, 1471-1473.

Young, B.J., Riera, N.I., Beily, M.E., Bres, P.A., Crespo, D.C., Ronco, A.E. 2012. Toxicity of the effluent from an anaerobic bioreactor treating cereal residues on Lactuca sativa. *Ecotoxicology and Environmental Safety*, 76, 182-186.

Yu, M.F., Files, B.S., Arepalli, S., Ruoff, R.S. 2000. Tensile loading of ropes of single wall carbon nanotubes and their mechanical properties. *Physical Review Letters*, 84, 5552-5555.

Yue, G.Z., Qiu, Q., Cheng, B.G.Y., Zhang, J., Shimoda, H., Chang, S., Lu, J.P., Zhou, O. 2002. Generation of continuous and pulsed diagnostic imaging x-ray radiation using a carbon-nanotube-based field-emission cathode. *Applied Physics Letters*, 81, 355-357.

Zarubina, A.P., Lukashev, E.P., Deev, L.I., Parkhomenko, I.M., Rubin, A.B. 2010. Biotesting the biological effects of single-wall carbon nanotubes using bioluminescent bacteria test-system. *Nanotechnologies in Russia*, 4, 871-875.

Zhang, Y., Bai, Y., Yan, B. 2010. Functionalized carbon nanotubes for potential medicinal applications. *Drug Discovery Today*, 15, 428-435.

Zhang, X., Burry, S., Dibiasio, D., Miller, J.E. 1989 Effects of immobilization on growth, substrate consumption, β-galactosidase induction, and byproduct formation in *Escherichia coli*. *Journal of Industrial Microbiology*. 4, 239-246.

Zhang, L., Petersen, E.J., Huang, Q. 2011. Phase distribution of (14)c-labeled multiwalled carbon nanotubes in aqueous systems containing model solids: peat. *Environmental Science and Technology*, 45, 1356-1362.

Zhang, J., Zou, H., Qing, Q., Li, Q., Liu, Z., Du, Z. 2003. Effect of chemical oxidation on the structure of single walled carbpn nanotubes. *The Journal of Physical Chemistry*

B, 107, 3712-3718.

Zhao, X. and Liu, R. 2012. Recent progress and perspectives on the toxicity of carbon nanotubes at organism, organ, cell, and biomacromolecule levels. *Environment International*, 40, 244-255.

Zhon, W., Winter, B., Zimmermann, W. 1993. Dechlorination of high-molecular-mass compounds in spent sulphite bleach effluents by free and immobilized cells of streptomycetes. *Applied Microbiology and Biotechnology*, 39, 418-423.

Zhu, L., Chang, D.W., Dai, L., Hong, Y. 2007. DNA damage induced by multiwalled carbon nanotubes in mouse embryonic stem cells. *Nano Letters*, 7, 3592-3597.

Zu, M., Li, Q., Zhu, Y., Wang, G., Byun, J-H., Chou. T-W. 2013. Stress relaxation in carbon nanotube-based fibers for load-bearing applications. *Carbon.* 52, 347-355.

APPENDIX A: OPTIMIZATION OF THE ENZYME ASSAYS CONDITIONS

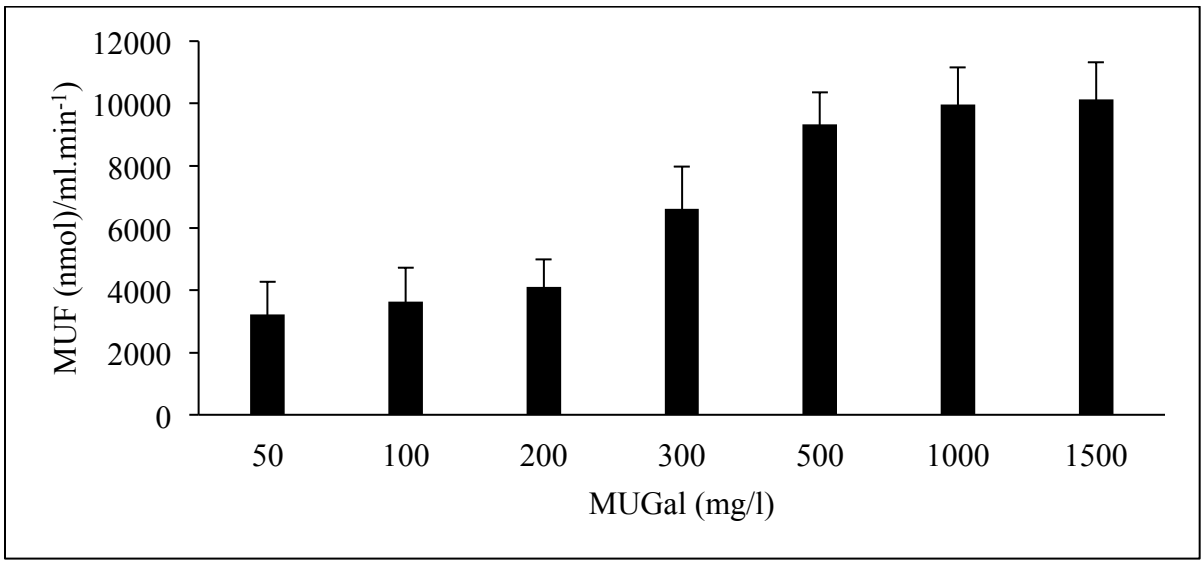

Figure A-1: Dependence of enzyme activity on the concentrations of MUGal.

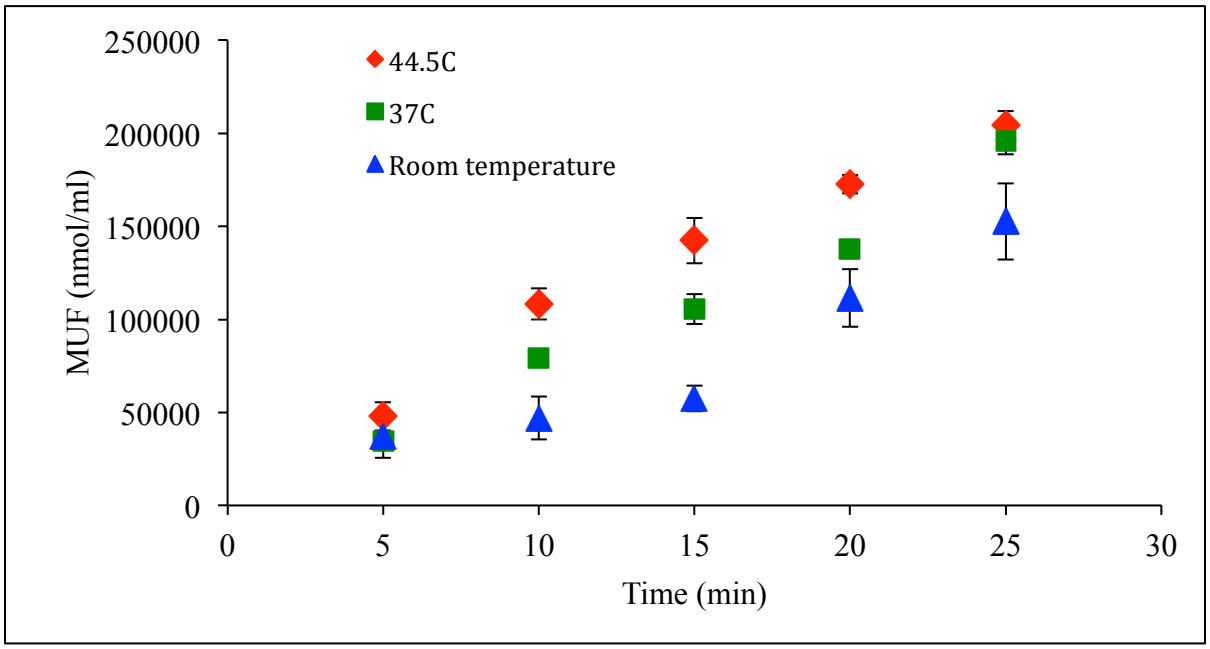

Figure A-2: Influence of different temperature on enzyme activity of *E. coli* ATCC 8739.

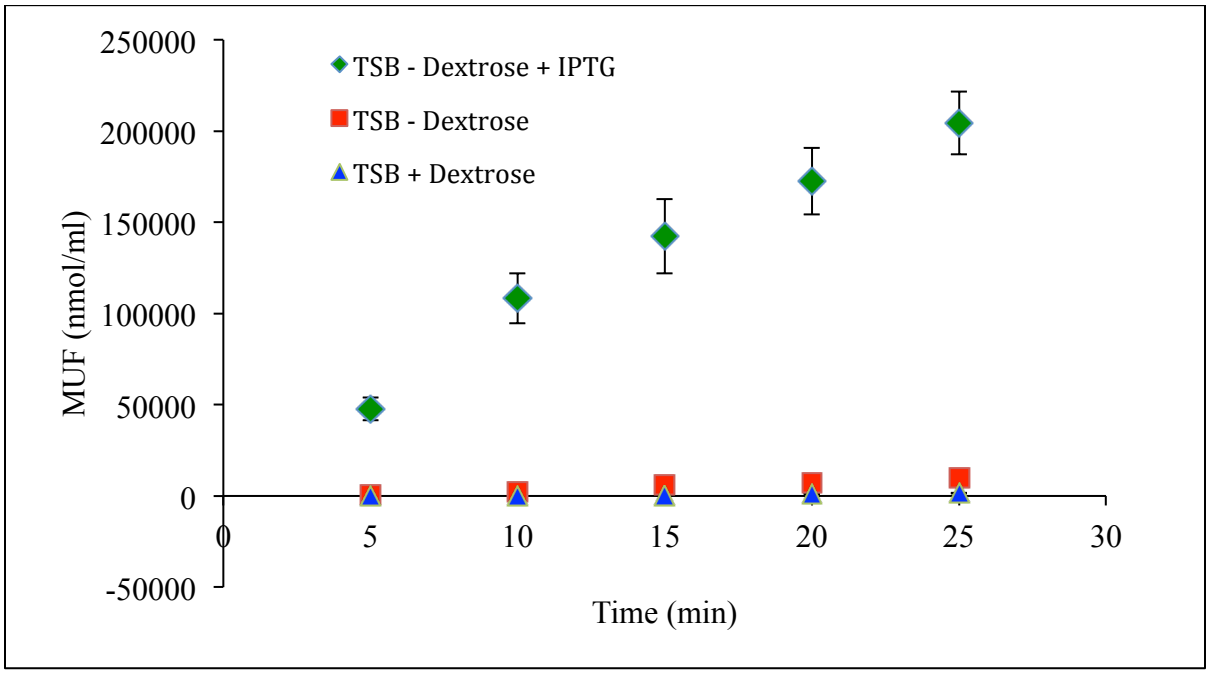

Figure A-3: Influence of different nutrient media components on the enzyme activity of *E. coli* ATCC 8739.

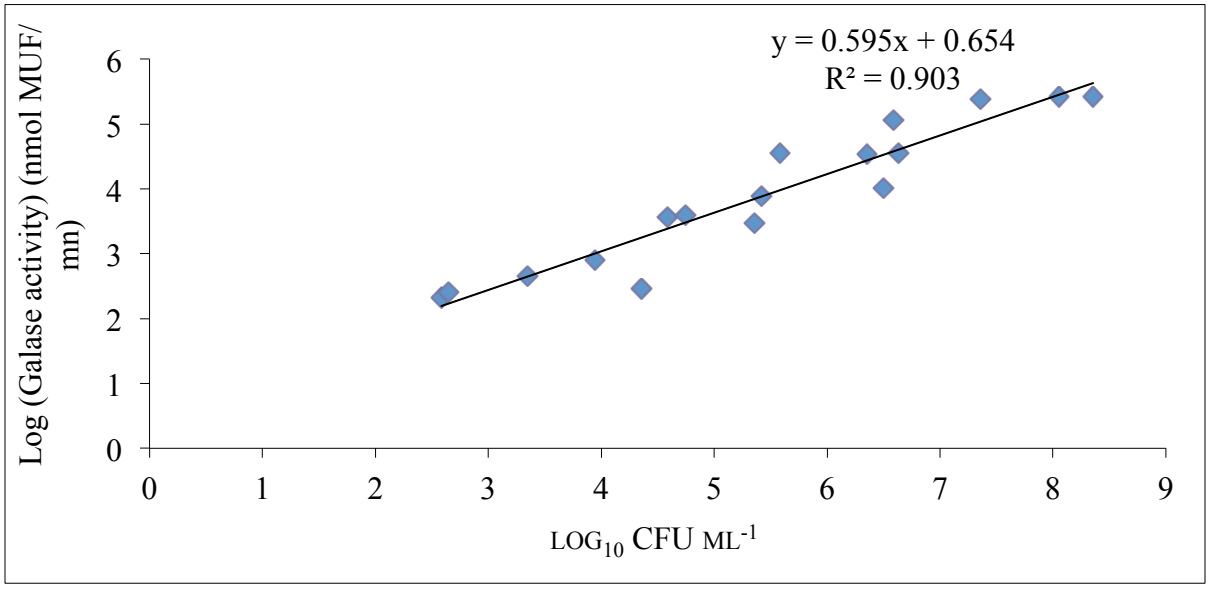

Figure A-4: Relationship between β-D-galactosidase activity and total bacteria (CFU) of *E. coli* ATCC 8739.

APPENDIX B: SDS-PAGE OF *ESCHERICHIA COLI* BEFORE AND AFTER EXPOSURE TO CNTS

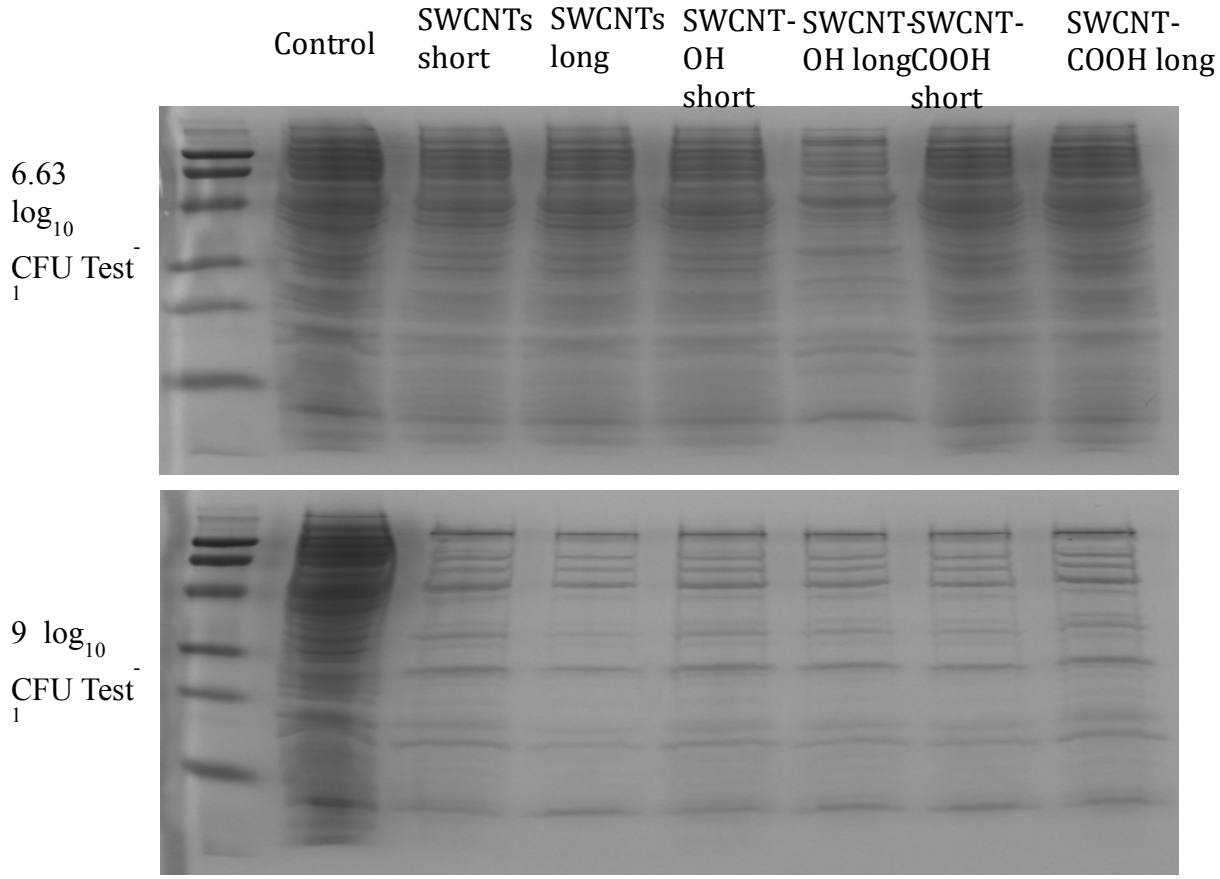

Figure B-1: SDS-PAGE of *E. coli* before and after exposure to CNTs.

APPENDIX C: EFFECTS OF CNT-FITC ON THE VIABILITY OF *ESCHERICHIA COLI*

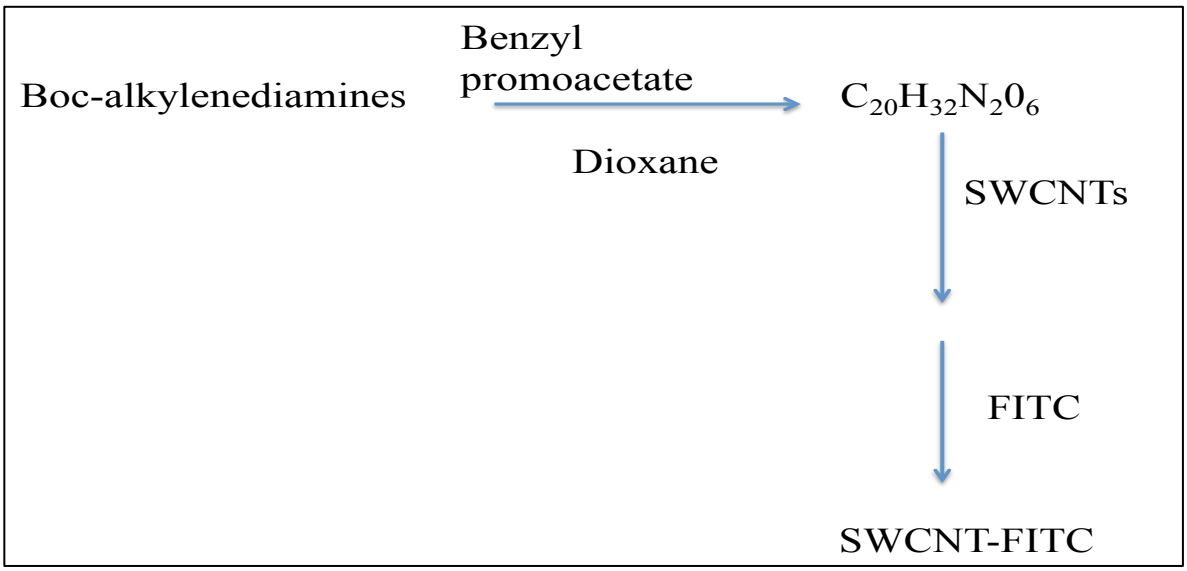

Scheme C-1: FITC functionalization procedure.

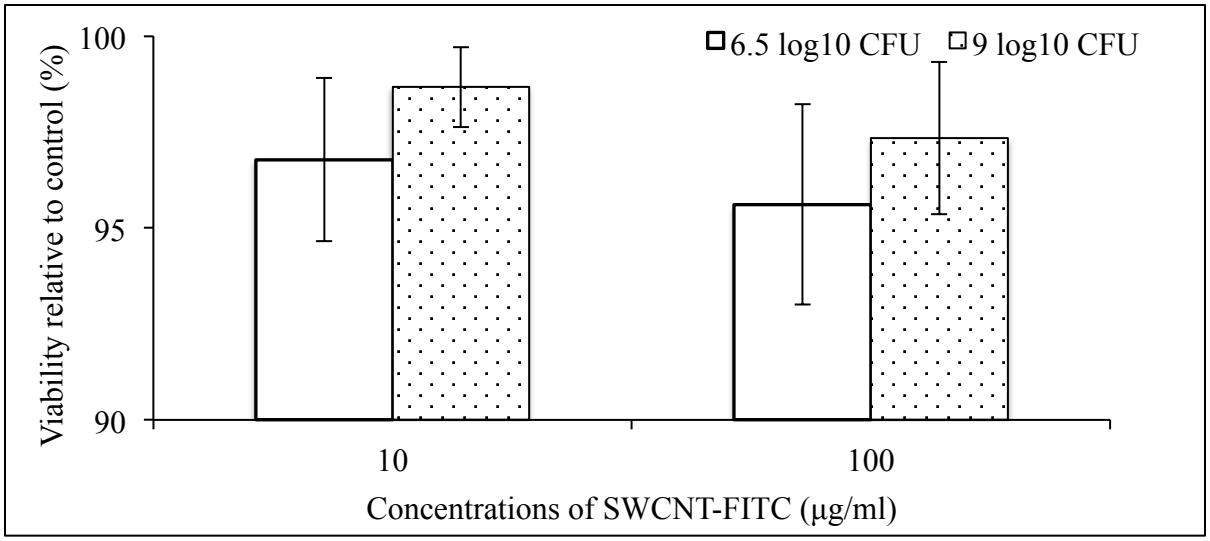

Figure C-1: Effect of SWCNT-FITC on viability of entrapped *E. coli*. By using enzyme assay method.

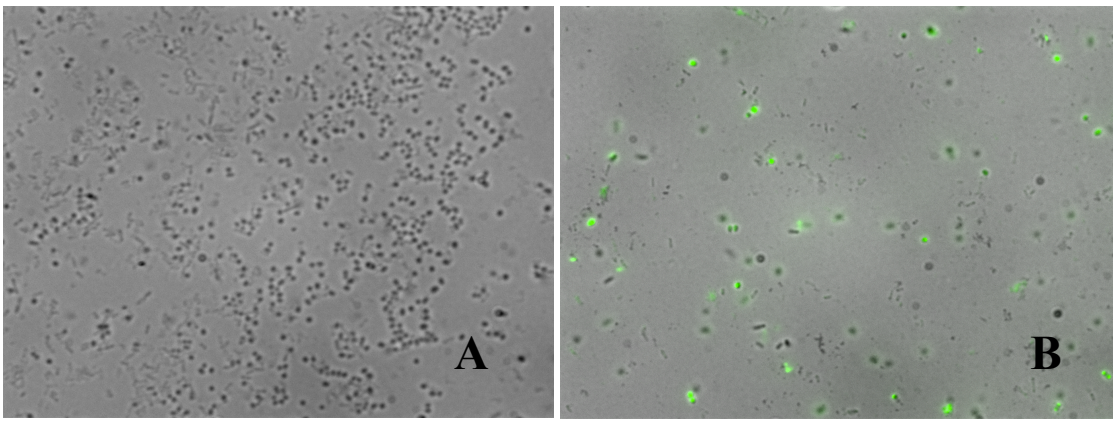

Figure C-2: Microscope images of *E. coli* after exposure to CNT-FITC, (A) *E. coli* without exposure to CNT-FITC, (B) *E. coli* exposure to CNT-FITC.